# GARMENT-BASED RESPIRATION AND PULSE OXIMETRY SENSING USING A STITCHED SENSOR AND CHEST MOUNTED PULSE OXIMETRY SENSOR

A Thesis

SUBMITTED TO THE FACULTY OF

THE UNIVERISTY OF MINNESOTA

BY

MEGAN E. CLARKE

IN PARITIAL FUFUILMENT OF THE REQUIRMENTS

FOR THE DEGREE OF

MASTER OF SCIENCE

Advisor: Dr. Lucy E. Dunne

August 2023

## Acknowledgements

I would like to give my deepest thanks to my fellow colleagues, advisors, family, and friends who have supported me during this project.

- Dr. Lucy E. Dunne, for her mentorship, guidance, patience, and kindness. I extend my deepest gratitude to you for all of your tireless work and advisement starting all the way back to my undergraduate studies. You have made me a better researcher and lifelong wearable technology enthusiast.

- Dr. Brad Holschuh, for his mentorship and advisement who helped me survive the first year of this degree. I thank you for your time and patience in helping a new researcher gain their footing.

- My lab mates in the Wearable Technology Lab, Heidi for keeping the lab running smoothly, Robbie for our video game analysis chats and support, and everyone else at the Wearable Technology Lab – thank you for cheering me on all these years.

- My friends and colleagues, Diana Wagner and Kait Becker (sticker club forever!), and my former colleagues at the Harvard BioDesign Lab who inspired me to pursue graduate studies.

- David Pollack, for his assistance in helping me figure out AcqKnowledge and expertly fielding my questions on unconventional use of Biopac systems.

- My family, Amy, Chris, and Emily Clarke whose love and encouragement have enabled me to face new challenges and experiences and pursue my passions wherever they led me.

- Finally, my wife, Danika Ragnhild, and Radish. Without you two there would be no words on these pages. I love you blue jay.

- This research is supported in part by the National Science Foundation Graduate Research Fellowship, award #2237827.

## Abstract

Garment-based wearable devices have the potential to make on-body sensing of vital signs a more seamless part of everyday life. This research seeks to investigate a wearable chest-mounted stitched strain sensor and pulse oximeter for the purpose of developing a garment-based sensing device. A wearable or garment-based device could be used for long term or long distance monitoring a wearer's respiratory health when regular access to healthcare is challenging due to distance, such as is the case in many rural communities. However, the effect of fit and sizing of a wearable device is a significant challenge when it comes to the balancing comfort and sensor accuracy needs in a wearable device. A stitched conductive thread sensor and an adapted pulse oximeter probe integrated into a chest-mounted mounted adjustable sensor belt were investigated to understand their performance relative to more typical sensing approaches. Two fit conditions were employed to measure effects on sensor performance and understand the challenges presented by garment-based sensing of respiratory signals. This research found that in general a tighter fit condition improved the performance of the stitched respiration sensor and chest mounted pulse oximeter, however sensor dropout greatly influenced both blood oxygen saturation ($SpO_2$) and beats-per-minute (BPM) data resulting in suboptimal readings. The stitched sensor was more accurate in measuring breath frequency than the comparison clinical device when fit was not optimized. As a result of this research, it is clear that the fit and sizing of a garment-based sensing device is a crucial factor in developing sensing garments suitable for everyday use.

# Table of Contents

## Table of Tables

## Table of Figures

# 1. Introduction

Respiration is a fundamental and vital part of life in humans and other living things requiring oxygen ($O_2$) to survive. Human respiration is responsible for oxygenating the blood and ridding the body of carbon dioxide ($CO_2$) via the pulmonary system which includes the trachea and lungs [1]. With the advent of the SARS-CoV-2 (COVID-19) pandemic there has been a sharp increase in research in the domain of respiratory illnesses, their symptoms, and the long-term aftereffects of these diseases within the medical and scientific communities. This renewed interest has demonstrated the need of pursuing novel methods of respiratory health monitoring that can be used for continuous remote monitoring of critical vital signs both in and outside of clinical settings.

## 1.1 Hospital closures and challenges presented by COVID-19

Access to healthcare can be limited due to a variety of factors such as distance due to hospital closures and remote populations [2], limited in-person healthcare options as an effort to reduce transmission of disease, and unavailability of necessary hospital beds in both rural and urban environments. Between 2005-2016, 120 rural U.S hospitals closed creating a barrier to access to essential healthcare and emergency services [2]. These closures force rural residents to travel greater distances to access even basic healthcare services and overwhelm a healthcare system that is already stretched thin. Rural populations suffer from a higher percentage of deaths from chronic lower respiratory disease [3] than their urban counterparts, and with reduced access to quality healthcare, are at greater risk of suffering from long term effects of COVID-19. Furthermore, survivors of COVID-19 may suffer long-term respiratory complications, similar to those of the 2003 severe acute respiratory syndrome (SARS) epidemic including reduced pulmonary function and lower quality of life post-recovery [4].

With nearly 60 million Americans living in rural areas [2] and a decline in available, and accessible, healthcare options, wearable technology has the opportunity to improve the quality of healthcare provided to rural populations. Wearable health monitoring devices paired with expanding telehealth options has the potential to allow rural patients to remain in their home communities, reduce the frequency of healthcare related long-distance trips, and provide vital information for professionals who care for rural patients.

As the COVID-19 pandemic has continued, the long-term complications resulting from the virus have been observed collectively named “long COVID” or “post-COVID” which can last weeks, months, and even years post recovery. Symptoms are varied and can include fatigue, poor concentration and memory (sometimes referred to as “brain fog”), and poor to little smell and taste in addition to continuing respiratory symptoms like difficulty/shortness of breath, cough, and heart palpitations [5]-[6]. Previous infectious respiratory epidemics such as the 2003 severe acute respiratory syndrome (SARS) epidemic also showed long-term effects, including reduced pulmonary function and lower quality of life post-recovery [4]. With 100,000,000+ confirmed cases of COVID-19 in the USA since 2019 [7] the potential impact of long covid in the years to come indicate that respiratory related monitoring may become an important aspect of ongoing healthcare for those who were the most severely affected.

Telehealth services are on the rise to fill these gaps which allow doctors and patients to interact and address a variety of health concerns using telecommunications via the internet and videoconferencing [8] potentially saving unnecessary trips and exposure to potential pathogens. Early in the pandemic hospitals and clinics limited in person healthcare to reduce the potential spread of the virus with many restrictions and new safeguards remaining to this day. The growth of telehealth services combined with long-term limitations to healthcare access highlight a need to develop specialized wearable technologies that can enable remote monitoring of respiratory disorders and disease. Additionally, wearable devices for the remote respiratory monitoring have the potential to reduce pressure on hospitals and allow for continuous monitoring of individuals in their home/communities in cases where distance presents a barrier to regular healthcare.

### 1.2 Why wearable devices?

As a field, wearable technology seeks to combine electronic and computing capabilities on the human body through a variety of means not limited to garments, accessories, and skin mounted devices. However, as the wearable technology market matures it becomes ever clearer that technologies for commercial and medical uses must prioritize user comfort and wearability. Developing textile-based wearable devices can often be a challenge due to the unique characteristics of textiles, yet it is these same characteristics that make using them all the more enticing for body worn garment-based technology. Garments have the ability to move with and conform to the body, can cover both large and small areas on the body, and are ubiquitous in

everyday life from clothing to home goods. Both woven and knit textiles can be manipulated or imbued with different desirable characteristics, such as embedded conductive yarns for electronic applications, selective increased or decreased areas of compression, and moisture wicking capabilities.

However, when translating technologies into garment-based wearables, there are often tradeoffs that must be made so that the desired technologies are able to work as intended. Electronic components can create heavy and stiff areas that can induce fatigue or impede range of motion, sensors may require direct, sustained contact with the skin which can be disrupted by movement, while other sensors or peripherals must be held in place in a tight, form fitting manner that can restrict movement [9], Therefore, the concept of "wearability" must be considered from the very start for a device to be worn on the body. As argued by Gemperle et al. [10], merely shrinking down computers and electronics only makes them that, smaller, and not necessarily considerate of the human body and its unique challenges and opportunities.

### 1.3 Wearable Sensing

Currently many sensors used for sensing and measuring respiration in clinical settings require more invasive and stationary devices such as spirometers [11] and capnography [12] monitors as well as wearable elastic-based sensors such as respiratory inductance plethysmography (RIP) sensors [13].

*Figure 1. Images of conventional respiration sensing devices including a stationary spirometer (left), a nasal capnography monitor (center), and RIP senor belts. Source: Images adapted from [14], [15], and [16].*

Adhesive wearable sensors have also begun to see use in clinical settings such as the Phillips Biosensor BX100 [14] which was given a 510(k) clearance from the FDA and CE mark in March 2020 [15] for use in response to the COVID-19 pandemic. There has been extensive research investigating novel on-body respiration sensors through a variety of methods that utilize

existing technology and merging them with textiles to develop wearable devices. The most common sensors used in this research include optical sensors such as fiber Bragg grating (FBG) [16]-[17], and polymeric optical fiber (POFs) [18]-[19], resistance-based piezoresistive sensors [20] and respiratory inductance plethysmography (RIP) sensors [21], and transducer sensors such as acoustic [22]-[23], accelerometers [24], and motion capture [25] methods.

In addition to more conventional respiration monitoring (breathing frequency), pulse oximetry measures such as blood oxygen saturation ($SpO_2$) and heart rate (measured in beats-per-minute or BPM) can be valuable vital signs indicating overall respiratory health of an individual. Pulse oximeters, a type of optical sensor, have been investigated for use as a respiration sensor using standard pulse oximeters [26] or algorithms [27], and in January of 2019 Masimo received FDA clearance for their MightySat™ Rx pulse oximeter [28] for home use using the same technology as their Respiration Rate from the Pleth (RRp® ) clinical devices which extracts respiration rate via analysis of the change in amplitude and frequency changes from the baseline plethysmography (PPG) waveform [29].

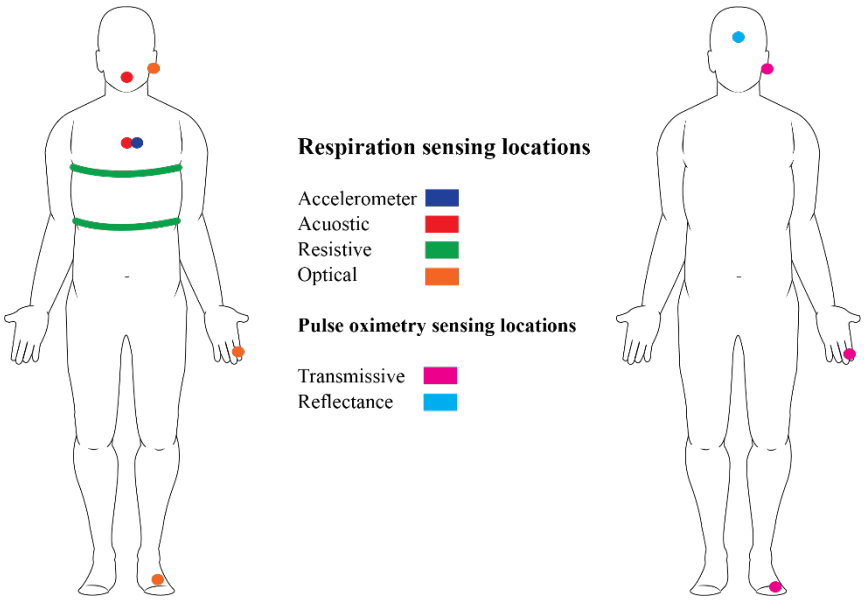


*Figure 2. Body map depicting typical respiration sensing (left) and pulse oximetry sensing locations (right).*

Of the sensors described above, practically all require the sensors to be prefabricated and mounted to the textile. For respiration, this is where the resistive stitched sensor's greatest potential lies, as they are at their basic level, a sensor that is made of a stitch/seam already

commonly used in garment fabrication. Stitched sensors are low cost, easily manufactured in garment factories, and look and feel like everyday clothing. Since the sensor is stitched directly onto the textile or desired substrate it eliminates the need to mount a prefabricated or off the shelf sensor using an additional means of anchoring. This allows for the stitched sensors to retain a low profile on the body, use established equipment and methods of fabrication in the apparel industry, and reduce the number of hard good components required for a device.


*Figure 3. Image of an industrial coverstitch machine used to fabricate the stitched sensor (left) and image of the underside of stitched sensor samples showing the conductive thread (right). Source: Images adapted from [33] and stitched sample provided by author.*

In the case of pulse oximeters, they are still typically relegated to the fingertip for both consumer and clinical devices. Even in wireless sensors such as the Masimo Radius PPG® [30] for tetherless continuous monitoring, the sensor is comprised of a fingertip probe with a smartwatch-like monitor on the wrist. While this may work in hospitals, the finger probe can be cumbersome, bulky, and impair full use of a wearer's hand. This limitation makes it appealing to develop a sensor that can be worn elsewhere on the body for use in everyday life.

In addition to the above benefits, textile- and garment-based sensors are a step in improving the wearability of sensing devices for the users. A garment-based device has the advantage of covering more of the body (unlike devices mounted on extremities) which affords a larger surface area for integrating needed components without the need for additional external harnesses or mounting systems. Garment-based sensors can be worn like regular clothing, do not require obtrusive head gear, and are relatively non-invasive compared to other sensing modalities. However, with these advantages, wearable sensors have their disadvantages that must

be overcome to create more durable and comfortable sensing garments. Garment-based and stitched sensors can be less accurate than their counterparts, fit of a garment can impact sensor performance (for example. looser fits, while more comfortable, produce noisier and/or inaccurate signals), and the electronics used can be affected by use, wear, and washing. As a result, it is necessary to continue investigating and refining garment-based sensing modalities to overcome these challenges to develop the next generation of wearable technologies.

This research endeavors to serve as an important step toward understanding the challenges posed by textile and garment-based respiratory monitoring. To do so, a sensor belt was developed and evaluated on a group of 12 healthy volunteer research participants to investigate a stitched respiration sensor for detecting breathing frequency and an adapted chest mounted pulse oximeter to detect $SpO_2$ and BPM measures. To understand the impact of fit and sizing on a garment-based sensing device, the sensor belt was assessed in two fit conditions. The wearers normal circumference of the upper chest at the armpit level while at rest served as the base fit condition, and a tight fit condition was established as the base circumference minus two inches. The reasoning for these two circumferences is provided in the pilot section of the methods chapter. The results of this research have implications for developing a greater understanding of the potential and limitations of multi-signal wearable sensors.

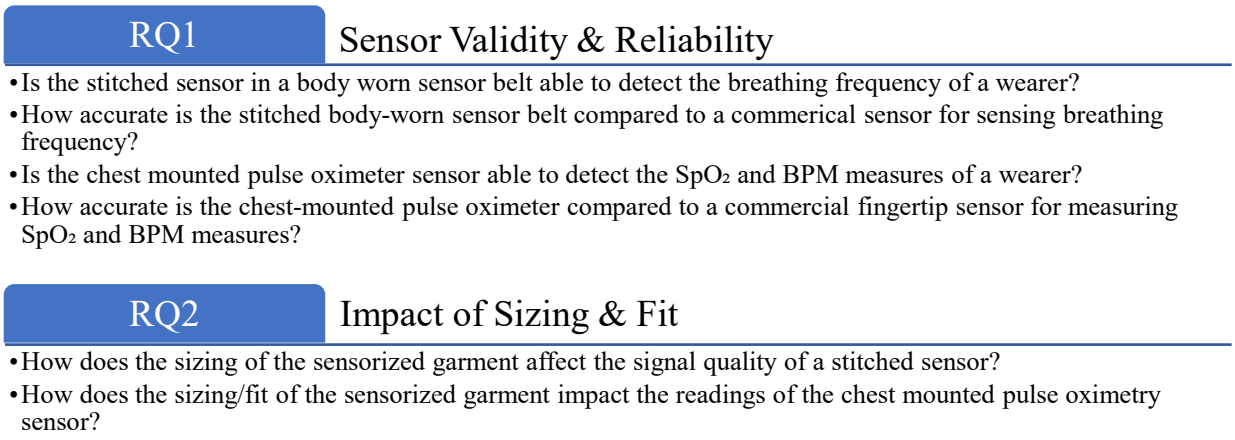


*Figure 4. Overview of research questions addressed in this thesis.*

# 2. Background

## 2.1 Respiration

Respiration is the process in which oxygen is introduced to the lungs from the outside atmosphere, diffused through bodily tissues through lung alveoli and blood, and carbon dioxide is expelled from the body [1]. Breathing is an essential action of life for humans and most life found on earth. The disruption of normal breathing patterns can indicate both acute and chronic respiratory disease and disorders, obstructed breathing, apnea (absence of breathing), respiratory distress, and other forms of abnormal breathing. Breathing can be broadly divided into two categories – normal "quiet" breathing and "heavy" breathing, depending on the action of the chest and abdominal cavities. During normal quiet breathing, the lungs are expanded and contracted by the downward and upward motion of the diaphragm. During inspiration (breathing in) the diaphragm contracts pulling the lungs downward, then during expiration (breathing out) the diaphragm relaxes causing the lungs to recoil assisted by compression of the chest walls and abdominal muscles to expel the air [1]. During heavy breathing the extra force needed to rapidly expire air from the lungs is mainly provided by the contraction of the abdominal muscles that pushes the abdominal contents against the diaphragm which compresses the lungs [1]. As a result, respiration is typically monitored at the chest level, abdominal level, or both to obtain the desired signals depending on the type of breathing or desired measurements.

### 2.1.1 Respiratory events & disorders

*Respiratory Disease & disorders:*

According to the World Health Organization respiratory disease is among one of the most common causes of death and illness [31]. Respiratory diseases make up 3 of the top 10 causes of death worldwide include chronic obstructive pulmonary disease (COPD), acute lower respiratory disease (including infections caused by influenza), and lung cancer and cause an estimated 8 million deaths per year and these numbers remain on the rise [31]. Other respiratory disease/disorders of note include tuberculosis, sleep-disordered breathing (such as sleep apnea), occupational lung disease (such as black lung disease), and now the highly infectious COVID-19 and its subvariants.

*Long covid:*

The emergence of the COVID-19 pandemic in 2019 has demonstrated the lasting impacts of a highly contagious respiratory disease and its impact on the healthcare system. When looking to the United States the Centers for Disease Control (CDC) reports that as of December 16th, 2022 there have been 100,600,000+ cases with 1,088,481 cases resulting in death attributed to SARS-CoV-2, which has put a considerable strain on the healthcare system and has brought healthcare disparities to the surface [7]. Long COVID or post-COVID conditions are still being defined by the broader medical community and categorized as the medium to long term consequences of the disease are being observed and studied. While the long-term effects of COVID-19 remain to be better understood as time goes by, we can look to currently available case studies, evidence from the field, and previous epidemics such as the SARS epidemic [32], [33] to get an idea of what impact COVID-19 will have in the future.

Current estimates by the CDC find that nearly 1 in 5 adults (18-64 years of age) report experiencing long covid symptoms (defined as symptoms lasting three or more months after contraction of the virus that were not present prior to infection) based on the Household Pulse Survey [34]. Respiratory-related symptoms include persistent cough, dyspnea (shortness of breath), increased respiratory effort, and chest pain which can impair activities of daily living [5], [35]. Individuals with long covid may also be at an increased risk for re-infection or susceptible to other disorders affecting the pulmonary system.

### 2.1.2 Respiration measurement and sensing

Respiration can be measured in several diverse ways based on the desired information to be gathered. Depending on what facet of respiration being measured, there are a variety of methods and apparatuses used in clinical settings. The most commonly used measurements include respiration rate/breathing frequency (rr), tidal volume (VT), and minute ventilation (VE) [36]. These can then be sub-divided into two categories, invasive vs. less-invasive measurements. Respiration rate, even in clinical settings, is typically measured by counting the number of times an individual breaths in a minute at rest based on the amount of times the chest rises [37]-[38]. However, tidal volume and minute ventilation both require the use of a spirometer which is an apparatus with a mouthpiece in which the patient blows into and a nose clip to keep the nostrils closed [39], [fig 5]. The ideal respiration rate for healthy adults is generally 12-20 breaths [40],

however this can vary depending age with elderly populations typically having higher rr values and ceiling for tachypnea (abnormally fast breathing) [41].

*Spirometry*

*Figure 5. Figure depicting two spirometers with a more typical spirometer device depicted (left) and a portable handheld spirometer. Source: Images adapted from [39] and [42].*

Spirometers measure the volume of air moving in and out of the lungs (ventilation) of an individual via mouthpiece that feeds into a machine. Spirometers can generally be divided into two groups: 1. Volume-measurement devices in which the flow is calculated by the time derivative of the volume signal and 2. Flow-measurement devices in which volume is calculated by integration over time of the flow signal [42]. These devices are typically used in a clinical setting, however there are smaller handheld portable versions such as that can be used such as the AioCare Respiratory Disease Management System (Vyaire™ Medical Inc., Chicago, IL, USA) [43]. These devices are typically only used for diagnostic tests to measure ventilation and not for general respiration sensing.

*Respiratory inductance plethysmography*

Respiratory inductance plethysmography (RIP) sensors are sensors that use a sinusoid wire array coupled with a transducer to measure the motion of the chest and abdomen and translate that movement into a readable output [44]. These sensors are frequently used in sleep centers [45] and on infants and young childern [44] to measure respiration rates in a simple and non-invasive manner. The sensors are typically comprised of a coated wire in a sinusiod pattern that is embedded in a elastic band that comes in a varitey of forms including disposable pre-sized or cut-to-size sensors or reusable sensor belts such as the Natus® XactTrace® RIP respiratory

effort belts (Natus®, Middleton, WI, USA) [46]. These bands are usually used in pairs with one belt positioned around the chest and the other belt positioned around the abdomen for the best readings/results, however in some cases they may be used indepentdently. RIP sensing has been used in commerical products for respiration monitioring such as the Hexoskin shirt (Carre Technologies Inc. (Hexoskin), Canada) [47] and the earlier LifeShirt (VivoMetrics, USA) [48], Fig. 6].

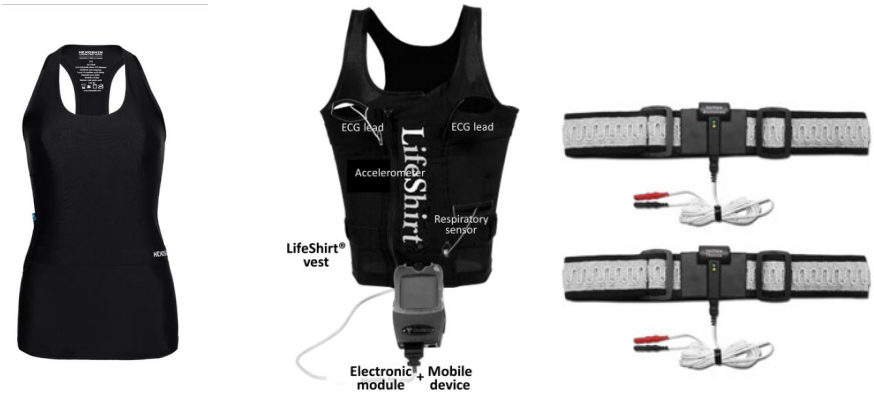


*Figure 6. Commercial products using Respiratory inductance plethysmography (RIP) sensors for respiration monitoring. Hexoskin Smart Shirt (left), LifeShirt® (center), Natus® XactTrace® RIP respiratory effort belts (right) Source: Images adapted from [47], [48], and [46]*

These devices show promise for a commercially viable garment for respiratory and vital sign monitoring that have the potential to be used along with telehealth modalities to create personalized remote health care programs for vulnerable patient populations who are immunocompromised, live long distances from specialist care, or otherwise homebound.

### 2.2.1 Pulse oximetry measurement and sensing

Pulse oximeters are used to measure oxygen saturation in blood as well as other derived information such as heart rate. These devices are typically used to detect hypoxia (low concentrations of oxygen in blood), apnea events, and have been used to determine if mechanical ventilation is required [49]. Pulse oximeters measure blood oxygen saturation ($SpO_2$) based on the principle of how oxyhemoglobin ($O_2Hb$) is distinguished from deoxyhemoglobin (Hhb) by measuring how they differently absorb red and near-infrared (IR) light [50]. Since $O_2Hb$ and Hhb absorb the red and near-IR lights at different levels pulse oximeters are able to detect the $SpO_2$ of only arterial blood which is influenced by the fluctuations of the cardiac cycle whereas other

tissues will generally remain stable [49]-[50]. By only measuring the changes in absorbance by the $O_2Hb$ and Hhb the pulse oximeter is able to filter out venous blood which can influence a $SpO_2$ reading. This can be expressed via the Beer Lambert Law, which demonstrates the relationship of the absorption of light, in this case the dual light wavelengths of the pulse oximeter, to the properties of the material through which the light is traveling. This relationship is expressed as:

$$A=\varepsilon bC$$

with "A" standings for absorbance, "ε" as the molar absorption coefficient, "b" as the length of the path traveled by the light, and "C" as the concentration of the solution [51].

Ideal $SpO_2$ and beats-per-minute (BPM) levels for healthy children and adults typically fall in the 95-100 range with FDA cleared pulse oximeters within a 2-3% [52] range of accuracy. If one of these monitors register a reading of 90% (a threshold for adverse health conditions [49]), with the 2-3% error the reading could indicate a range of a 86-94% reading.

*Pulse oximetry devices*

These devices are often tethered via a cable to a machine that reads the sensor outputs such as the Nellcor™ Bedside Respiratory Patient Monitoring System (Medtronic, USA) [53], however Masimo has developed a wireless adhesive Respiration Rate from the Pleth (RRp®) device which is a tetherless pulse oximeter probe that can also be used to derive breathing frequency of a patient [54] [fig. 7].


*Figure 7. NellcorTM Bedside Respiratory Patient Monitoring System (left) and Masimo Pleth (RRp®) pulse oximetry monitors. Source: Images adapted from [53], [54].*

While convenient and simple to use, these probes are somewhat bulky, impede use of the hand if a finger probe is used, and are less able to detect specific adverse events such as shortness of breath or coughing.

### 2.2.2 Methods of pulse oximetry sensing

There are currently two methods of pulse oximetry sensing, transmissive and reflectance. Transmissive pulse oximeters work by shining the light created by the photodiodes through a thin area of the body, such as the finger, earlobe, or ankle in the case of infants, directly to the receiver. These areas are preferred sensing locations due to the high perfusion of blood vessels and are thin enough to be able to pass the light through with the photodiode and receiver directly opposite to each other.

Reflectance pulse oximeters are set up in a different manner with the emitter and receiver components are placed adjacent to each other and the oxygen saturation is estimated from the back-scattered light [49], [55]. The most common placement for these types of probes is the forehead as it can take advantage of the supraorbital artery which is less likely to be affected by vasoconstriction than a peripheral artery such as those found in the fingers. Reflectance pulse oximeters have also gained some interest by companies since they require low power consumption and fast sensor response time [49].

### 2.2.3 Atypical sensing locations

While the forehead is the standard location for reflectance-based pulse oximeters, researchers are exploring alternative sensor placement from internal locations such as the esophagus [56]-[57] to external locations including the torso, bicep, wrist, and calf [58], [59]. These external locations are of great interest, particularly in the design and development of wearable sensing garments. These atypical sensing locations show promise in the case of Kramer et al. [58], the tested sensing locations – chest at the pectoral and sternum, arm at the bicep and forearm, and leg at the calf, achieved accuracies (ARMS, root-mean-square difference) of 1.7% (n = 26) at the calf, 3.1% (n = 12) at the bicep, 3.4% (n = 11) at the forearm, 2.9% (n = 42) at the pectoral, and 2.9% (n = 13) at the sternum. These measurements fall within regulatory guidance calibrations with an ARMS of less than 3.5% as acceptable error.

### 2.3 Respiration and pulse oximetry

While both respiration and pulse oximetry measures both provide insight into an individual's physical state, $SpO_2$ and rr aren't necessarily always tightly tied to each other [60]-[61], (silent hypoxia – covid, low Spo2 levels without shortness of breath), but give a more targeted understanding of potential symptoms. Those with COVID-19 can be affected by a phenomenon called "silent hypoxia" in which an individual can display low $SpO_2$ levels without a shortness of breath (>18-22 rr). As a result, $SpO_2$ and rr measures, while informative alone, the two measures together give a better understanding of an individual's respiratory health.

With many hospitals and clinics limiting in-person and non-essential healthcare services to reduce the spread of the virus, telemedicine has been increasingly implemented to bridge the gap between patients and physicians. This gap motivates the purpose of this research to develop a garment-based sensing system to monitor respiration and blood oxygen saturation patterns with the ability to reliably detect adverse respiratory events such as coughing, shortness of breath, and respiratory distress remotely and provide this information in real-time to clinicians. These garments have the potential to allow for both short and long-term monitoring of respiratory symptoms while remaining unobtrusive enough to not affect activities of daily living (ADLs) within their own homes and communities.

### 2.4 Textile Structures

For the development of fiber and textile-based sensors and garment-based wearable devices, conductive yarns and textiles are of great importance. In the case of respiration sensing, conductive threads can be used for fabricating sensors by replacing conventional wires like those used in RIP sensing. Conductive textiles, in conjunction with insulating dialectic layers, can also be used to make capacitive sensors capable of strain and pressure sensing. The advantages of these fiber and textile-based sensors are that they are by nature, comprised of the same materials already used in garment manufacturing. Conductive thread can be sewn directly into a seam or over a textile surface and conductive textiles can be used in the construction of a smart garment or top applied and stitched to a garment using conventional sewing machinery.

### 2.4.1 Conductive Threads

Thread is a specialized yarn used in sewing to join sewn goods, such as garments, which can be made from natural, manufactured, and synthetic fibers. These fibers are processed into yarns by spinning or twisting the fibers that can then be plied and further processed. Synthetic fibers (e.g., polyester, acrylic, nylon, etc.) are manufactured by extruding the melted or dissolved material through a spinneret via a spinning pump to create filaments which can be further processed into yarn or extruded in a monofilament [62]. During this process conductive materials can be added to create a conductive yarn. Fine metal wires can be twisted around a fiber core, carbon nanotubes or carbon black particles can be mixed in with the synthetic fibers pre-extrusion, and finished yarns can be coated with a fine layer of metal, such as silver or copper, to impart conductive characteristics to the thread [62].

The yarns can then be used in the production of conductive textiles or threads to develop smart textiles and textile-based sensors. These textile-based systems are particularly attractive for use in wearable sensing systems as they are flexible, deformable, and easily integrated into garments and textile-based systems, using existing equipment and/or processes. However, these conductive yarns are not without their disadvantages. In the case of yarns containing conductive particles, the more conductive materials in the assembly, the higher the conductivity. However, increasing the proportion of conductive particles impacts the mechanical properties of the yarn, which typically becomes stiffer and sometimes more brittle than typical sewing threads. Yarns that have been coated with a layer of metal are susceptible to friction during the production process, manufacturing process, washing, and wear and tear which causes the conductive materials to crack and rub off. Therefore, careful consideration and selection of materials must be done when developing a sensor or garment for the best results using these materials.

### 2.4.2 Stitch Architectures

The stitch is a fundamental element of sewn goods with applications that range from strictly functional to purely decorative. ATSM International defines a stitch as a “configuration of the interlacing of sewing thread in a specific repeated unit” [63]. Just as there is a wide variety of fibers and textiles used for sewn goods, there are an equally considerable number of stitch architectures with each having unique properties and uses. The type of textile being used, such as woven or knit textiles, determines the proper stitch architecture for a product.

Stitches in the 400-600 stitch classes are particularly suited for use on knit fabrics as once they are sewn to the textile, they are less likely to break and impede the elongation of the textile while being stretched. Additionally, the three thread stitch types, such as that of a typical coverstitch seam, allow for a seam configuration with both conductive and non-conductive threads that helps prevent shorting of a stitched sensor since the conductive fibers are insulated from each other [fig. 8]

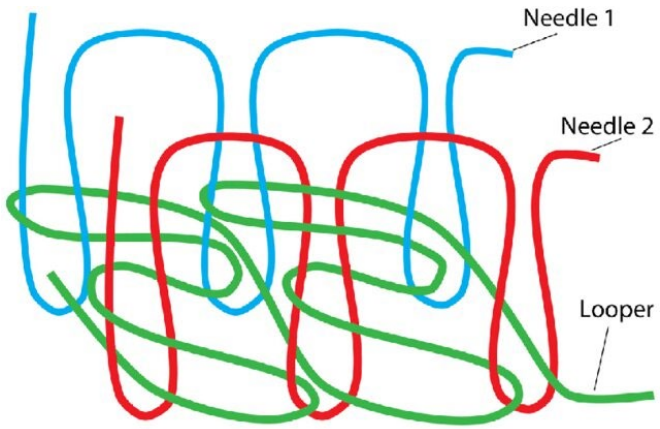


Figure 8. Diagram of a two needle three thread coverstitch seam. Source: Image adapted from [64]. The two needle threads are visible on the top of the textile with the lower looper thread on the bottom of the textile.

The stitched sensors used in this study are formed with the coverstitch architecture as seen above [fig. 8] with conductive thread in the lower looper. They are particularly exciting as they can be easily integrated into garments that are unobtrusive, conform to the human body, and can be fabricated using existing sewing equipment and processes. This thesis research study aims to validate these textile-based stitched sensors as an accurate and reliable method of respiration monitoring.

### 2.5 Methods of textile-based strain sensing

At their most basic level, sensors are described as a device that responds to a physical stimulus and then translates that input into a resulting impulse/output [64]. Depending on the school of thought, textile-based sensors can be categorized into sensors that are comprised of textiles, or sensors applied or integrated into textiles via methods such as stitching, bonding, or printing, among others. This section will discuss the characteristics and uses of three types of

fiber and textile-based sensors used for strain sensing including: optical, capacitive, and resistive sensors.

### 2.5.1 Optical Strain Sensing

One method of textile-based strain sensing is optical strain sensing in which an optical fiber integrated into a woven or knit textile structure [fig. 9]. These sensors are typically comprised of a coated polymer fiber with a light source at one end and a photodiode at the other end [65]. These sensors measure the light changes as the light moves through the fiber as it is bent or strained between the light source and receptor. Optical sensors have previously been studied for respiration sensing including the use of polymer optical fiber (POF) sensors and fiber bragg grating (FBG) sensors mounted via extensible straps/bands, particularly for monitoring respiration in magnetic resonance imaging (MRI) contexts due to their inert, flexible, lightweight, and relatively unobtrusive nature [65]-[66]. Other researchers have also looked to validate using a series FBG sensors integrated into a garment as a method of measuring normal quiet breathing and apnea while the wearer is in both standing and supine positions [66]-[17].

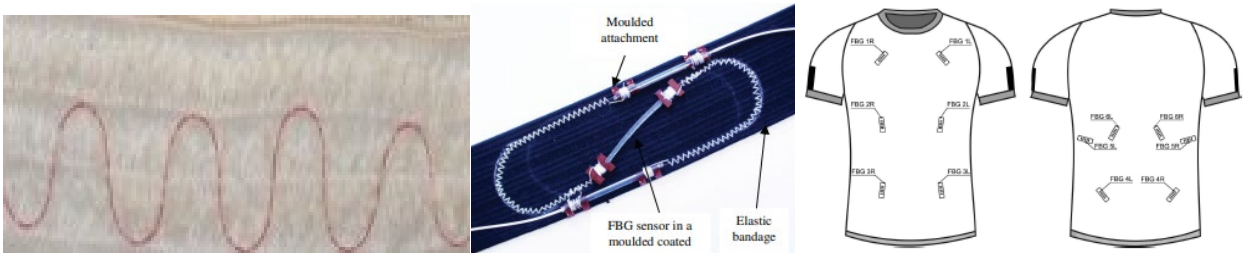


*Figure 9. Figure depicting optical sensors. POF sensor in a sinusoidal pattern integrated into an elastic band (left) and fiber bragg grating sensor array on an elastic band (middle), fiber bragg grating sensors integrated into a garment (right). Source: Adapted from [65], [66], and [17].*

*Optical sensor pros & cons*

While effective, this optical method of sensing does have distinct disadvantages over other methods of fiber and textile-based sensing. Since the fibers require both a light source and detector a certain amount of bulk is inevitable as well as the fact that the system requires an active input (light source) which adds another element in the system that must be accounted for and powered. Additionally, optical sensors are not as easily integrated into a garment during the

manufacturing process requiring top application of the fiber, manual insertion into a woven or knit structure, or specialized process to couple the sensor to a textile base.

### 2.5.2 Capacitive Strain Sensing

Textile capacitive sensors are typically comprised of two conductive textile layers that have been bonded or adhered to an inner dielectric insulator layer. These sensors have been explored for both pressure and strain sensing for wearable devices and soft sensing systems due to their conformable nature and relative ease of production. Capacitive sensors exhibit good sensitivity to forces (including strain and pressure) and can be made in a variety of shapes and sizes to match the required need for a project. Researchers at Harvard University have developed a method of batch manufacturing highly stretchable textile-based capacitance sensors using two layers of Shieldex Medtex-130 (V Technical Textiles Inc., USA), a silver-plated knit textile with a silicone elastomer (Ecoflex 00-30, SmoothOn Inc., USA) as the middle dielectric layer [67]-[68] which can be cut to project specifications using a laser cutting machine [fig. 10].

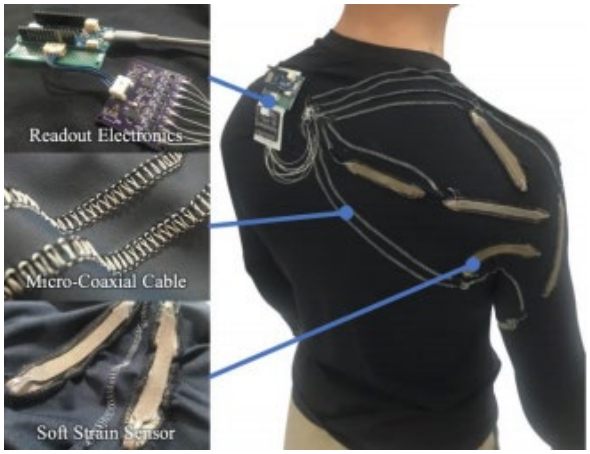


*Figure 10. A shirt-based sensing garment utilizing capacitive strain sensors for shoulder kinematic estimation. Source: Adapted from [69]*

Capacitive sensors have also been used for respiration sensing integrated into belts by laminating layers of polyester fabric with Ni-Cu-Ni plated fabric [69] and sliver plated knit textiles [70], and garments by stitching conductive yarns in a specific stitching pattern [71].

*Capacitive sensor pros & cons*

While capacitive sensors are able to effectively detect respiration, they are susceptible to mechanical degradation over time, particularly sensors with an elastomeric layer if not properly encapsulated. There is also the chance for the sensors to short due to frayed fibers from the conductive textiles coming loose due to repeated use and mechanical wear if not shielded from the environment.

### 2.5.3 Piezoresistive Strain Sensing

Another form of textile-based strain sensing is piezoresistive strain sensing which encompasses a variety of methods including coated-textiles, film-based sensors, and stitched sensors. These sensors measure the change in resistance of the sensor as it is strained. These sensors demonstrate excellent deformity and flexibility which is ideal when developing sensors and wearable devices for daily use to mitigate interference of daily tasks and comfort for the wearer. Piezoresistive sensors are commonly fabricated by coating a textile with a film of an elastomer that has conductive materials mixed in such as carbon-based fillers. In [20] the researchers used ELASTOSIL® LR 3162 (Wacker Chemie AG, Germany) which is a conductive silicone rubber combined with carbon-black particles and coated a knit (95% PES (Supplex®), 5% Lyrca®) textile to create two sensors that were adhered at the chest and abdomen on a vest-like garment. The sensors were then connected using conductive yarns (Shieldex® 235f34 dtex 4-ply HC, Statex) and snaps to connect the sensors to the electronic box [Fig. 11].


*Figure 11. Examples of textile-based piezoresistive sensors include a conductive elastomer sensor (left) and a conductive thread stitched piezoresistive sensor (right). Source: Adapted from [20]-[73].*

Another approach to textile-based resistive strain sensors is using conductive threads stitched into a substrate, such as a knit textile. In Gioberto & Dunne, 2012 [72] a 602 two needle thread

coverstitch with Shieldex silver-coated 235/34 dtex 4-ply thread was used to fabricate a sensor that exploits the loop configuration the threads that generate a piezoresistive response [Fig. 7]. This research has found that these stitch types are viable architectures for textile-based strain sensing for detecting elongation and movements such as respiration and bending [72]-[73].

*Stitched sensor pros & cons*

These stitched sensors are of particular interest for developing a respiration sensing garment as they are simple, are easily be integrated into sewn goods and garments, have a small form factor, conform to the human body, and relatively unobtrusive to the wearer. However, it must be noted that the threads used for stitched sensors are coated to impart the desired conductive characteristics. These coatings can be damaged due to friction during the fabrication process, due to rubbing during wear/use, and performance can be diminished during washing causing the sensors to be less sensitive overtime and limiting the lifetime of the senor unless properly shielded. Previous work by Berglund et al. showed that both un-insulated and insulated stitched sensors are subject to baseline drift and peak-to-peck response after washing and drying, especially those exposed to both machine washing and drying [74].

Stitched sensors show good sensitivity to detecting elongation/strain and require a simple power system that can be integrated in a small electronic package. The sensors have a small form factor that is flexible and can be directly sewn to textiles and other stretchable substrates. With proper shielding from the environment to improve sensor lifetime, these sensors show promise for developing a low-cost, simple to manufacture, and comfortable garment-based sensors are suited for long-term respiration sensing.

### 2.6 Wearable device sizing & Fit

When developing worn devices that integrate sensors and electronics into textiles, how these devices are sized becomes an important consideration. There is near infinite variability of human body shapes and anthropometrics that influence how garments interact and move with the body during both static and dynamic postures. As a result, sensorized garments present additional challenges in developing sizing systems that accommodate a diverse population and while retaining sensor functionality.

### 2.6.1 Impact of anthropometric variability on smart garment functionality

In much of ready-to-wear (RTW) garment design the size ranges are based on traditional methods of pattern making and rely on grade rules to size a pattern up or down a size range from a base pattern. RTW focuses primarily on developing a size system that limits the number of sizes needed and maximizes the efficiency of production and resulting profit. This method of sizing garments introduces a variety of challenges that must be overcome to ensure proper placement of a sensor on the body for optimal performance. Work by Griffin et al. [75] examined the variability of body landmarks of selected individuals from two anthropometric databases, Anthropometric Survey of US Army Personnel (ANSUR) comprised of U.S. military personnel and Civilian American and European Surface Anthropometry Resource Project (CAESAR) comprised of American and European civilians, using the ASTM standards for gender specific sizing and ANSUR "unisex" sizing based on the ANSUR men data set to examine the variability of location of the $10^{th}$ rib landmark relative to the high point shoulder (HPS) landmark. The results found large variability in the vertical spread of $10^{th}$ rib location, ranging from 30 to 131mm in gender-specific sizes and 69-146mm in the unisex condition. Their results demonstrate the difficulties of integrating sensors in garments, in this case an ECG electrode, and that sizing system considerations must be a part of smart garment development from the very beginning.

### 2.6.2 Impact of sizing & fit on sensor performance

To address the issue of fit and sizing, there has been efforts by researchers looking to improve the design and manufacture of smart garments using methods such as computer 3D model simulations [76]-[77] and anthropometric databases [75]-[78] to inform sizing systems that will retain device functionality through a size range. Work done by Harms et al. have extensively explored the effects of garment wrinkling and movement [76], [79] on posture recognition. They noted an average 13% loss in sensor system accuracy [79], however a decrease in error was also observed in participants for whom the sensorized shirt was nearly tight-fitting as a result of increased body dimensions. Work by Gioberto & Dunne [80] also found that garment positioning can have an effect on potential sensor placement in lower body garments (in this case denim trousers) observing positioning error of up to 14 cm at the ankle and observing variable drift error across difference weights of denim textiles and marker locations. In the case

of particularly sensitive technologies where precision is of great importance, sizing and fit of sensorized devices is an essential element in optimal sensor performance and reducing undesirable sensor drift and error.

In the studies mentioned earlier in this chapter, sensor error is as a result of human movement or other physiological functions are noted on. However, the fit conditions in which the sensors are tested are unknown for [45], [66], [17], [70], and [71] (which was only tested on a mannequin with an inflatable cuff bladder), or by having the participant tighten the sensor themselves to accomplish an approximate 2% pre-stretch [20]. As a result, understanding the relationship between sensor performance and wearer circumference in these studies is difficult outside of the general consensus that tight and undersized fits tend to provide optimal results.

### 2.6.3 Wearable device comfort

Another consideration for garment-based devices is the relative comfort of the device. Frequently, a worn device is snug and close-fitting in an effort to ensure sensor contact with the body for best functionality. However, this method can be problematic as it does not necessarily consider the long-term comfort of the wearer, optimal sensor placement could conflict with high-wear areas leading to premature degradation or impede free range of motion of that body part/region. As a result both the requirements of the sensor being integrated and needs of the user must be considered to develop an optimal finished product [81].

# 3. Methodology

## 3.1 Purpose & research aims

In this chapter the research questions [fig. 12] are investigated through exploratory pilot testing culminating in a research study with *n=12* participants. Sensor development will be discussed in section 3.2, pilot testing in section 3.3, and study procedures and data analysis from section 3.5 onward. Each section describes the testing methods, variables, and data analysis methods for each sensor and fit condition.

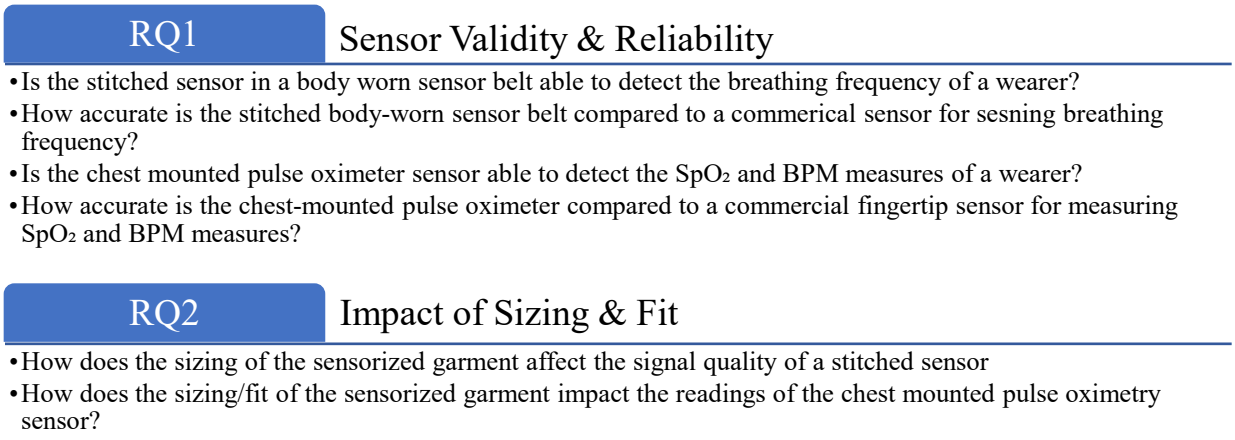


*Figure 12. Overview of research questions addressed in this research study.*

## 3.2 Prototype development

*Device summary*

To develop a study to evaluate the stitched sensor's ability to detect respiration rate and the chest mounted pulse oximeter's ability to detect blood oxygen saturation a prototype was developed and refined through a series of pilot tests. An adjustable sensing band was developed to enable ease of testing the stitched respiration sensor on a variety of locations and individuals as well as being able to precisely set the band to a fixed circumference. A data acquisition system (MP160, BIOPAC Systems, Inc) was used for collecting data from both the experimental and reference sensors during pilot testing and study. AcqKnowledge 5 (BIOPAC Systems Inc., version 5.0.8) was used to collect, process, and analyze data and Microsoft Excel (Microsoft Corporation, version 2305 Build 16.0.16501.20074) used for additional data analysis.

*Respiration sensor development*

The stitched sensor and its implementation is based on work by G. Gioberto [82] whose first investigated the use of a stitched sensor for garment-based strain sensing and Patil et. al. [83] who investigated the use of worn sensors for characterizing and observing cigarette smoking behaviors. The sensor is comprised of a silver-coated Nylon conductive thread (235/36 x4 HCB, V Technical Textiles/Shieldex® USA) stitched with a two needle coverstitch configuration with polyester thread in the needles and conductive thread in the lower looper, on a 80% polyamide/20% spandex jersey knit textile base layer [fig #]. The stitched sensors were sewn on a stretch textile substrate in 1.5-inch lengths and cut into individual sensors. The wire leads applied to the sensors using 7mm rivets as the contact points with a rivet press, "sandwiching" the wire leads and conductive thread between the two halves of the rivets. In later prototypes a small amount of conductive epoxy was applied to the rivets and wires prior to pressing to improve the connection and signal. The resulting sensor was one inch in length between the two rivets [fig. 2].

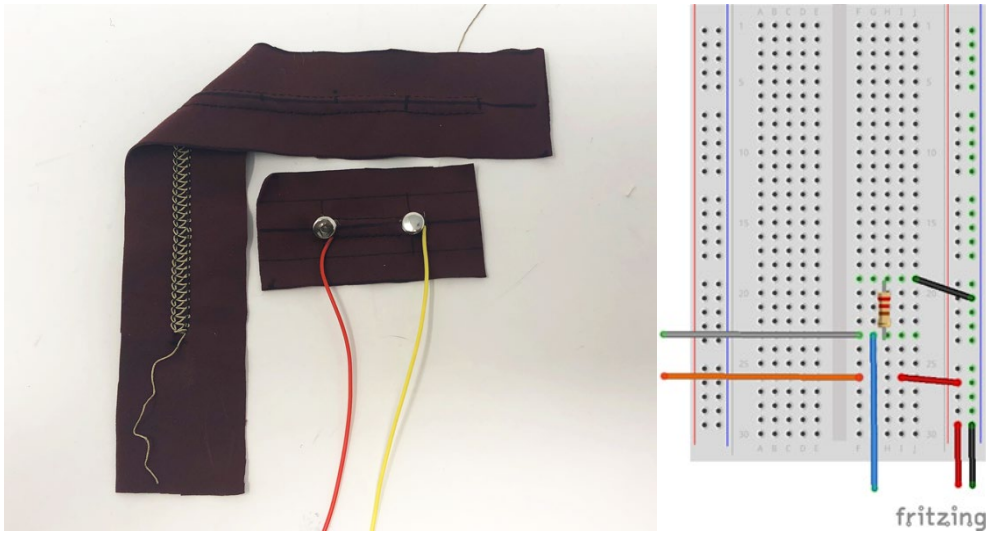


*Figure 13. Left image: Twin needle coverstitch sample with conductive thread in the bottom looper and sensor with riveted connections and wire leads. Right image: Voltage divider schematic for interfacing the custom stitched sensor (grey and orange wires to the l eft) and the Biopac HLT100C module (blue, black, and red wires) via a RJ25 connector.*

Respiration data was collected using the HLT100C high level transducer interface module with a voltage divider from the experimental stitched sensor and the RESP100C respiration

pneumogram module with the TSD201 respiration transducer as a reference measure. A voltage divider was used to interface the custom sensor with the Biopac HTL100C module [fig. 13]. It is comprised of a standard breadboard and with a 10-ohm resistor between the custom sensor and HTL100C.

*Pulse oximeter development*

The Biopac TSD124C flex wrap transducer was used for the chest mounted pulse oximeter as its construction allowed for simpler modification than a traditional finger clip transducer. Previous research conducted by Schreiner et al. [59] found that their sensors produced the best signals between 0° to 10° relative to the reference plane, in this case the chest of the wearer. In this study the emitter and receiver of the flex wrap transducer were spaced 6 mm apart and set at an angle of 10° inside of a 3D printed housing [fig. 14]. Exploratory testing was undertaken to test the sensor's ability to detect blood oxygen saturation levels in both taped (sensor + housing taped to the body) and no tape (sensor + housing held in place with the conditions.

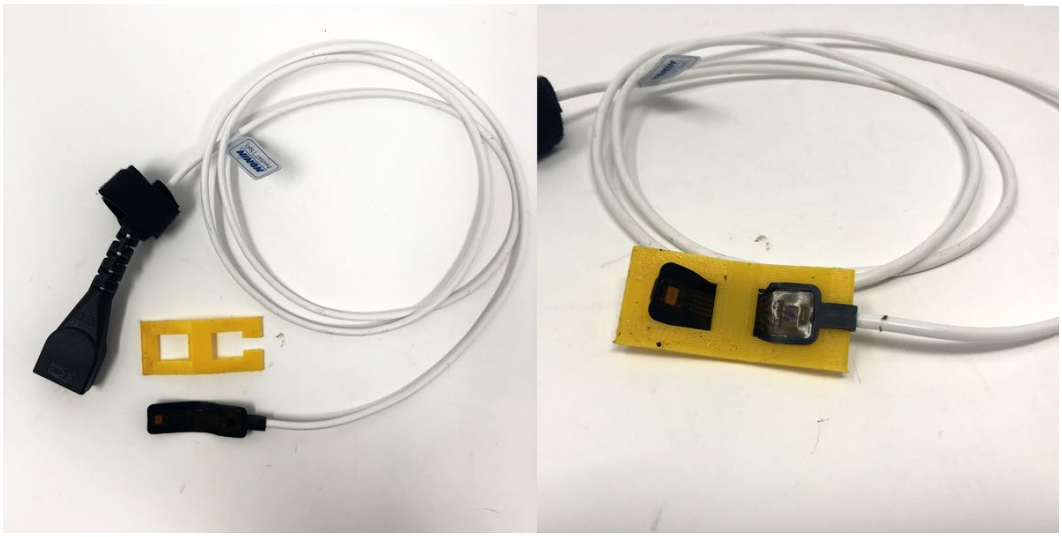

*Figure 14. Biopac TSD124C flex wrap pulse oximeter sensor with 3D printed housing.*

Pulse oximetry data was collected using the OXY100E and TSD124C flex wrap transducer as the experimental sensor with the OXY100C and TSD123 finger clip transducer serving as a reference measure. The OXY100E module is used to measure beat-by-beat $SpO_2$ values, pulse plethysmogram, and heart pulse rate. The TSD124C flex wrap transducer is used in

this study for measuring pulse oximetry signals on the upper chest on the manubrium where the upper section of the sternum and clavicles and first ribs meet. The OXY100C along with the finger clip TSD123A $SPO_2$ finger transducer is used the reference measure to compare against the data from the chest mounted TSD124C flex wrap transducer. These modules work using the Lambert-Beer law as described in the background chapter.

### 3.3 Pilot testing

To test the stitched sensor, the prefabricated sensors were sewn to an inextensible nylon webbing to isolate the strain to the sensor itself to improve sensor responsivity. A side release buckle was added to the band as an adjustable closure to allow for testing a variety of fit conditions. In later iterations of the sensing band prototype, markings were added in 1, ½, and ¼ inch increments to make for faster and more efficient size adjustments during testing. During initial testing of the pulse oximetry sensor, it was not included in the same sensor belt as the stitched respiration sensor and instead was either taped to the body or held in place with a different sensor belt. Both sensors were integrated into a singular sensor belt for final pilot testing and use in the following study.

*Stitched sensor performance*

During exploratory testing it was found that in tighter fit conditions the sensor oversaturated and produced a nosier signal [fig. 15].

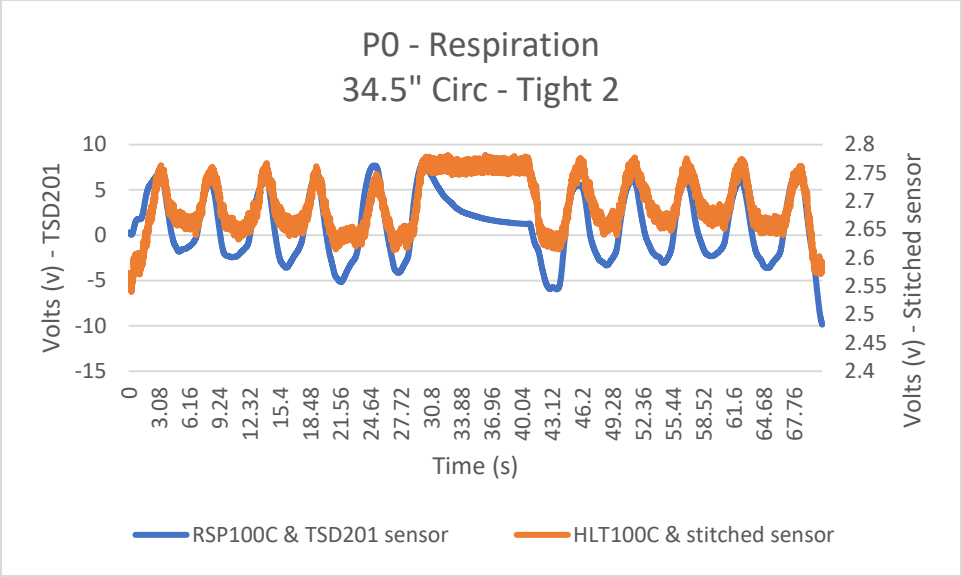


*Figure 15. Graph of the Biopac reference sensor and experimental stitched sensor response in a tight fit condition (sensor belt is set two inches smaller than participant's base circumference at the armpit level on the upper chest) during normal breathing.*

In an effort to mitigate some of the oversaturation effects a soft braided elastic was added as a backing to the sensor before being sewn to the nylon band [fig. 16].

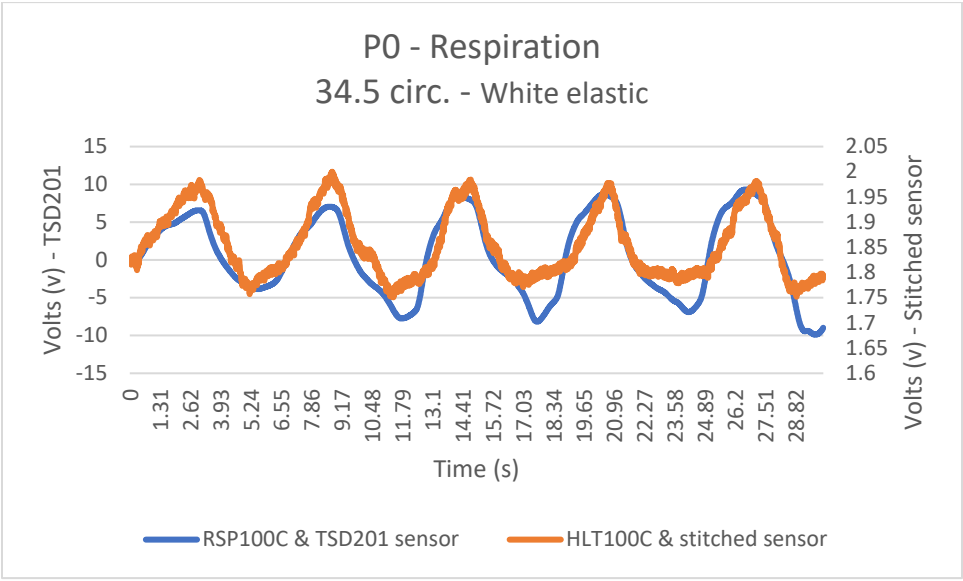


*Figure 16. Graph of Biopac reference sensor and experimental stitched sensor response in a tight fit condition (sensor belt is set two inches smaller than participant base circumference) during normal breathing, with a braided elastic backing.*

The elastic backing improved the stitched sensor signal by reducing noise as a result of mitigating some of the direct strain on the sensor, especially in the tighter fit conditions, by limiting the stretch of the sensor preventing it from completely oversaturating. The resulting data could then be further filtered in AcqKnowledge to produce a smoother waveform.

To determine potential sizing conditions the sensor was evaluated in a series of gradually reduced circumferences starting with the wearer's base circumference and reduced in one inch increments up to six inches smaller than the base circumference [fig. 17].

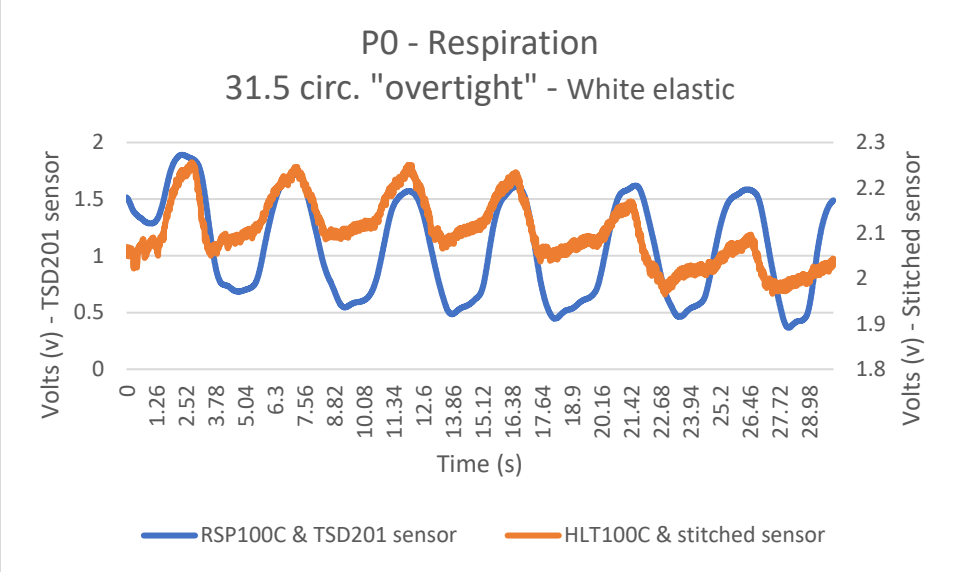


*Figure 17. Graph of the Biopac reference sensor and experimental stitched sensor response in a tight fit condition with the sensor belt set to five inches smaller circ. than participant base circ. when compared to [fig. 15] graph with the two-inch circ. difference.*

Based on this testing, a two-inch circumference reduction for the tight condition was chosen for the study. The two-inch circumference difference was best able to balance sensor signal clarity and wearer comfort and was not too dissimilar to a compression garment. Tighter circumferences (3–5-inch differences from base circ.) were found to be far too restrictive to the wearer's rib cage during breathing and caused a significant amount of discomfort even post doffing of the sensor belt.

*Chest mounted pulse oximeter performance*

The adapted chest mounted pulse oximeter had the most variable performance of the experimental sensors. While it worked best in tight and taped [fig. 18] conditions, both conditions were still prone to dropping out even at rest in seated and laying down positions. However, the overtight condition demonstrated that in theory $SpO_2$ readings in the >90% range could be obtained from a chest mounted probe in line with those of a conventional finger probe. The overtight condition saw the best results during pilot testing readings comparable with or in many cases better than the taped condition [fig. 19]. During pilot testing the "overtight" condition was defined by cinching the pulse oximetry sensor belt to the point of wearer discomfort, which is the condition that [fig. 19] was evaluated in.

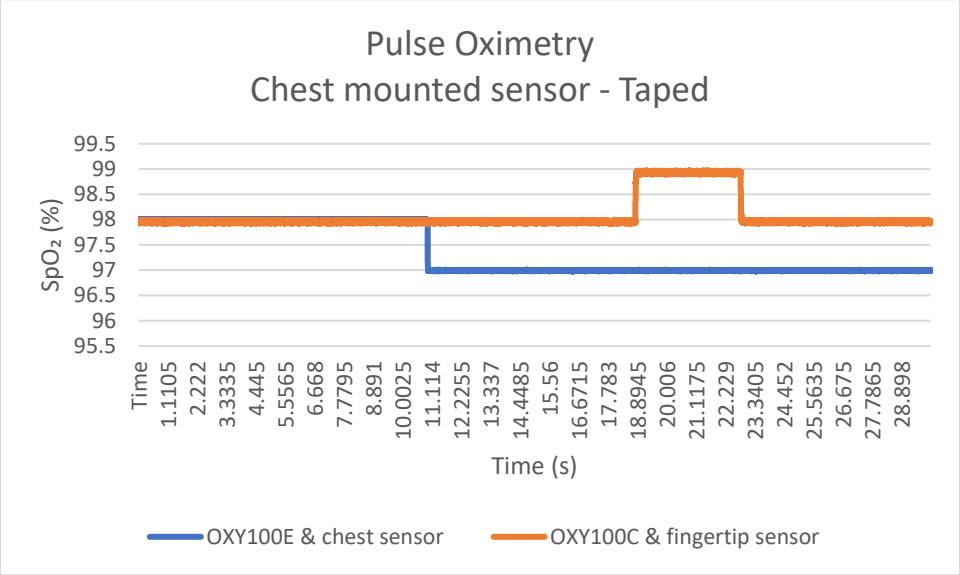


*Figure 18. Graph of $SpO_2$ sensor readings from the chest sensor and fingertip sensor in a taped condition.*

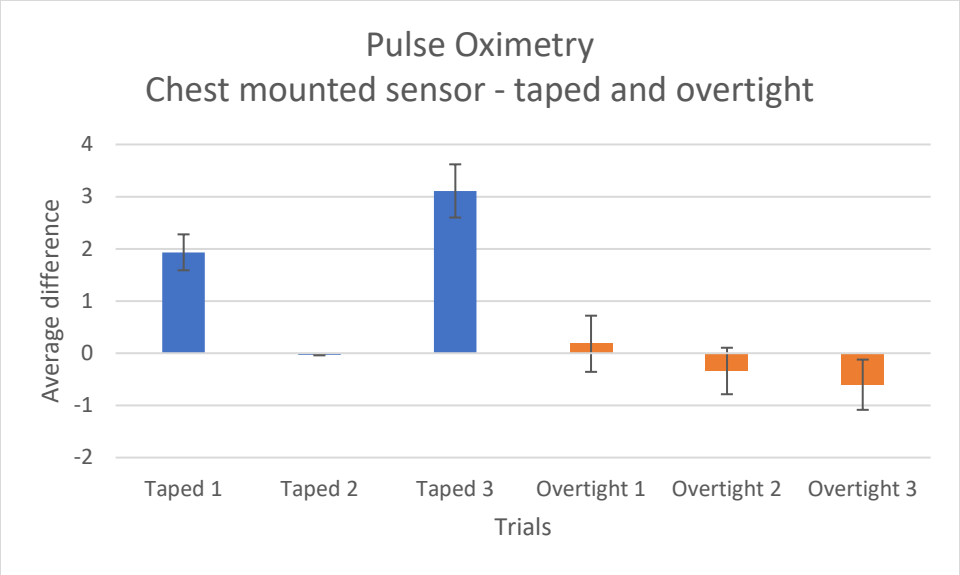


*Figure 19. Graph of average difference of the chest mounted sensor in taped and overtight conditions.*

*Summary*

As a result of insight gained from pilot testing the final study device and study parameters were determined. An elastic backing was applied to the respiration sensor to reduce oversaturation of the sensor, the adapted pulse oximeter probe was validated for use mounted on the chest, and the sizing variables for the base and tight conditions were established. To understand the effect of sizing and fit for both respiration and pulse oximetry sensors the sensor belt was tested in a base condition equal to the participant's circumference at the armpit level of the upper chest (the level at which the manubrium is generally located) at rest, and a tight condition that is two inches smaller that the base circumference.

### 3.4 Final study device

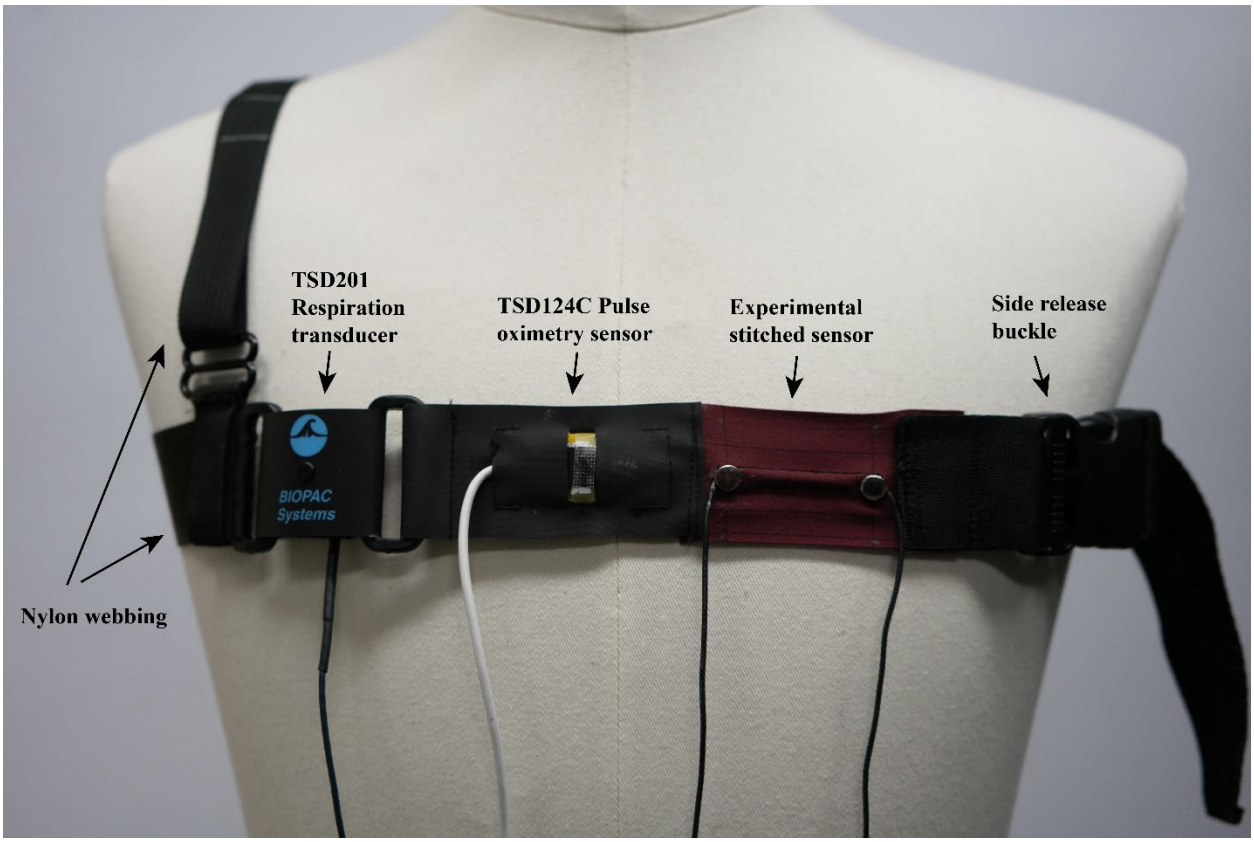


*Figure 20. Figure of final prototype used for the study on a mannequin.*

The final prototype used for the study took the form of a belt with all of the sensors integrated in such a way to make it simple to resize and adjust for each participant. The base belt is comprised of 1.5-inch-wide nylon webbing to which the sensor array was sewn on to using a standard lockstitch sewing machine [fig. 20]. The Biopac TSD201 transducer (respiration), Biopac TSD124C (pulse oximetry), and stitched sensor were arranged and sewn into an array before being sewn to the nylon webbing. A side release buckle was added for adjustability of the belt and to serve as a closure. The TSD124C pulse oximeter transducer presented a unique challenge in developing a way to integrate it with the rest of the sensor belt. Due to the rigid 3D printed housing and lack of attachment points, a small enclosure was developed to hold the sensor in place. The enclosure was made using an inextensible textile with two small sections of elastic sewn to it to create a “pocket” that the 3D printed housing could be nested into, to hold it in place without obstructing the emitter and receiver of the transducer. A small hole was cut in

the textile to allow for the transducer cable to be routed to the outside for unobstructed interfacing with the MP160 hardware.

An additional 1-inch nylon webbing strap was attached to the belt with a triglide buckle for adjusting the strap (not pictured) and a triglide bar to anchor it to the belt. This strap was added to prevent the belt from slipping down the body during study trials. Prior to the start of the study the participant was asked to change into a tank top shirt to allow access to the upper chest where the sensors were placed. Then the sensor belt was adjusted to the appropriate size based on the participants measurements and donned at the upper chest level so that the TSD124C sensor was at the height of the manubrium during testing.

### 3.5 Research study design

In this study participants were recruited to evaluate a stitched respiration sensor and chest mounted pulse oximeter probe to investigate the sensors potential for use in a wearable respiratory health monitoring device.

*Participants*

A group of 12 participants were recruited and consented into the study, following the protocol approved by the UMN IRB. Inclusion criteria were: 18-45 years of age, fit a woman's size small, medium, or large fitted shirt, have no history of chronic respiratory disorders (ex. asthma or COPD), and are not currently experiencing symptoms of or diagnosed with a respiratory disorder.

*Study variables*

In this study both respiration and pulse oximeter sensors were tested to observe the responsiveness of the sensors and the impact of sizing and fit on the performance of the sensors. The variables for each sensor are described in the following sections:

*Respiration variables*

To investigate the stitched sensor's ability to detect respiration rate (rr), the stitched respiration sensor was compared with the Biopac TSD201 respiratory effort transducer. The circumference of the sensing band was treated as an independent variable which was adjusted for each participant based on their individual measurements. The resulting strain response and respiration rate are the dependent variables as the fit of the sensing band influences sensor

performance. Both sensing bands were tested simultaneously with the following conditions: sensor/garment fit (circumference in in/cm) and type of breathing.

Sensor fit is tested in two fit conditions, the participant's normal resting circumference at the upper chest, and then again by subtracting two inches from the base circumference as determined by previous pilot testing. The circumference of the sensor band is recorded and set to match before donning.

*Table 1. Table of respiration sensor variables*

| **Respiration variables** | | |
|---|---|---|
| **Independent Variables** | **Sensor band fit** | |
| **Dependent Variables** | Base circ. | Tight circ. (base circ. minus 2 inches) |
| Respiration rate (rr) | | |
| Coefficient of determination (r-squared value) | | |

*Pulse Oximetry variables*

To investigate the pulse oximeter probe's ability to sense blood oxygen ($SpO_2$) and heart rate (beats per minute or BPM), the chest mounted TSD124C flex wrap transducer was compared with the TSD123A $SPO_2$ fingertip transducer.

*Table 2. Table of chest-mounted pulse oximeter variables*

| **Independent Variables** | **Sensor band fit** | |
|---|---|---|
| **Dependent Variables** | Base circ. | Base circ. minus 2 inches |
| Dropout rate | | |
| Coefficient of determination (r-squared value) of SpO2% with Biopac fingertip sensor | | |
| Average difference and standard deviation of | | |

| | | |
|---|---|---|
| SpO2% values as compared to Biopac fingertip sensor | | |
| Average difference and standard deviation of Beats-per-minute (BPM) as compared to Biopac fingertip sensor | | |

*Study Procedures*

Prior to the start of the study, informed consent was obtained from each participant. The measurement of the upper chest was taken with a soft tape measure and recorded, then two inches were subtracted from this measurement and recorded. The participant was then instructed to sit in a backed chair with both feet on the ground and arms at rest on their laps. Once the participant indicated they were ready, the researcher gave a five second countdown before each trial began. The participant was asked to breathe normally for five breaths, hold their breath for 10 seconds, and then take five more breaths for each trial. Three trials were recorded for both fit conditions for a total of six trials per participant.

### 3.6 Data analysis

Data analysis took place in AcqKnowledge (Biopac Systems Inc.) and Microsoft Excel (Microsoft). All data was initially collected in AcqKnowledge then exported as a *.xls file for further processing in Excel.

*Participant data*

The base circumference was gathered from each participant by measuring their upper chest at the armpit level while at rest. To determine the tight circumference two inches were subtracted from the base circumference based on findings from pilot testing.

### Respiration

*Coefficient of determination*

Linear regression analysis was performed in Microsoft Excel to measure the variance in analog respiration responses between the two sensors. The r-squared coefficient of determination

was calculated for the full respiration dataset as well as with the breath hold section removed. In the breath hold removed dataset, the breath hold section was segmented and analyzed separately from the full respiration data set. This separate analysis was done as it was found that the sensors drifted non-uniformly during the breath hold section which affected the resulting r-squared values due to the different sensor response. To extract the breath hold section, the timestamps for the start and end of the breath hold section were identified in AcqKnowledge file, then the corresponding data was eliminated from the data in Excel. A linear regression was then performed on the new dataset. For both datasets, the experimental stitch sensor served as the y-value and the Biopac TSD201 transducer as the x-value.

*Breathing frequency analysis*

Breathing frequency was calculated via the peak detector function in AcqKnowledge 5.0. The algorithm was calibrated by identifying and selecting the smallest peak within a given respiration sensor's data channel. This peak was used to establish the minimum voltage used as the peak detection threshold that was then used to automatically find all peaks at or above the set minimum threshold in the channel. The same procedure was used for each respiration sensor data channel (experimental and reference sensors) for each trial and fit condition for all participants. For this study, the algorithm's ability to detect the breaths from the sensors (represented by peaks) was investigated, and beyond the identification of the smallest peak by the researcher no other refining was applied to the peak detector before running the program. The goal of this was to understand what registered as a "breath" and how many were detected by the software rather than what was the "correct" number of breaths to simulate how a stitched sensor integrated into a garment might behave on users in a non-clinical environment. The AcqKnowledge derived breathing frequency values for both the stitched sensor and Biopac TSD201 transducer were then compared against the "actual" number of breaths which were manually counted by the researcher.

*P12 case study*

In contrast to the fit conditions for participant's 1-11, P12 was evaluated by calibrating the Biopac TSD201 sensor following Biopac guidelines for the sensor. The TSD201 transducer was removed from the sensor belt and calibrated separately by having the participant exhale completely and then adjusting the provided extensible nylon strap so that it was snug on the body

and in no way loose in the exhaled state. The full study procedure was then repeated keeping the TSD201 sensor at the same circumference and only manipulating the circumference of the stitched sensor. This is discussed more in-depth in the discussion section with the respiration results.

**Pulse oximetry**

*Dropout rate*

The pulse oximetry data was first analyzed to determine the dropout rate of the experimental sensor compared to the reference sensor for both the $SpO_2$ and BPM data. Sensor dropout was calculated using the =IF and =SUM functions in Excel. The =IF function was used to make a logical TRUE/FALSE comparison to determine if any given data point is dropped out or not. For $SpO_2$ values, dropped out data was defined as TRUE = if blood oxygen saturation was within a 0-100 range as detected by the sensor and returned as a "0" and FALSE = blood saturation above the 121 range as detected by the sensor and returned as a "1". During pilot testing it was noted that when the chest mounted sensor lost contact with the body, or was otherwise obstructed, the value displayed in AcqKnowledge at approximately 127%. As a result a cutoff of 121 was applied to the $SpO_2$ values to flag invalid data points. The dropout was then calculated in a percentage using the =SUM function, which is used to add values, in this case the values calculated by the =IF function.

These formulas were applied to each data point in the data column for both the experimental chest sensor and the reference fingertip sensor for each trial and participant. The dropped-out portions of the experimental sensor data were then extracted, and the valid data analyzed separately with a linear regression to find the coefficient of determination between the two sensors with the chest probe sensor serving at the y-value and fingertip sensor as the x-value.

*Average difference and standard deviation*

To understand how similar the $SpO_2$ and BPM values were between the two sensors the average difference and standard deviation were calculated in Excel. The difference was calculated by subtracting the experimental sensor data points from the reference sensor data points, then the average was calculated from the differences. The standard deviation was calculated from the difference values using the =STDEV.P function for each trial and participant.

# 4. Results

Data analysis was split into two categories, respiration and pulse oximetry. For respiration, the stitched sensor was compared against the Biopac reference sensor to determine their relationships for breathing frequency error and coefficient of determination measures between the sensor signals in both fit conditions. For pulse oximetry, the chest probe sensor was compared against the reference sensor to determine their relationships for $SpO_2$% coefficient of determination, $SpO_2$% dropout percentage, $SpO_2$% average difference and standard deviation, and BPM average difference and standard deviation. Additional respiration graphs can be found in Appendix A and pulse oximetry graphs in Appendix B.

## 4.1 Participant data

*Participant measurements*

*Table 3. Table of participant base and tight circumferences in inches rounded to the closest 1/8th of an inch.*

| Participant number | Base circumference (inches) | Tight circumference (inches) |
|---|---|---|
| **P1** | 34 | 32 |
| **P2** | 33.25 | 31.25 |
| **P3** | 33.75 | 31.75 |
| **P4** | 35.5 | 33.5 |
| **P5** | 33.5 | 31.5 |
| **P6** | 39.25 | 37.25 |
| **P7** | 38.5 | 36.5 |
| **P8** | 32 | 30 |
| **P9** | 35 | 33 |
| **P10** | 36.625 | 34.63 |
| **P11** | 36.25 | 34.25 |
| **P12** | 34.5 | 32.5 |

## 4.2 Respiration data

Below are two examples of time-series graphs demonstrating worst [fig. 21] and best [fig. 22] case scenarios for the respiration sensors in both fit conditions.

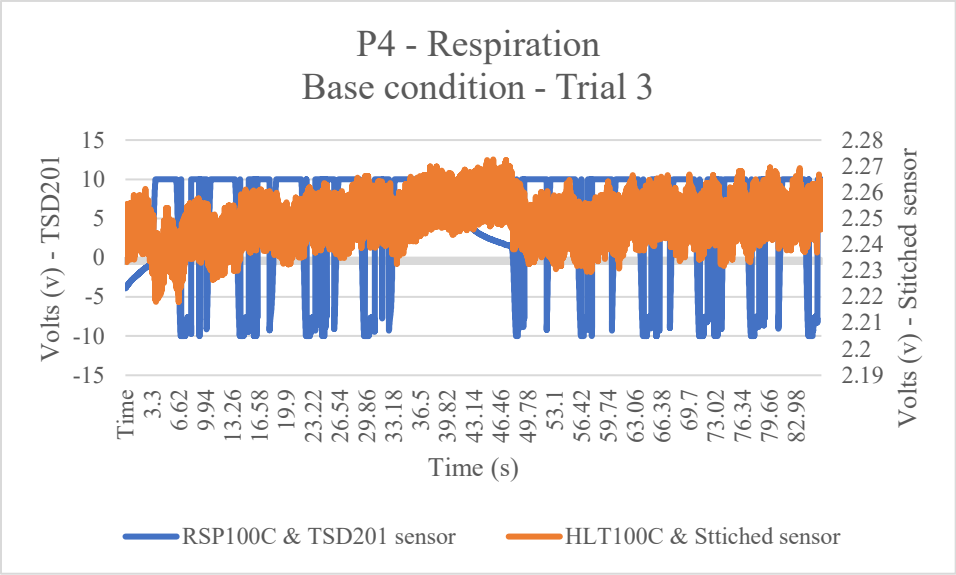


*Figure 21. Time-series graph of P4 base condition trial depicting a "worst-case" scenario in which only two breaths were detected for the stitched sensor and 68 were detected for the Biopac TSD201 sensor.*

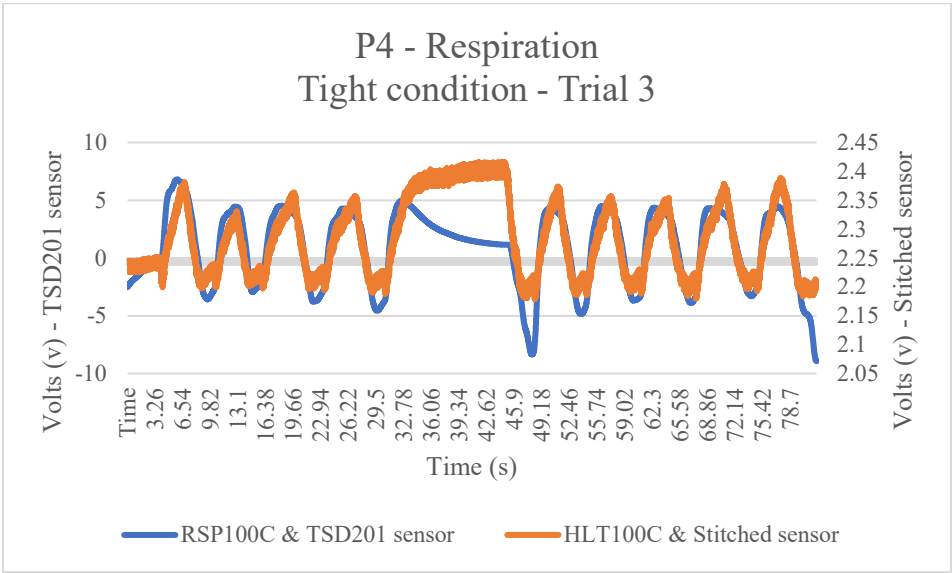


*Figure 22. Time-series graph of P4 tight condition trial depicting a "best-case" scenario with both the stitched sensor and Biopac TSD201 sensor in which both sensors detected ten breaths, the same as the number of manually counted breaths.*

*Coefficient of determination*

The full respiration dataset required no additional processing, and a linear regression analysis was run with the experimental stitched sensor as the X variable and reference sensor as the Y variable for each participant. The breath hold removed dataset was further processed by identifying the timestamps of the breath hold section in each AcqKnowledge file and removing it from the data in Excel. A linear regression in the same manner as the full dataset was then performed. The resulting data was then averaged for both fit conditions across all trials and participants.

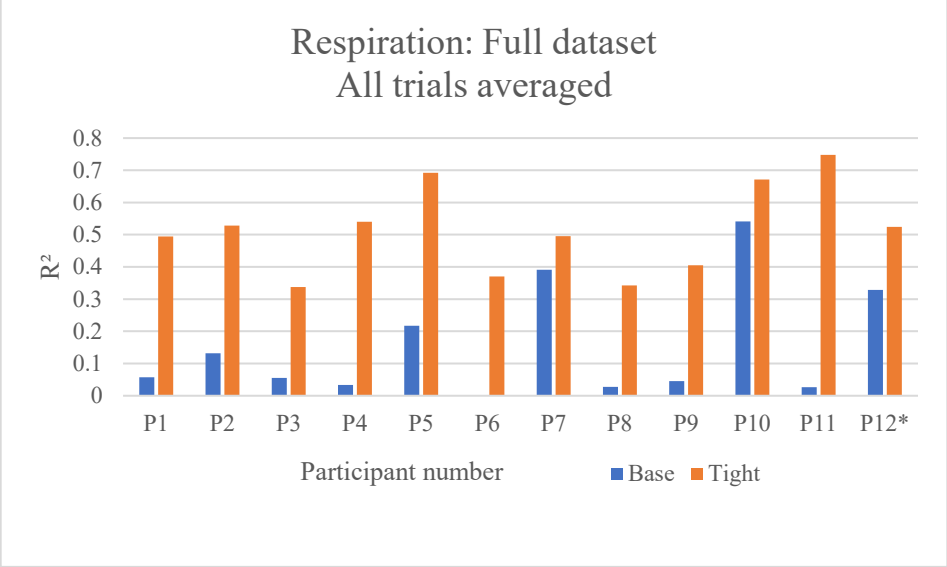


*Figure 23. Graph of coefficients of determination (r-squared values) for full respiration dataset with all trials averaged for each participant.*

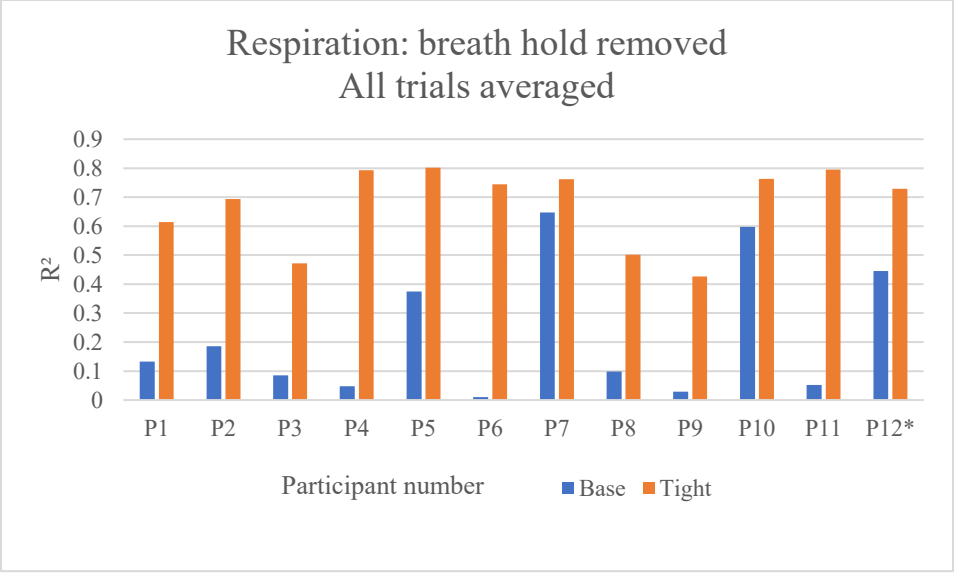


*Figure 24. Graph of coefficient of determination (r-squared values) for breath hold removed respiration dataset with all trials averaged for each participant.*

*Breath frequency*

Breathing frequency error was extracted from the AcqKnowledge peak detector and the average difference and standard deviations were calculated in Excel. The stitched and Biopac

values were subtracted from the manually counted number of breaths for each trial and condition and then all trials averaged for both fit conditions across all participants.

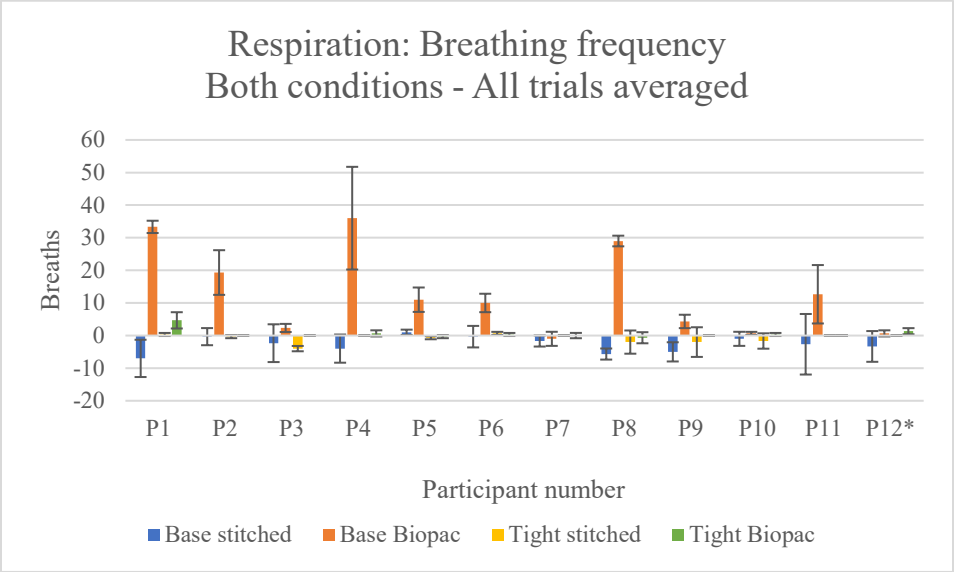


*Figure 25. Graph of average difference and standard deviations of breathing frequency for both experimental stitched sensor and Biopac reference transducer in both fit conditions (difference in breath frequency detected by the AcqKnowledge peak detector compared with the actual number of breaths manually counted, and all trials averaged for each participant).*

### 4.3 Pulse oximetry data

Below are two time-series graphs showing examples of worst [fig. 26] and best [fig. 27] case scenarios for the chest mounted pulse oximetry sensor in both base and tight conditions.

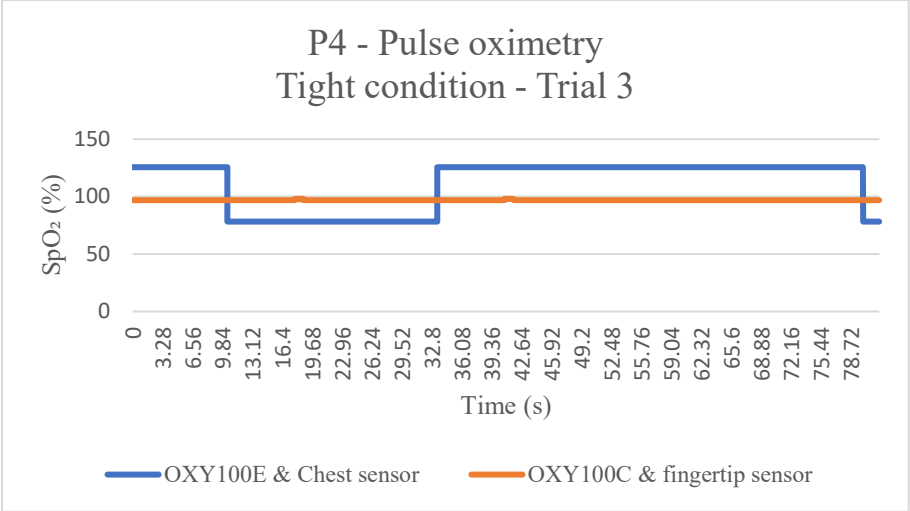


*Figure 26. Time-series graph of a worst-case scenario with the chest sensor with a 69.71% dropout rate from participant 4 who had the greatest amount of dropout averaged across all participants in the tight fit condition [fig. 21].*

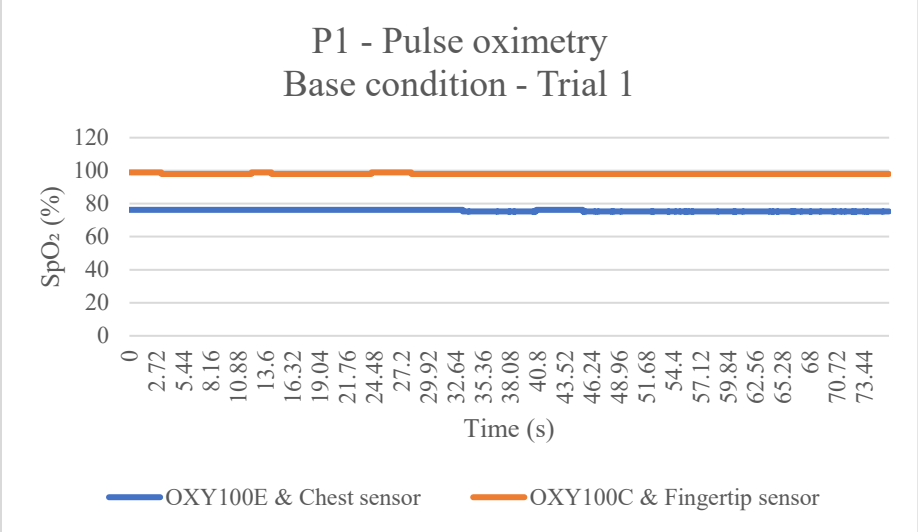


*Figure 27. Time-series graph of a best-case scenario with the chest sensor with a 0% dropout rate from participant 1 who had the least amount of dropout averaged across all participants in the base fit condition [fig. 28].*

### *Dropout rate*

The dropout rate of the $SpO_2$ data was calculated in Excel by identifying the dropped-out sections of the data, indicated by value exceeding 121% $SpO_2$ and calculating the percentage of data that was dropped out. This was done only for the chest probe sensor as the fingertip sensor

displayed no dropped out values. The resulting data was then averaged for both fit conditions across all trials and participants.

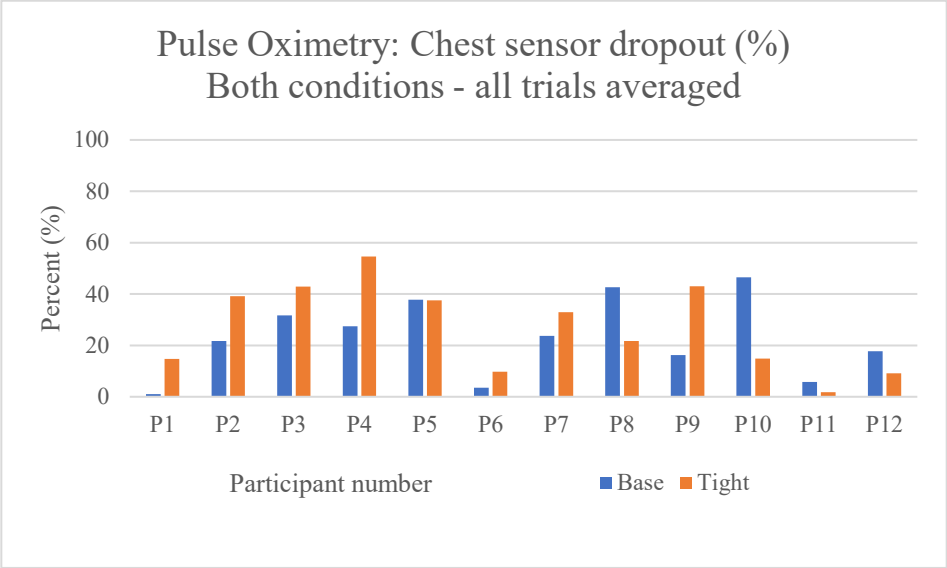


*Figure 28. Graph of chest probe sensor dropout rate of $SpO_2$ values for both fit conditions with all trials averaged for each participant.*

### *$SpO_2$ coefficient of determination*

The $SpO_2$ data with the dropout removed was then used to run a linear regression analysis with the chest probe sensor as the X variable and reference fingertip sensor as the Y variable for each participant and trial. The resulting data was then averaged for both fit conditions across all trials and participants.

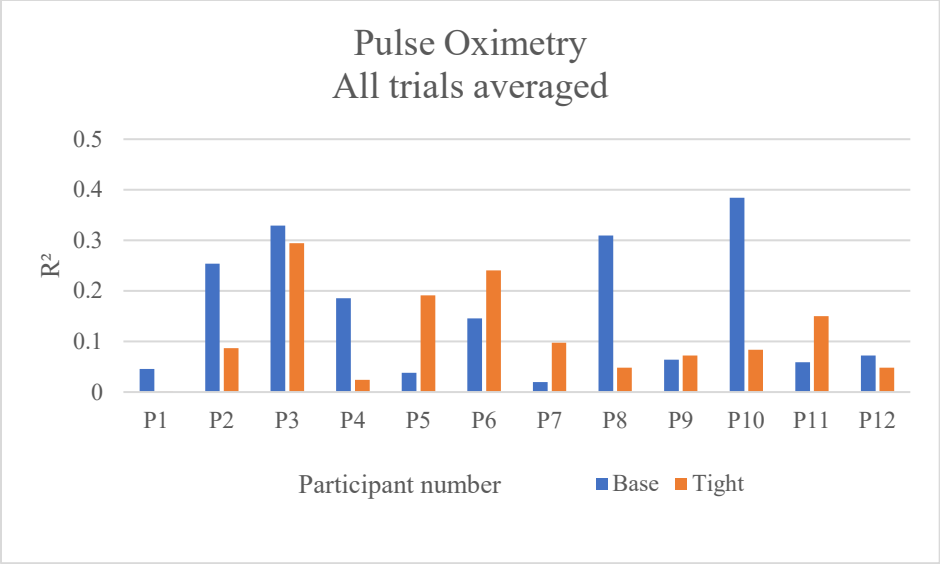


*Figure 29. Graph of coefficient of determination (r-squared values) for pulse oximetry $SpO_2$ values with dropped out data removed, and all trials averaged for each participant.*

### *$SpO_2$ average difference and standard deviation*

The average difference and standard deviations for the $SpO_2$ values were calculated from the dropout removed dataset. The difference was taken between the fingertip sensor values and the chest probe sensor values from which the average and standard deviations were calculated. The resulting data was then averaged for both fit conditions across all trials and participants.

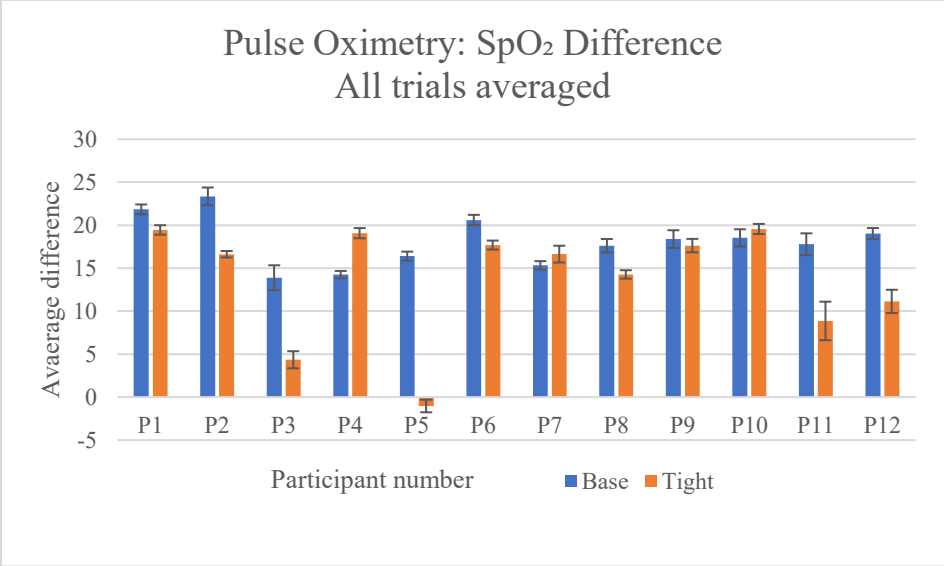


*Figure 30. Graph of average difference and standard deviations of $SpO_2$ values with dropped out data removed, and all trials averaged for each participant.*

*BPM average difference and standard deviation*

The average difference and standard deviations for the BPM values were calculated from the dropout removed dataset. The difference was taken between the fingertip sensor values and the chest probe sensor values from which the average and standard deviations were calculated. The resulting data was then averaged for both fit conditions across all trials and participants.

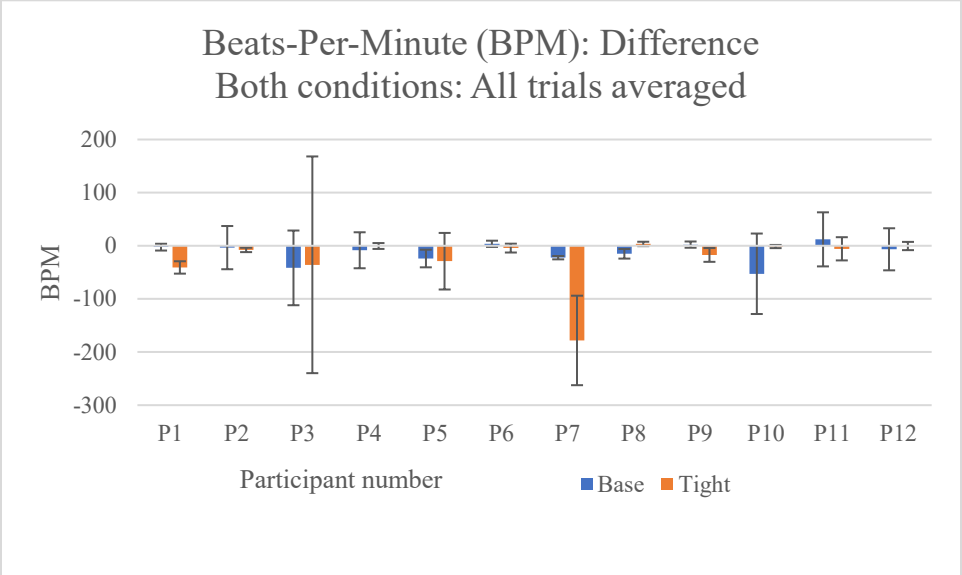


*Figure 31. Graph of average difference and standard deviations of chest probe BPM values with dropped out data removed, and all trials averaged for each participant.*

# 5. Discussion

## 5.1 Respiration

The stitched sensor performed the best in the tight fit condition in all metrics with an average of -0.81 ±1.29 breaths of breathing frequency error [fig. 25], 0.51 ±0.13 coefficient of determination for the full dataset [fig. 23], and 0.67 ±0.13 coefficient of determination for the breath hold removed dataset [fig. 24], averaged across all participants. Most r-squared values fell between 0.6-0.8. The base condition demonstrated a weaker relationship between the stitched sensor and the reference sensor, with an average coefficient of determination of 0.15 ±0.17 for the full dataset and 0.22 ± 0.22 for the breath hold removed dataset. However, although less accurate than in the tight condition, the stitched sensor still outperformed the Biopac TSD201 reference sensor for breathing frequency measures in the base condition, with an average error of -2.70 ±2.30 breaths compared to the Biopac sensor's average error of 13.20 ±12.71 breaths. The breathing frequency error data [fig. 25] shows that breaths detected by the AcqKnowledge peak detector function for the stitched sensor were typically more consistent with manually counted breaths than the Biopac reference sensor. The TSD201 uses a pressure-based sensor to detect the change in circumference of a wearer while breathing, and as a result is more susceptible to false positives when inappropriately sized which is most evident in participants 1, 4 and 8. Participant 4 saw the highest number of miscounted breaths in the base condition in trial 3 with 68 detected breaths compared to the 10 manually counted breaths. These results lead to a case study in which the Biopac reference sensor was appropriately calibrated separately from the sensor belt as described below (P12 case study).

*P12 case study*

After the initial study of P1-P11 it was observed that the Biopac TSD201 sensor performed poorly compared to the stitched sensor and manually counted breaths in the breathing frequency measure. During the testing of P1-P11 the Biopac sensor was included in the same sensor array as the stitched sensor to observe the effect of the two fit conditions in sensor performance. However, the TSD201 measures respiration using a pressure-based sensor and as a result the data, particularly in the base fit condition, was subject to a large amount of error as the sensor came in and out of contact with the participant's body during breathing as a result of the sensor belt's inextensible band resting loosely on the body during exhalation. When the

AcqKnowledge peak detector function was run on resulting data, the sharp spikes [fig. 21] in the data waveform were detected and identified as “breaths.” To better understand how the Biopac sensor compared to the stitched sensor in ideal conditions the TSD201 sensor was calibrated according to Biopac best practices which involved having the participant exhale completely and tightening the extensible nylon belt so that it was always slightly undersized on the participant’s chest. Then the full study was performed again with the Biopac sensor remaining the same circumference and only the stitched sensor was manipulated. This resulted in better results for the Biopac sensor with an average error of $0.71 \pm 0.94$ in the base condition. When compared to the stitched respiration sensor, the average error for the properly calibrated Biopac reference sensor was nearly the same as the stitched sensor in the tight condition (breathing frequency error of $-0.81 \pm 1.29$).

Overall, the stitched sensor consistently performed better in the tight condition compared to the base condition across all metrics. While the coefficient of determination for both respiration datasets [fig. 23]-[fig. 24] did not show a strong relationship between the two sensors, it is likely due to the two sensors drifting differently than each other during the static load during the breath hold section [fig. 22]. However, when it came to the breathing frequency measure, the stitched sensor performed just as well or better than the Biopac TSD201 sensor indicating that the stitched sensor is less sensitive to error due to fit than the Biopac reference sensor These results demonstrate a need for careful consideration of device sizing and sensor anchoring to ensure the best possible readings in worn systems. Based on the above results it can be reasonably assumed that undersized wearable devices akin to compression garments are more likely to perform favorably than non-compression garments in regard to respiration sensing.

### 5.2 Pulse oximetry

The pulse oximetry probe sensor mounted on the chest was generally able to detect $SpO_2$ levels and BPM values, however when compared to the reference finger probe its reliability and accuracy suffered. Compared to the 0% dropout rate of the fingertip reference sensor the chest mounted sensor saw an average dropout rate of 22.1% ±14.4% in the base condition and 26.85% ±16.19% in the tight condition [fig. 28]. Some instances saw a minimal dropout as low as 1.08% in the case of P1 in the base condition, to dropout as high as 54.62% in the case of P4 in the tight condition, which demonstrated that fit did not seem to have a notable impact on sensor dropout.

The exact reasons for sensor dropout are not known, but sensor band drift during trials and other motion artifacts were likely contributors. While the base condition had less average dropout across all participants, it was still similar to that of the tight condition.

The chest mounted sensor showed poor correlation with the fingertip sensor [fig. 29] with all $r^2$ values <0.5 in both fit conditions. The chest mounted sensor saw an average coefficient of determination of 0.16 ±0.12 in the base fit condition and 0.11 ±0.08 in the tight fit condition. Fit did not seem to have a notable effect on the $SpO_2$ readings with the base condition having better results than the tight condition by a very slim margin.

When it came to the average difference between the $SpO_2$ values, the chest sensor's $SpO^2$ values were often quite different from the reference sensor values, varying as little as -1.03275 for P5 in the tight condition and as much as 23.34411 for P2 in the base condition [fig. 30]. The average difference was largely steady between the fingertip and chest sensor with an average difference of 18.08 ± 2.77 in the base condition and 13.7 ±6.32 in the tight condition when averaged across all participants. BPM measures values [fig. 31] also differed from their reference sensor counterparts with average differences of up to -178.18 ± 84.21 in the case of P7 at worse and 3.71 ± -4.39 at best for P6 [fig. 31]. Like the above $SpO_2$ average difference measure, the BPM average difference measure was also largely steady with and average difference of -13.25± 18.27 in the base fit condition and -26.49 ± 47.91 in the tight fit condition when averaged across all participants. Like the coefficient of determination measure for the chest mounted pulse oximeter, fit did not seem to have a noticeable impact on sensor performance, with both fit conditions demonstrating large amounted of error compared to the reference sensor.

One potential reason for the amount of error demonstrated by the chest mounted sensor is the algorithm used to derive these measures in the AcqKnowledge software. Both the $SpO_2$ and BPM measures are extracted from the raw signal using undisclosed proprietary algorithms that pre-condition the waveform [84], and as aggregate measures they likely involve a moving average or sliding window approach that would be influenced by dropped-out data. As a result, it is difficult to determine how error and/or dropout affects the resulting values with the algorithm used by AcqKnowledge. Another potential factor is that the sensor is calibrated for use on the finger which has more perfuse blood vessels compared to that of the chest. This error in part

could be alleviated with a sensor properly calibrated for reflectance pulse oximetry sensing which does not rely on the thin tissues like that of transmissive pulse oximetry sensing. With an appropriate sensor developed with reflectance sensing in mind and an appropriate algorithm that accounts for dropped out data to normalize the difference measures, it could be possible for the sensor to detect values closer to those of the fingertip sensor.

*Summary*

Generally, both the stitched sensor and chest mounted pulse oximeter sensor both able to detect their respective measurements to a degree. Between the two experimental sensors, the stitched sensor performed the most similarly to its respective reference sensor, particularly in the tight fit condition, and better than the reference sensor in the base condition in the case of breathing frequency under sub-optimal fit conditions [fig. 25]. It was observed that the smaller the sensor belt circumference relative to the wearer's base circumference, the better quality of signals were obtained from the stitched respiration sensor, however diminishing returns on sensor quality was observed when the sensor was extremely undersized [fig. 17] with the sensor signal flattening out and causing pain and discomfort to the wearer. The stitched sensor demonstrated error similar to human counting error of manually counted breaths which typically falls within a 2-6 miscounted breaths-per-minute [38]-[85]. The base condition had an average of -4.50 miscounted breaths, putting it close to the higher end of human error. This demonstrates that in a looser fit condition the stitched sensor is still able to detect breaths comparable to that of a trained individual and better than the mis-calibrated Biopac reference sensor with an error of 22.1 miscounted breaths. The tight fit condition performed better with an average of -1.34 miscounted breaths, demonstrating that it can perform within the limits of manual counts by trained individuals and on par with the Biopac sensor in the tight condition which had 0.91 miscounted breaths. These results indicate that the sensor has potential to perform as well as trained individuals in both fit conditions in its current state.

The chest mounted pulse oximeter was able to detect $SpO^2$ and BPM measures, but when compared to the reference fingertip sensor it did not perform nearly as well in either fit condition. There was significant dropout in both conditions [fig. 28] and the $SpO_2$ values were poorly correlated with the reference sensor with all r-squared values $<0.5$ for both fit conditions

[fig. 29]. The average difference values for both $SpO_2$ and BPM also showed fairly large differences compared to the reference sensor. It is likely that the pulse oximetry data was highly influenced in part by the dropped-out data due and the algorithms used to derive high-level measures in AcqKnowledge. The missing data points potentially influenced these derivative measures, particularly if a moving average method is employed. It is possible that an appropriate algorithm capable of taking dropped out values into account was deployed for the pulse oximetry data, the resulting derived measures may have been improved. In its current form the chest mounted pulse oximeter sensor is poorly suited for use in a wearable system.

All of these results demonstrate the challenges inherent to developing garment-based sensing devices, from the sizing considerations down to the algorithms used to filter and process resulting data. The stitched sensor performed the best in the tight condition, while the pulse oximeter sensor's results were much more mixed with no fit condition performing significantly better than the other. Tradeoffs of absolute accuracy of a device and the comfort of the wearer must be considered, particularly if a device is intended for daily medium to long term use

# 6. Conclusion

This research investigated the use of a stitched sensor and chest mounted pulse oximeter for the purpose of sensing and monitoring respiratory health metrics. This was accomplished by integrating the stitched respiration sensor and chest mounted pulse oximeter sensor into an adjustable belt to test the device in two fit conditions: a base fit condition, which refers to the resting circumference of an individual at the armpit level on the upper chest, and a tight fit condition which is the base fit condition minus two inches. A set of reference sensors (pulse oximetry measured from the traditional fingertip location and a commercial chest-mounted respiration sensor) were also evaluated, with the respiration sensor tested in the same two fit conditions as well as a single case-study trial with the sensor calibrated according to the manufacturer's instructions. This was done to evaluate the impact of fit and sizing on the performance of the sensors in the two fit conditions, as compared to the performance of the reference sensors.

Due to the difference in the direction of drift of the sensor's signals, the stitched sensor showed poor correlation with the Biopac reference sensor. However, the stitched sensor performed better in the breathing frequency measure with the base fit condition having an average of -4.50 miscounted breaths-per-minute, similar to that of manually counted breaths (error of 2-6 breaths-per-minute), and the tight condition with an average of -1.34 miscounted breaths-per-minute. In clinical settings respiration error can vary widely due to the nature of manual counting by an observer to derive rr. As a result, due to lack of time or staffing the reported rr is often clustered around the 18-20 range even if the patient is already showing signs of tachypnea, or is in crisis shortly after [38]-[86]. This indicates that there is a need for more automated monitoring of rr in clinical settings to assist hospital staff. The stitched sensor demonstrates an ability to accurately detect respiration rate, however additional testing and development is needed before it can be used in hospital settings. In the short term the sensor needs to be evaluated to assess the effects of other variables that may influence accuracy, such as different body postures and activity positions such as laying down or quiet sitting tasks (as common in hospital bed settings). Additionally, characterization of the sensor and elastic are needed to investigate the effect of textile and material choices needed to develop a robust sensor.

The chest mounted pulse oximeter sensor had far more mixed results when compared to the fingertip reference sensor. The chest sensor was prone to dropout and both fit conditions had poor correlations with the fingertip sensor with all chest sensor $r^2$ values <.5. The average difference in $SpO_2$ and BPM values of the chest sensor was largely steady across both fit conditions, but the measures still showed a large variance in values compared to the fingertip sensor with an average difference of 15.90% ±5.35 across all participants and fit conditions for the $SpO_2$ values, and -19.91 ±36.95 for the BPM values. FDA cleared pulse oximeters can have up to a 2-3% variance in values, which can result in an approximately ±4 difference in $SpO_2$%[52] at most. The average differences output by the chest mounted sensor are much greater than the acceptable 2-3%. The fit conditions did not seem to have a notable effect on sensor readings with both fit conditions performing better in different metrics, and the base fit condition often outperforming the tight fit condition.

While some of the poor performance of the adapted sensor can potentially be attributed to the sensor being calibrated for use as a transmissive-style pulse oximeter and the proprietary algorithms used to derive the $SpO^2$ and BPM values in AcqKnowledge, the study results show that chest mounted pulse oximetry, while possible, still requires a great deal of work. If a pulse oximeter is to be developed for sensing at the chest, substantial work is required to improve sensor performance. First steps toward developing a more accurate chest mounted pulse oximeter include adapting or fabricating a pulse oximeter sensor specifically intended for reflectance-based sensing. An appropriate algorithm for filtering the pulse oximeter data is also crucial to test if a different method of deriving $SpO_2$ and BPM values from the raw signal that considers the effect of sensor dropout on the values. Once a more robust sensor is developed, future testing can be done to assess accuracy of the sensor with the wearer at rest before moving to more dynamic movement.

Of the two sensors, the fit of the sensor belt most influenced the stitched respiration sensor. The stitched sensor performed as well or better than the Biopac reference sensor in the base fit condition with the stitched sensor showing an average -2.70 ± 2.30 breaths of breathing frequency error, while the tight fit condition showed a smaller average error of -0.80 ± 1.30 breaths. These results indicate that fit and sizing does have an impact on respiration sensor performance. Future work on fit and sizing for the respiration sensor should focus on

understanding how the sensor performs during different activity conditions such as laying down, standing up, or performing quiet tasks as dynamic postures and movement can affect body measurements like length and circumference. If the sensor is to be used during normal daily life, it must be able to perform similarly in different activities and postures typical of activities of daily living. Additionally, in this study the sensor circumference was carefully controlled by sewing it to an inextensible webbing band. Future work should look to understand how the sensor performs in a more garment-like form factor and without the constraint imposed by the webbing that similar to that of a compression garment.

Limitations presented by this study include those of the participants and sensors themselves. A small number of participants (n=12) were recruited in limited range of sizes (fitted small, medium, and large shirt sizes), and gender of the participants (female-identified only). The knit jersey textile used to fabricate the stitched sensor was not characterized, nor the elastic used to back the sensor with a tensile testing machine, so the exact properties imparted by the textile and elastic is unknown. Related to both the participants and sensors, is that there is limited space available on the body at the upper chest to place sensors. In future iterations of this device, the optimization of the sensors, their required electronics and cables must be addressed to develop a smaller footprint on the body, however this is outside of the scope of this particular research.

This research found that a stitched respiration sensor can reliably detect respiration, and with careful consideration of fit and sizing during device development, a stitched sensor shows great promise. Reliable pulse oximetry at the chest however is more difficult to achieve and requires a different approach than taken with this research study. While there is evidence for pulse oximetry metrics being measured successfully at the chest, factors such as sensor type and appropriately calibrated algorithms are necessary to produce the best results irrespective of fit conditions. Sizing and fit should be carefully considered in future wearable sensor device development as it has the potential to affect not only the accuracy of the sensors, but also comfort of the user. While tighter fit conditions will result in better sensor signals (particularly for strain sensors) and more effectively hold sensors in place on the body, they can also cause discomfort to the point that users may inappropriately size the smart garment or abandon its use altogether. Therefore, future wearable devices must weigh the tradeoffs between absolute sensor

accuracy and its user population to ensure optimal sensor performance in a device that is tolerable for wearers during use.

## References.


[1] J. E. Hall, *Guyton and hall textbook of medical physiology*, 13th ed. London, England: W B Saunders, 2015.

[2] K. J. Mueller *et al.*, “After Hospital Closure: Pursuing High Performance Rural Health Systems without Inpatient Care,” p. 23.

[3] M. C. Garcia *et al.*, “Potentially excess deaths from the five leading causes of death in metropolitan and nonmetropolitan counties - United States, 2010-2017,” *MMWR Surveill. Summ.*, vol. 68, no. 10, pp. 1–11, 2019.

[4] J. C. NGAI, F. W. KO, S. S. NG, K. TO, M. TONG, and D. S. HUI, “The long-term impact of severe acute respiratory syndrome on pulmonary function, exercise capacity and health status,” *Respirology*, vol. 15, no. 3, pp. 543–550, Apr. 2010, doi: 10.1111/j.1440-1843.2010.01720.x.

[5] CDC, “Long COVID or post-COVID conditions,” *Centers for Disease Control and Prevention*. Dec. 2022. [Online]. Available: https://www.cdc.gov/coronavirus/2019-ncov/long-term-effects/index.html

[6] “COVID-19: Long-term effects,” *Mayo Clinic*. https://www.mayoclinic.org/diseases-conditions/coronavirus/in-depth/coronavirus-long-term-effects/art-20490351 (accessed Jan. 03, 2023).

[7] CDC, “COVID data tracker,” *Centers for Disease Control and Prevention*. Mar. 2020. [Online]. Available: https://covid.cdc.gov/covid-data-tracker/

[8] D. M. Mann, J. Chen, R. Chunara, P. A. Testa, and O. Nov, “COVID-19 transforms health care through telemedicine: Evidence from the field,” *J Am Med Inform Assoc*, vol. 27, no. 7, pp. 1132–1135, Jul. 2020, doi: 10.1093/jamia/ocaa072.

[9] L. E. Dunne and B. Smyth, “Psychophysical elements of wearability,” in *Proceedings of the SIGCHI Conference on Human Factors in Computing Systems - CHI ’07*, San Jose, California, USA: ACM Press, 2007, pp. 299–302. doi: 10.1145/1240624.1240674.

[10] F. Gemperle, C. Kasabach, J. Stivoric, M. Bauer, and R. Martin, “Design for wearability,” in *Digest of Papers. Second International Symposium on Wearable Computers (Cat. No.98EX215)*, IEEE Comput. Soc, 2002.

[11] N. E. Lange, M. Mulholland, and M. E. Kreider, “Spirometry: don’t blow it!,” *Chest*, vol. 136, no. 2, pp. 608–614, 2009.

[12] R. Ortega, C. Connor, S. Kim, R. Djang, and K. Patel, “Monitoring Ventilation with Capnography,” *N Engl J Med*, vol. 367, no. 19, p. e27, Nov. 2012, doi: 10.1056/NEJMvcm1105237.

[13] G. K. Wolf and J. H. Arnold, “Noninvasive assessment of lung volume: Respiratory inductance plethysmography and electrical impedance tomography,” *Critical Care Medicine*, vol. 33, no. 3, p. S163, Mar. 2005, doi: 10.1097/01.CCM.0000155917.39056.97.

[14] “Biosensor BX100,” *Philips*. http://www.usa.philips.com/en/healthcare/product/HC989803203011/biosensor-bx100-wearable-remote-measurement-device (accessed Feb. 27, 2022).

[15] “Philips launches next generation wearable biosensor for early patient deterioration detection, including clinical surveillance for COVID-19,” *Philips*. May 2020. [Online]. Available: https://www.usa.philips.com/a-w/about/news/archive/standard/news/press/2020/20200526-philips-launches-next-generation-wearable-biosensor-for-early-patient-deterioration-detection-including-clinical-surveillance-for-covid-19.html

[16] M. Ciocchetti *et al.*, “Smart textile based on fiber Bragg grating sensors for respiratory monitoring: Design and preliminary trials,” *Biosensors (Basel)*, vol. 5, no. 3, pp. 602–615, 2015.

[17] D. Lo Presti, C. Massaroni, P. Saccomandi, M. A. Caponero, D. Formica, and E. Schena, “A wearable textile for respiratory monitoring: Feasibility assessment and analysis of sensors position on system response,” in *2017 39th Annual International Conference of the IEEE Engineering in Medicine and Biology Society (EMBC)*, Jul. 2017, pp. 4423–4426. doi: 10.1109/EMBC.2017.8037837.

[18] J. De Jonckheere *et al.*, “OFSETH: smart medical textile for continuous monitoring of respiratory motions under magnetic resonance imaging,” *Annu. Int. Conf. IEEE Eng. Med. Biol. Soc.*, vol. 2009, pp. 1473–1476, 2009.

[19] J. Witt *et al.*, “Medical Textiles With Embedded Fiber Optic Sensors for Monitoring of Respiratory Movement,” *IEEE Sensors Journal - IEEE SENS J*, vol. 12, pp. 246–254, Jan. 2012, doi: 10.1109/JSEN.2011.2158416.

[20] L. Guo, L. Berglin, U. Wiklund, and H. Mattila, “Design of a garment-based sensing system for breathing monitoring,” *Textile Research Journal*, vol. 83, no. 5, pp. 499–509, Mar. 2013, doi: 10.1177/0040517512444336.

[21] C. F. Clarenbach, O. Senn, T. Brack, M. Kohler, and K. E. Bloch, “Monitoring of Ventilation During Exercise by a Portable Respiratory Inductive Plethysmograph,” *Chest*, vol. 128, no. 3, pp. 1282–1290, Sep. 2005, doi: 10.1378/chest.128.3.1282.

[22] P. Gupta, H. Wen, L. Di Francesco, and F. Ayazi, “Detection of pathological mechano-acoustic signatures using precision accelerometer contact microphones in patients with pulmonary disorders,” *Sci Rep*, vol. 11, no. 1, Art. no. 1, Jun. 2021, doi: 10.1038/s41598-021-92666-2.

[23] P. Gupta, Y. Jeong, J. Choi, M. Faingold, and F. Ayazi, “Precision high-bandwidth out-of-plane accelerometer as contact microphone for body-worn auscultation devices,” in *2018 Solid-*

*State, Actuators, and Microsystems Workshop Technical Digest*, San Diego: Transducer Research Foundation, 2018.

[24] A. Jin, B. Yin, G. Morren, H. Duric, and R. M. Aarts, "Performance evaluation of a tri-axial accelerometry-based respiration monitoring for ambient assisted living," *Annu. Int. Conf. IEEE Eng. Med. Biol. Soc.*, vol. 2009, pp. 5677–5680, 2009.

[25] F. Ernst and P. Saß, "Respiratory motion tracking using Microsoft's Kinect v2 camera," *Curr. Dir. Biomed. Eng.*, vol. 1, no. 1, pp. 192–195, 2015.

[26] P. Leonard, "Standard pulse oximeters can be used to monitor respiratory rate," *Emergency Medicine Journal*, vol. 20, no. 6, pp. 524–525, Nov. 2003, doi: 10.1136/emj.20.6.524.

[27] P. S. Addison, J. N. Watson, M. L. Mestek, and R. S. Mecca, "Developing an algorithm for pulse oximetry derived respiratory rate (RRoxi): a healthy volunteer study," *J Clin Monit Comput*, vol. 26, no. 1, pp. 45–51, Feb. 2012, doi: 10.1007/s10877-011-9332-y.

[28] "Masimo Announces FDA Clearance of RRp®, Respiration Rate from the Pleth, on the MightySat™ Rx Spot-Check Fingertip Pulse Oximeter," Jan. 28, 2019. https://www.businesswire.com/news/home/20190128005178/en/Masimo-Announces-FDA-Clearance-of-RRp%C2%AE-Respiration-Rate-from-the-Pleth-on-the-MightySat%E2%84%A2-Rx-Spot-Check-Fingertip-Pulse-Oximeter (accessed Aug. 11, 2023).

[29] "Respiration Rate from the Pleth (RRp® )," Masimo, Product Information. [Online]. Available: https://www.masimo.com/siteassets/us/documents/pdf/plm-12300a_product_information_respiration_rate_from_the_pleth_rrp_us.pdf

[30] "Masimo - Radius PPG Tetherless Pulse Oximetry." https://www.masimo.com/products/sensors/radius-ppg/ (accessed Aug. 11, 2023).

[31] *Forum of International Respiratory Societies. The global impact of respiratory disease*. European Respiratory Society, 2021.

[32] J. C. Ngai, F. W. Ko, S. S. Ng, K.-W. To, M. Tong, and D. S. Hui, "The long-term impact of severe acute respiratory syndrome on pulmonary function, exercise capacity and health status," *Respirology*, vol. 15, no. 3, pp. 543–550, 2010, doi: 10.1111/j.1440-1843.2010.01720.x.

[33] A. Nalbandian *et al.*, "Post-acute COVID-19 syndrome," *Nat Med*, vol. 27, no. 4, Art. no. 4, Apr. 2021, doi: 10.1038/s41591-021-01283-z.

[34] "Nearly One in Five American Adults Who Have Had COVID-19 Still Have 'Long COVID,'" Jun. 22, 2022. https://www.cdc.gov/nchs/pressroom/nchs_press_releases/2022/20220622.htm (accessed Jan. 02, 2023).

[35] L. Bull-Otterson *et al.*, “Post–COVID conditions among adult COVID-19 survivors aged 18–64 and \geq65 years — United States, march 2020–November 2021,” *MMWR Morb. Mortal. Wkly. Rep.*, vol. 71, no. 21, pp. 713–717, 2022.

[36] J. B. Scott and R. Kaur, “Monitoring Breathing Frequency, Pattern, and Effort,” *Respiratory Care*, vol. 65, no. 6, pp. 793–806, Jun. 2020, doi: 10.4187/respcare.07439.

[37] “Vital Signs (Body Temperature, Pulse Rate, Respiration Rate, Blood Pressure).” https://www.hopkinsmedicine.org/health/conditions-and-diseases/vital-signs-body-temperature-pulse-rate-respiration-rate-blood-pressure (accessed Apr. 24, 2022).

[38] J. Badawy, O. K. Nguyen, C. Clark, E. A. Halm, and A. N. Makam, “Is everyone really breathing 20 times a minute? Assessing epidemiology and variation in recorded respiratory rate in hospitalised adults,” *BMJ Qual Saf*, vol. 26, no. 10, pp. 832–836, Oct. 2017, doi: 10.1136/bmjqs-2017-006671.

[39] “Spirometry - Mayo Clinic.” https://www.mayoclinic.org/tests-procedures/spirometry/about/pac-20385201 (accessed Feb. 27, 2022).

[40] C. Chourpiliadis and A. Bhardwaj, “Physiology, Respiratory Rate,” in *StatPearls*, Treasure Island (FL): StatPearls Publishing, 2023. Accessed: Aug. 16, 2023. [Online]. Available: http://www.ncbi.nlm.nih.gov/books/NBK537306/

[41] A. Rodríguez-Molinero, L. Narvaiza, J. Ruiz, and C. Gálvez-Barrón, “Normal Respiratory Rate and Peripheral Blood Oxygen Saturation in the Elderly Population,” *Journal of the American Geriatrics Society*, vol. 61, no. 12, pp. 2238–2240, 2013, doi: 10.1111/jgs.12580.

[42] F. de Jongh, “Spirometers,” *Breathe*, vol. 4, no. 3, Mar. 2008.

[43] “AioCare respiratory disease management system,” *Vyaire Medical*. [Online]. Available: https://intl.vyaire.com/products/aiocare-respiratory-disease-management-system

[44] O. H. Mayer, R. G. Clayton Sr, A. F. Jawad, J. M. McDonough, and J. L. Allen, “Respiratory inductance plethysmography in healthy 3- to 5-year-old children,” *Chest*, vol. 124, no. 5, pp. 1812–1819, 2003.

[45] Z. Zhang, J. Zheng, H. Wu, W. Wang, B. Wang, and H. Liu, “Development of a Respiratory Inductive Plethysmography Module Supporting Multiple Sensors for Wearable Systems,” *Sensors (Basel)*, vol. 12, no. 10, pp. 13167–13184, Sep. 2012, doi: 10.3390/s121013167.

[46] “Natus® XactTrace® RIP respiratory effort belts,” *Natus*. [Online]. Available: https://neuro.natus.com/products-services/natus-xacttrace-rip-respiratory-effort-belts

[47] Hexoskin, “Hexoskin Smart shirt - women’s,” *Hexoskin*. [Online]. Available: https://www.hexoskin.com/collections/all/products/hexoskin-shirt-women

[48] M. Suh, “12 - Wearable sensors for athletes,” in *Electronic textiles: Smart fabrics and wearable technology*, T. Dias, Ed., Cambridge, England: Woodhead Publishing, 2015, pp. 257–273.

[49] A. Jubran, “Pulse oximetry,” *Critical Care*, vol. 19, no. 1, p. 272, Dec. 2015, doi: 10.1186/s13054-015-0984-8.

[50] E. D. Chan, M. M. Chan, and M. M. Chan, “Pulse oximetry: Understanding its basic principles facilitates appreciation of its limitations,” *Respiratory Medicine*, vol. 107, no. 6, pp. 789–799, Jun. 2013, doi: 10.1016/j.rmed.2013.02.004.

[51] S. Bell, “absorbance,” in *A Dictionary of Forensic Science*, Oxford University Press, 2013. Accessed: Aug. 12, 2023. [Online]. Available: https://

[52] C. for D. and R. Health, “Pulse Oximeter Accuracy and Limitations: FDA Safety Communication,” *FDA*, Dec. 2022, Accessed: Mar. 27, 2023. [Online]. Available: https://www.fda.gov/medical-devices/safety-communications/pulse-oximeter-accuracy-and-limitations-fda-safety-communication

[53] “Continuous monitoring. With a single finger,” *Medtronic.com*. [Online]. Available: https://www.medtronic.com/content/dam/covidien/library/us/en/product/pulse-oximetry/nellcor-respiration-rate-technology-info-sheet.pdf

[54] “Masimo - Respiration Rate from the Pleth (RRp®).” https://www.masimo.com/technology/co-oximetry/rrp/ (accessed Mar. 27, 2023).

[55] M. Nitzan, A. Romem, and R. Koppel, “Pulse oximetry: fundamentals and technology update,” *Med. Devices (Auckl.)*, vol. 7, pp. 231–239, 2014.

[56] P. A. Kyriacou, “Pulse oximetry in the oesophagus,” *Physiol. Meas.*, vol. 27, no. 1, pp. R1–R35, Jan. 2006, doi: 10.1088/0967-3334/27/1/R01.

[57] P. A. Kyriacou, S. Powell, R. M. Langford, and D. P. Jones, “Esophageal pulse oximetry utilizing reflectance photoplethysmography,” *IEEE Transactions on Biomedical Engineering*, vol. 49, no. 11, pp. 1360–1368, Nov. 2002, doi: 10.1109/TBME.2002.804584.

[58] M. Kramer, A. Lobbestael, E. Barten, J. Eian, and G. Rausch, “Wearable Pulse Oximetry Measurements on the Torso, Arms, and Legs: A Proof of Concept,” *Military Medicine*, vol. 182, no. suppl_1, pp. 92–98, Mar. 2017, doi: 10.7205/MILMED-D-16-00129.

[59] C. Schreiner, P. Catherwood, J. Anderson, and J. McLaughlin, *Blood oxygen level measurement with a chest-based Pulse Oximetry prototype System*, vol. 37. 2010, p. 540.

[60] W. R. Mower, C. Sachs, E. L. Nicklin, P. Safa, and L. J. Baraff, “A comparison of pulse oximetry and respiratory rate in patient screening”.

[61] N. A. Chatterjee *et al.*, “Admission respiratory status predicts mortality in COVID-19,” *Influenza and Other Respiratory Viruses*, vol. 15, no. 5, pp. 569–572, 2021, doi: 10.1111/irv.12869.

[62] J. Eichhoff, A. Hehl, S. Jockenhoevel, and T. Gries, “Textile fabrication technologies for embedding electronic functions into fibres, yarns and fabrics,” in *Multidisciplinary know-how for smart-textiles developers*, T. Kirstein, Ed., Cambridge, England: Woodhead Publishing, 2013, pp. 191–226.

[63] “ASTM D6193 - 16(2020) Standard Practice for Stitches and Seams.” https://www.astm.org/Standards/D6193.htm (accessed Dec. 17, 2020).

[64] “Definition of SENSOR,” Aug. 03, 2023. https://www.merriam-webster.com/dictionary/sensor (accessed Aug. 12, 2023).

[65] J. D. jonckheere *et al.*, “OFSETH: Smart medical textile for continuous monitoring of respiratory motions under magnetic resonance imaging,” in *2009 Annual International Conference of the IEEE Engineering in Medicine and Biology Society*, Sep. 2009, pp. 1473–1476. doi: 10.1109/IEMBS.2009.5332432.

[66] M. Ciocchetti *et al.*, “Smart Textile Based on Fiber Bragg Grating Sensors for Respiratory Monitoring: Design and Preliminary Trials,” *Biosensors (Basel)*, vol. 5, no. 3, pp. 602–615, Sep. 2015, doi: 10.3390/bios5030602.

[67] A. Atalay *et al.*, “Batch Fabrication of Customizable Silicone-Textile Composite Capacitive Strain Sensors for Human Motion Tracking,” *Adv. Mater. Technol.*, vol. 2, no. 9, p. 1700136, Sep. 2017, doi: 10.1002/admt.201700136.

[68] Y. Jin *et al.*, “Soft Sensing Shirt for Shoulder Kinematics Estimation,” in *2020 IEEE International Conference on Robotics and Automation (ICRA)*, Paris, France: IEEE, May 2020, pp. 4863–4869. doi: 10.1109/ICRA40945.2020.9196586.

[69] S. D. Min, Y. Yun, and H. Shin, “Simplified Structural Textile Respiration Sensor Based on Capacitive Pressure Sensing Method,” *IEEE Sensors Journal*, vol. 14, no. 9, pp. 3245–3251, Sep. 2014, doi: 10.1109/JSEN.2014.2327991.

[70] N. Molinaro *et al.*, “Wearable textile based on silver plated knitted sensor for respiratory rate monitoring,” in *2018 40th Annual International Conference of the IEEE Engineering in Medicine and Biology Society (EMBC)*, Jul. 2018, pp. 2865–2868. doi: 10.1109/EMBC.2018.8512958.

[71] T. Agcayazi, M. A. Yokus, M. Gordon, T. Ghosh, and A. Bozkurt, “A stitched textile-based capacitive respiration sensor,” in *2017 IEEE SENSORS*, Oct. 2017, pp. 1–3. doi: 10.1109/ICSENS.2017.8234234.

[72] G. Gioberto and L. Dunne, “Theory and characterization of a top-thread coverstitched stretch sensor,” in *2012 IEEE International Conference on Systems, Man, and Cybernetics (SMC)*, Oct. 2012, pp. 3275–3280. doi: 10.1109/ICSMC.2012.6378296.

[73] G. Gioberto and L. E. Dunne, “Overlock-Stitched Stretch Sensors: Characterization and Effect of Fabric Property,” *Journal of Textile and Apparel, Technology and Management*, vol. 8, no. 3, Art. no. 3, Dec. 2013, Accessed: Aug. 16, 2023. [Online]. Available: https://jtatm.textiles.ncsu.edu/index.php/JTATM/article/view/4417

[74] M. E. Berglund, J. Coughlin, G. Gioberto, and L. E. Dunne, “Washability of e-textile stretch sensors and sensor insulation,” in *Proceedings of the 2014 ACM International Symposium on Wearable Computers*, Seattle Washington: ACM, Sep. 2014, pp. 127–128. doi: 10.1145/2634317.2634326.

[75] L. Griffin, C. Compton, and L. E. Dunne, “An analysis of the variability of anatomical body references within ready-to-wear garment sizes,” in *Proceedings of the 2016 ACM International Symposium on Wearable Computers*, Heidelberg Germany: ACM, Sep. 2016, pp. 84–91. doi: 10.1145/2971763.2971800.

[76] H. Harms, O. Amft, and G. Troester, “Does loose fitting matter? Predicting sensor performance in smart garments.,” in *Proceedings of the 7th International Conference on Body Area Networks*, Oslo, Norway: ACM, 2012. doi: 10.4108/icst.bodynets.2012.249968.

[77] H. Harms, O. Amft, and G. Tröster, “Estimating Posture-Recognition Performance in Sensing Garments Using Geometric Wrinkle Modeling,” *IEEE Transactions on Information Technology in Biomedicine*, vol. 14, no. 6, pp. 1436–1445, Nov. 2010, doi: 10.1109/TITB.2010.2076822.

[78] R. Granberry, J. Duvall, L. E. Dunne, and B. Holschuh, “An analysis of anthropometric geometric variability of the lower leg for the fit & function of advanced functional garments,” in *Proceedings of the 2017 ACM International Symposium on Wearable Computers*, Maui Hawaii: ACM, Sep. 2017, pp. 10–17. doi: 10.1145/3123021.3123034.

[79] H. Harms, O. Amft, and G. Troster, “Influence of a loose-fitting sensing garment on posture recognition in rehabilitation,” in *2008 IEEE Biomedical Circuits and Systems Conference*, Nov. 2008, pp. 353–356. doi: 10.1109/BIOCAS.2008.4696947.

[80] G. Gioberto and L. E. Dunne, “Garment Positioning and Drift in Garment-Integrated Wearable Sensing,” in *2012 16th International Symposium on Wearable Computers*, Jun. 2012, pp. 64–71. doi: 10.1109/ISWC.2012.35.

[81] L. Dunne, “Beyond the second skin: an experimental approach to addressing garment style and fit variables in the design of sensing garments,” *Int. J. Fash. Des. Technol. Educ.*, vol. 3, no. 3, pp. 109–117, 2010.

[82] G. Gioberto, “Measuring joint movement through garment-integrated wearable sensing,” Apr. 2015, Accessed: Aug. 12, 2023. [Online]. Available: http://conservancy.umn.edu/handle/11299/172666

[83] Y. Patil, S. Tiffany, and E. Sazonov, “Understanding smoking behavior using wearable sensors: Relative importance of various sensor modalities,” in *2014 36th Annual International Conference of the IEEE Engineering in Medicine and Biology Society*, Aug. 2014, pp. 6899–6902. doi: 10.1109/EMBC.2014.6945214.

[84] Biopac Ssytems, INC., “PRODUCT SHEET - PULSE OXIMETRY.” Accessed: Aug. 14, 2023. [Online]. Available: https://www.biopac.com/wp-content/uploads/Pulse-Oximetry.pdf

[85] G. B. Drummond, D. Fischer, and D. K. Arvind, “Current clinical methods of measurement of respiratory rate give imprecise values,” *ERJ Open Res*, vol. 6, no. 3, pp. 00023–02020, Sep. 2020, doi: 10.1183/23120541.00023-2020.

[86] P. C. Loughlin, F. Sebat, and J. G. Kellett, “Respiratory Rate: The Forgotten Vital Sign—Make It Count!,” *The Joint Commission Journal on Quality and Patient Safety*, vol. 44, no. 8, pp. 494–499, Aug. 2018, doi: 10.1016/j.jcjq.2018.04.014.

## Appendix A. Respiration Data

Additional graphs of respiration coefficient of determination (r-squared values) and breathing frequency analysis measures comparing the experimental stitched sensor against the reference (Biopac) sensor.

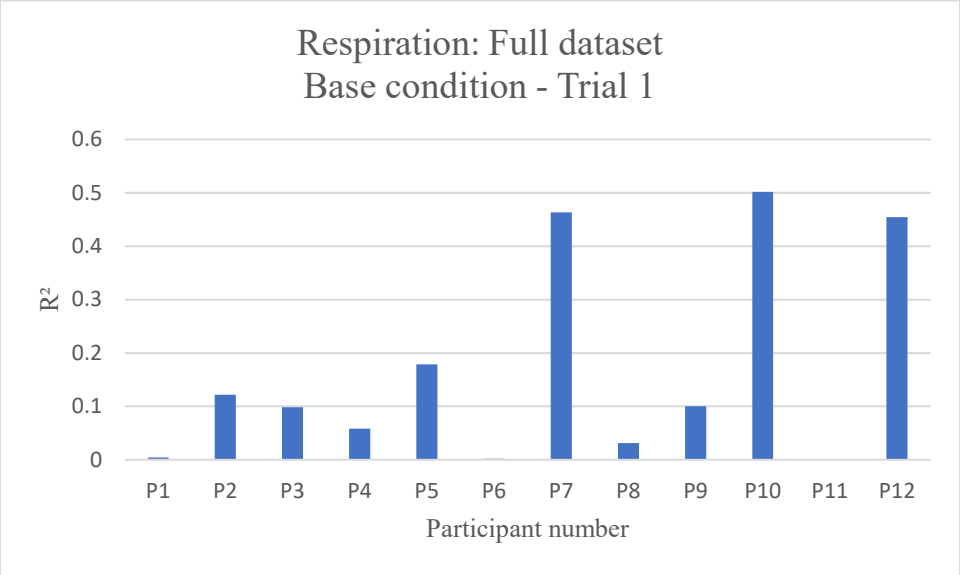


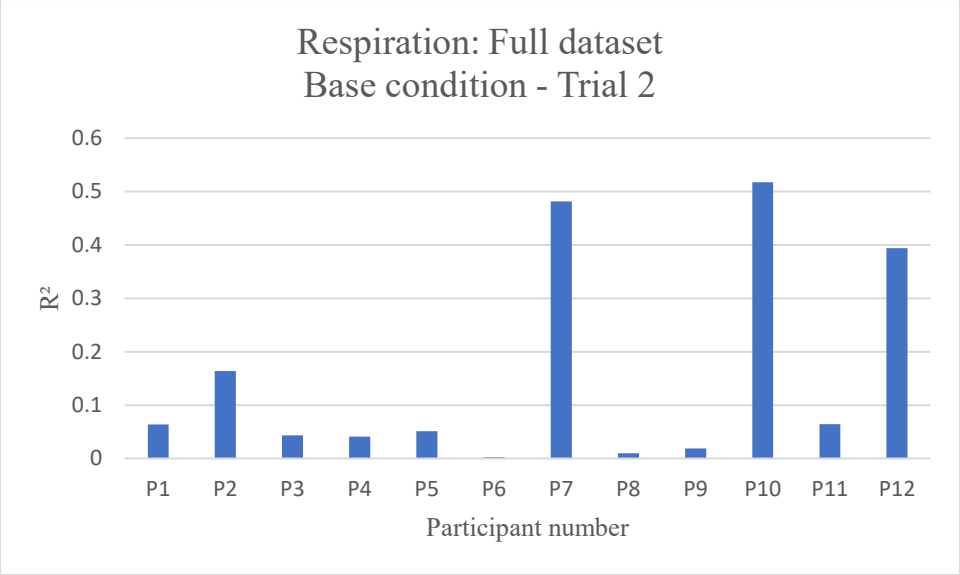

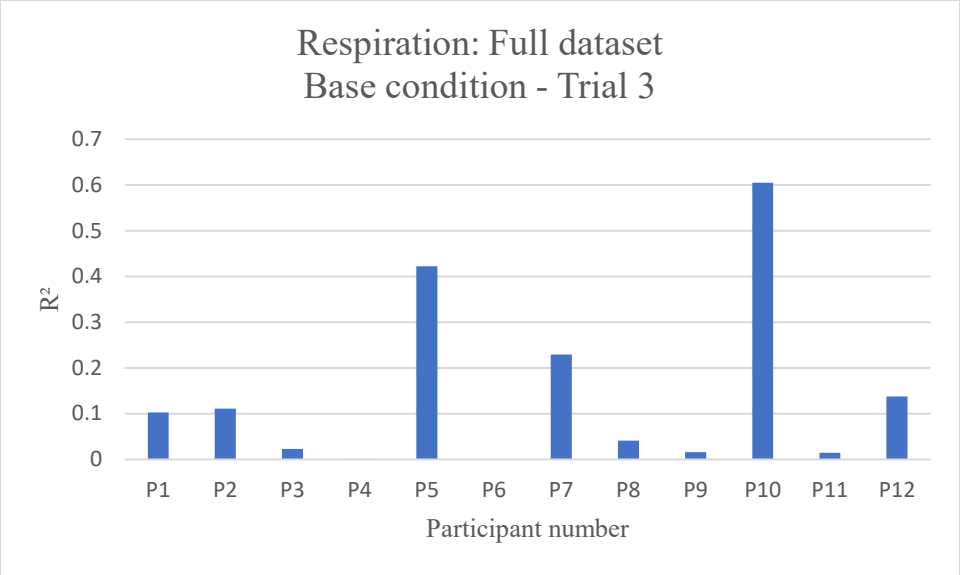


*Fig. A1-A3. Respiration full data set (breath hold included) base fit condition trials 1-3.*

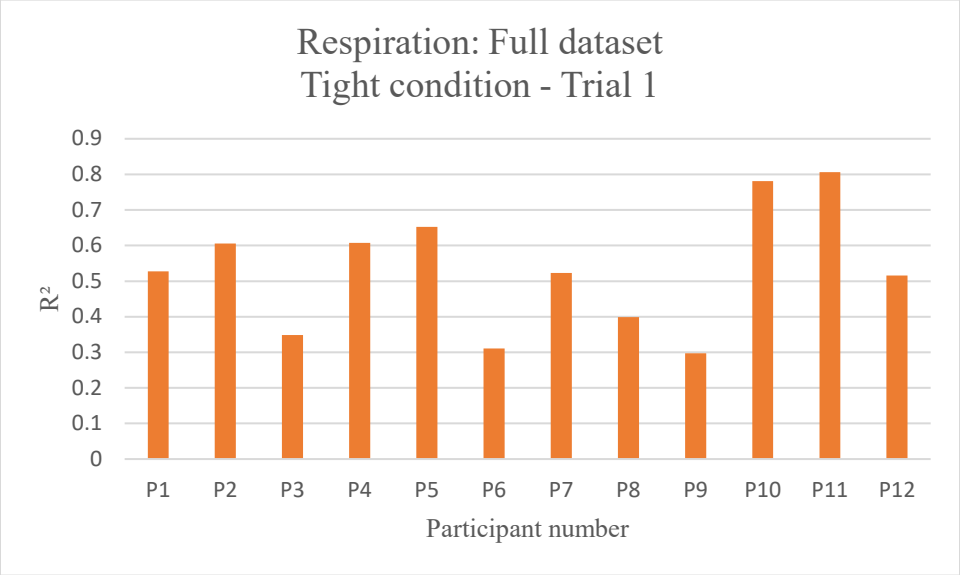

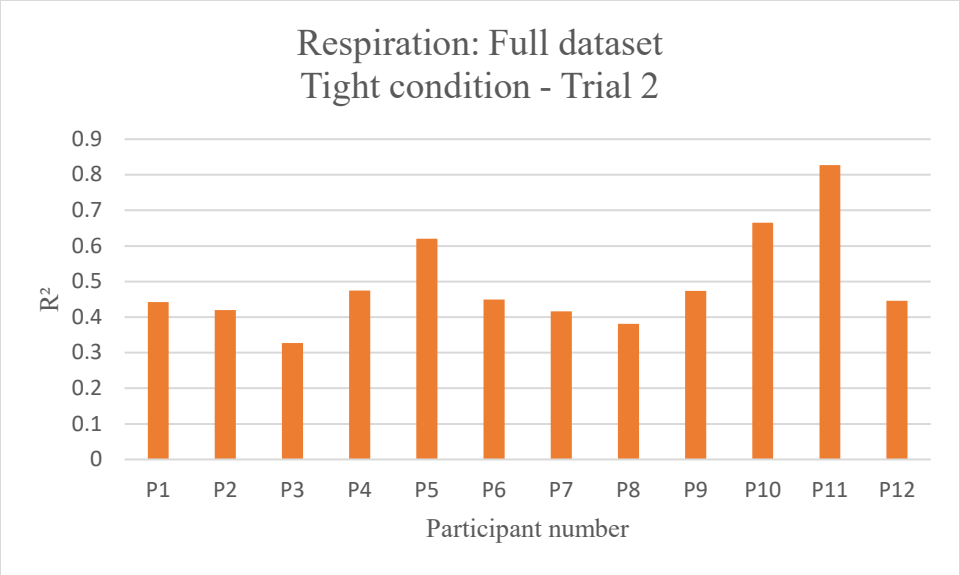


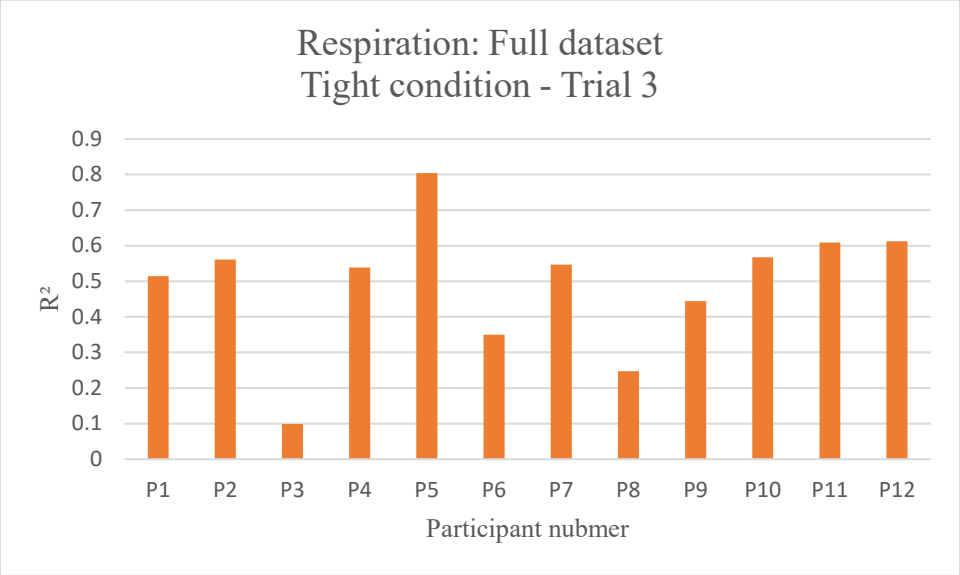


*Fig. A4-A6. Respiration full data set (breath hold included) tight fit condition trials 1-3.*

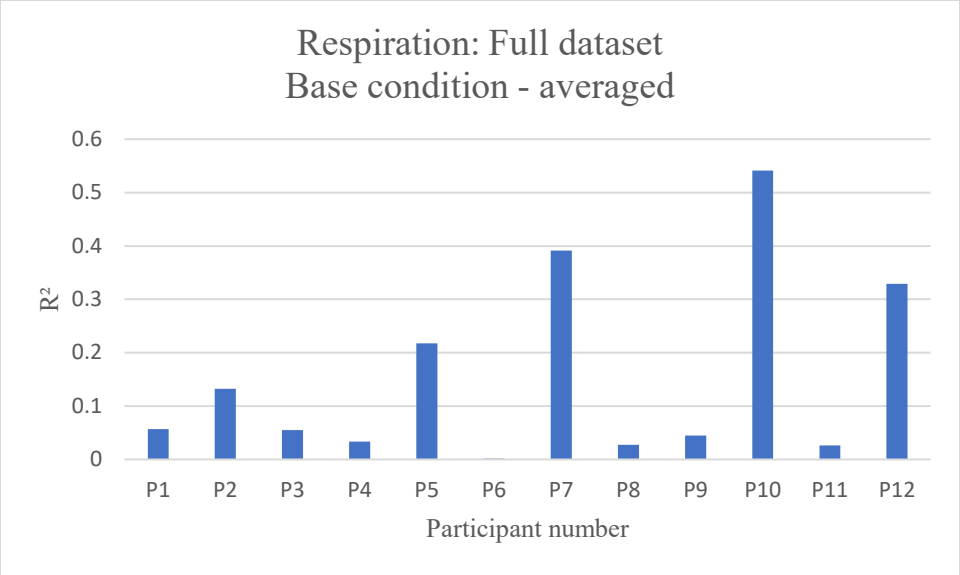


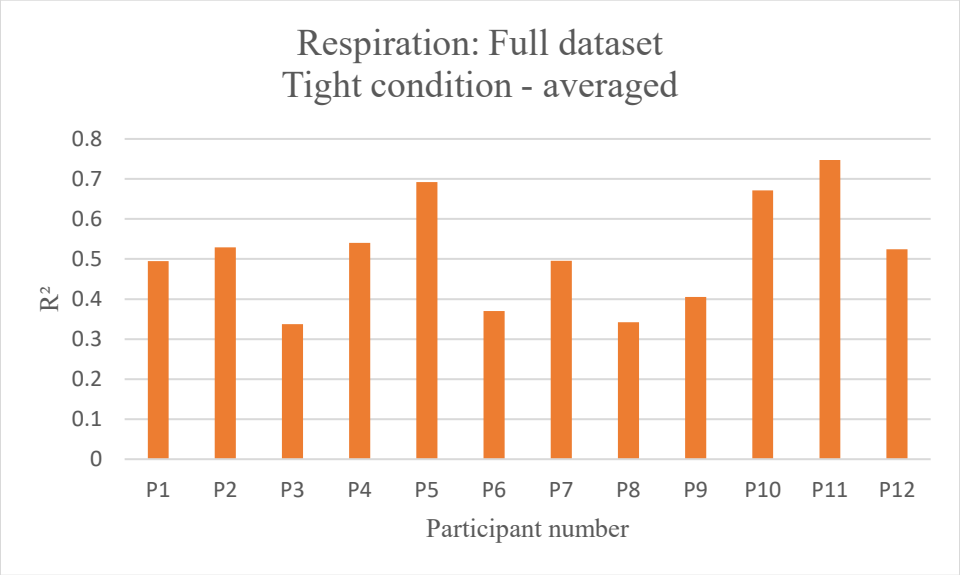


*Fig. A7-A8: Respiration full data set (breath hold included) all trials averaged for each participant.*

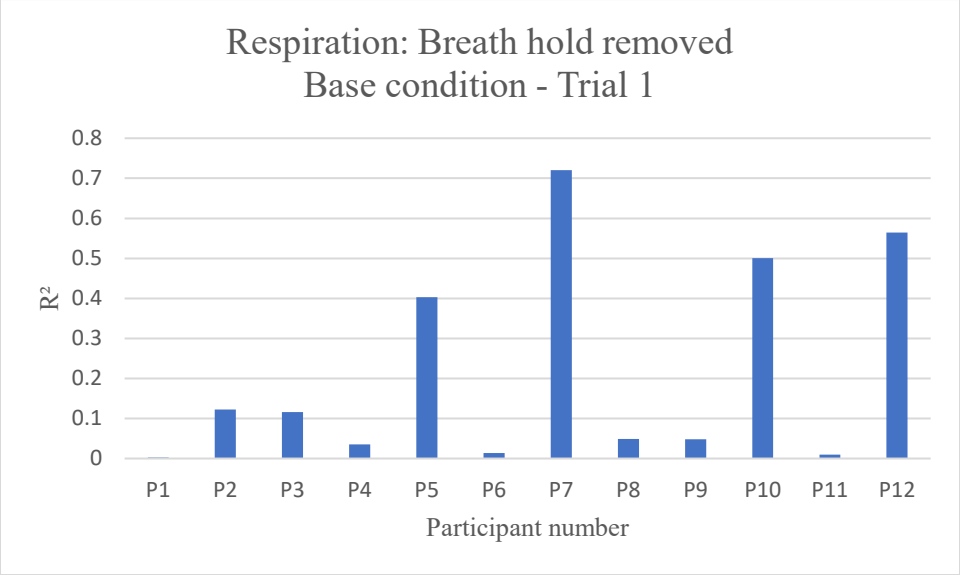
Respiration: Breath hold removed
Base condition - Trial 1
R²
0.8
0.7
0.6
0.5
0.4
0.3
0.2
0.1
0
P1
P2
P3
P4
P5
P6
P7
P8
P9
P10
P11
P12
Participant number

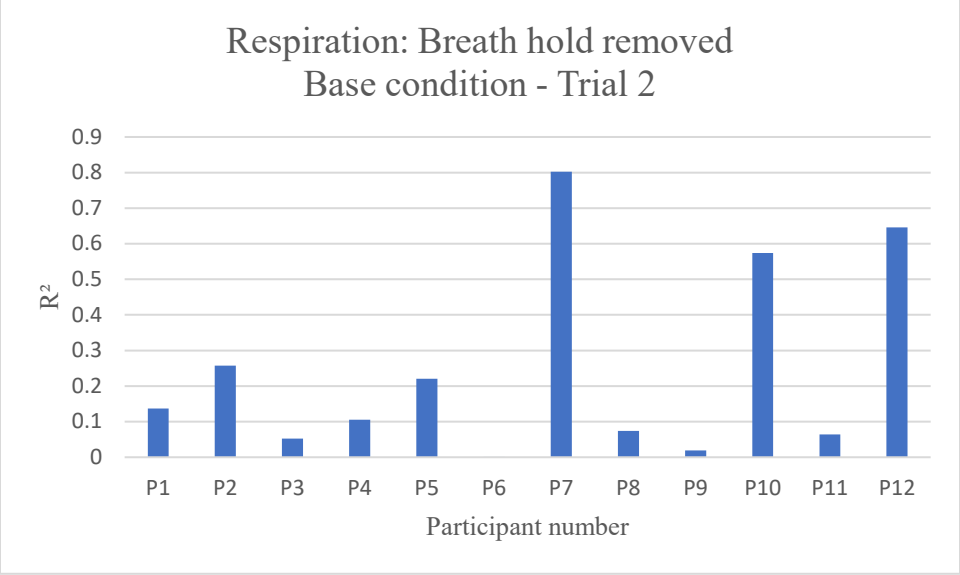
Respiration: Breath hold removed
Base condition - Trial 2
R²
0.9
0.8
0.7
0.6
0.5
0.4
0.3
0.2
0.1
0
P1
P2
P3
P4
P5
P6
P7
P8
P9
P10
P11
P12
Participant number

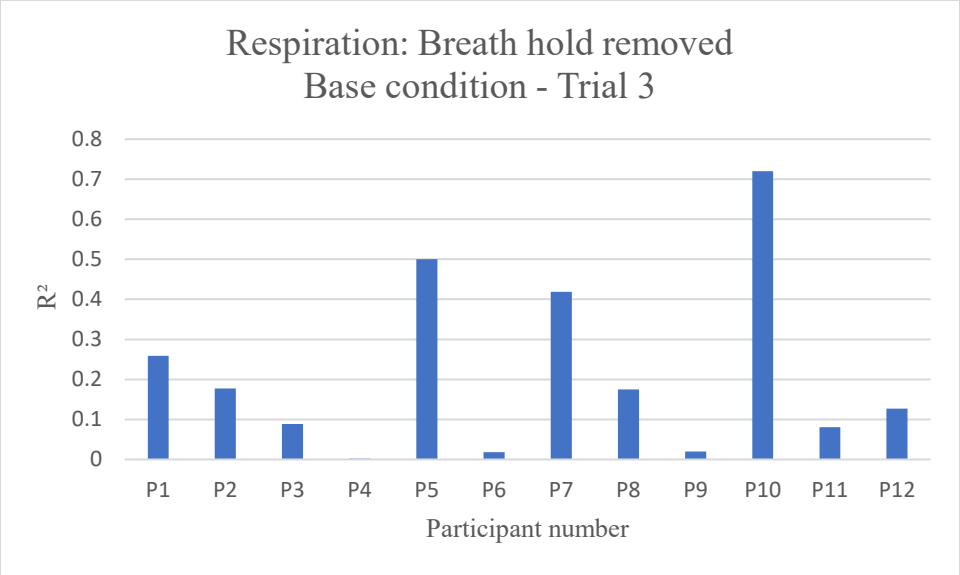


*Fig. A9-A11. Respiration, breath hold section removed, base fit condition trials 1-3.*

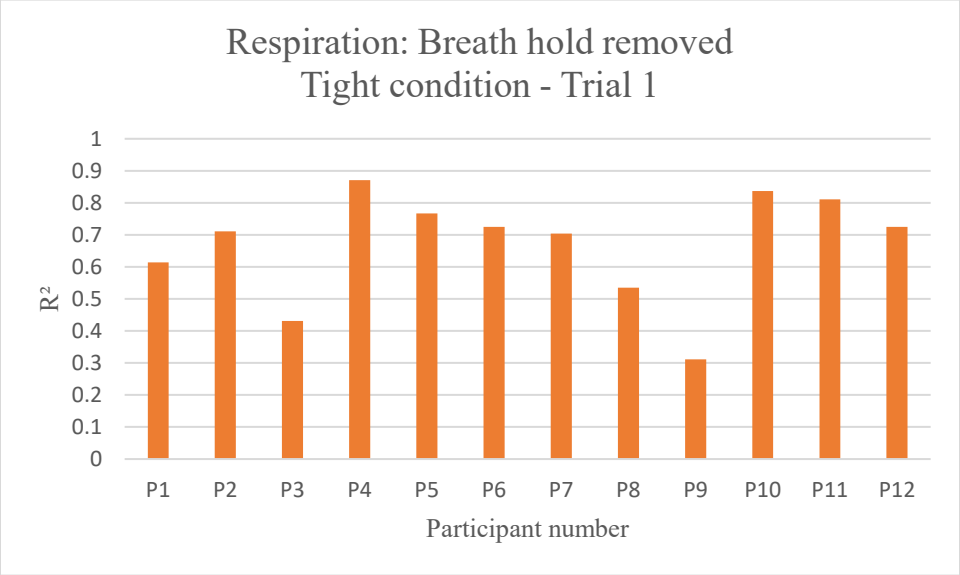

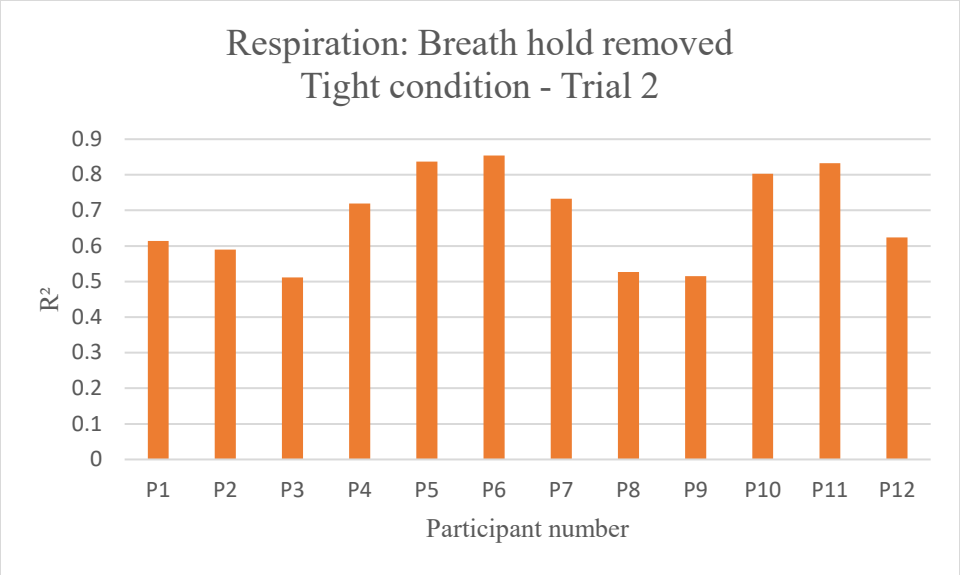


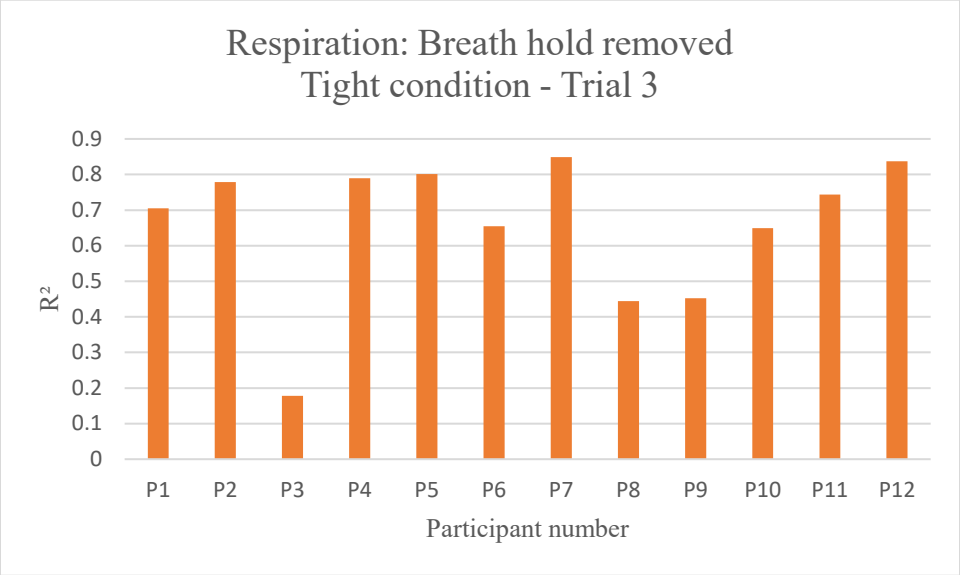


*Fig. A12-A14. Respiration, breath hold section removed, tight fit condition trials 1-3.*

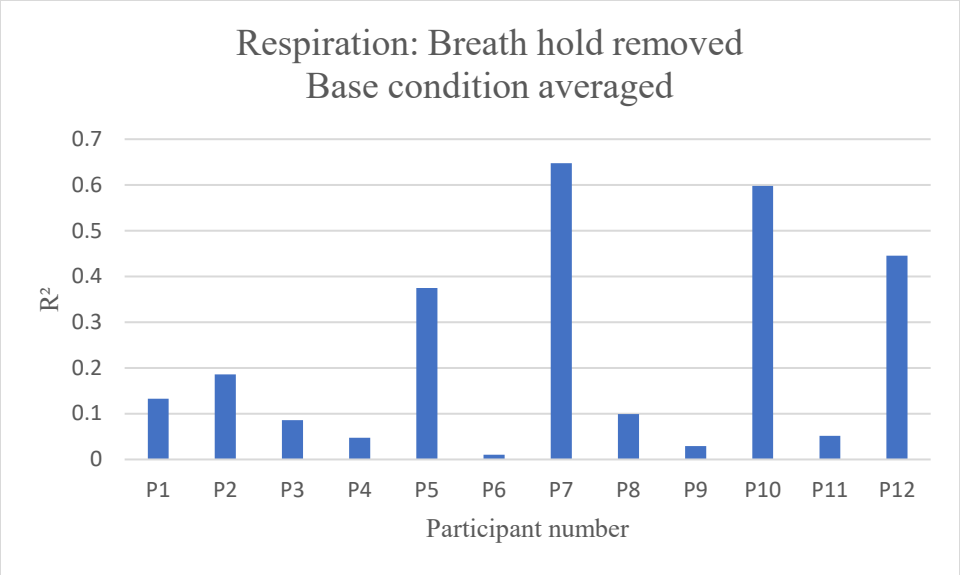


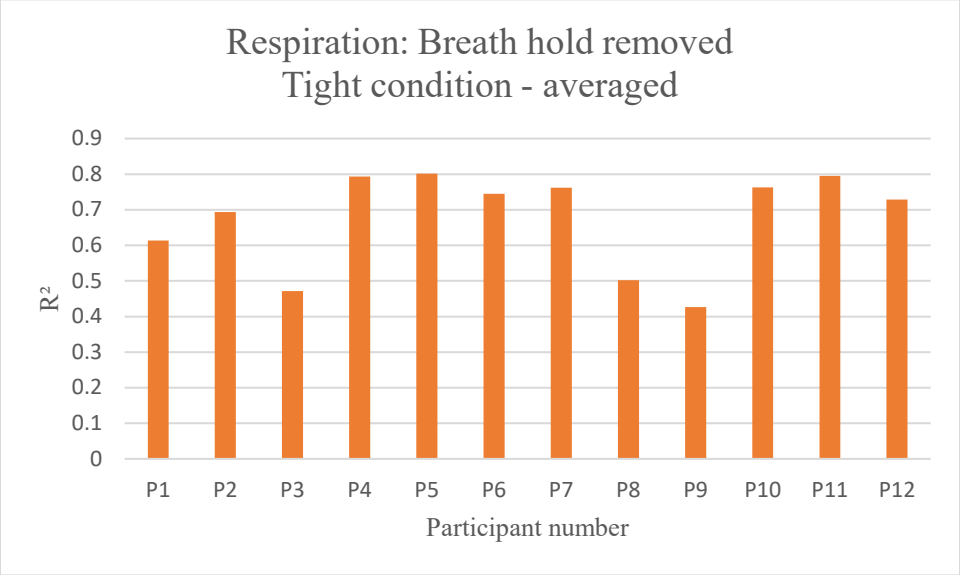


*Fig. A15-A16: Respiration, breath hold section removed, all trials averaged for each participant.*

## Appendix B. Pulse Oximetry Data

Additional graphs of pulse oximetry coefficient of determination (r-squared values) and average difference and standard deviation measures for $SpO_2$ and average difference and standard deviation measures for beats-per-minute (BPM) comparing the experimental chest probe sensor against the reference fingertip sensor.

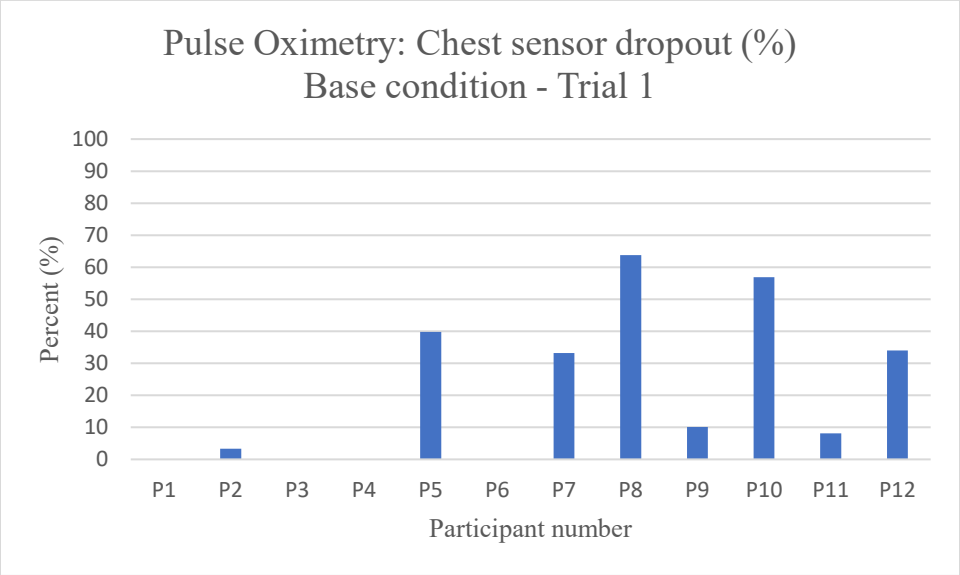


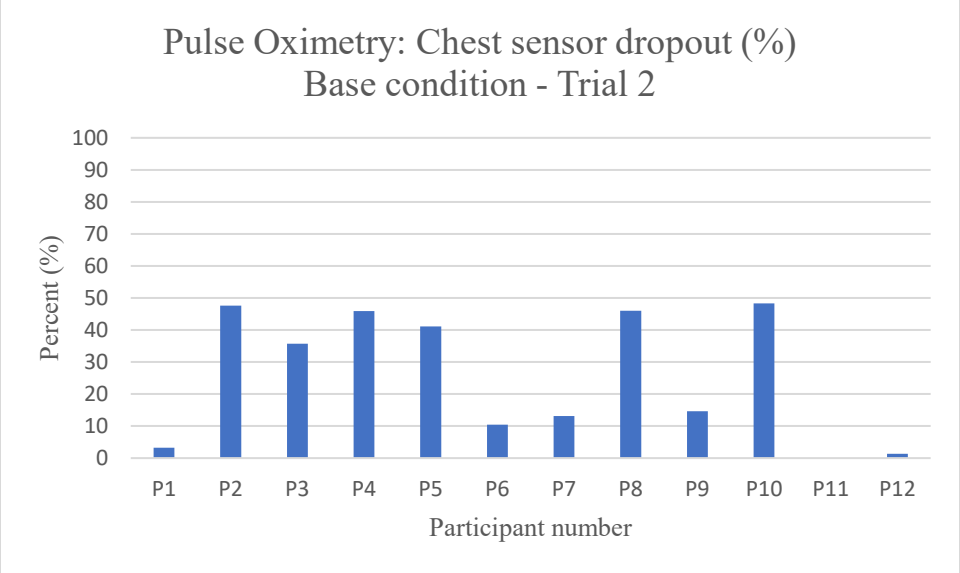

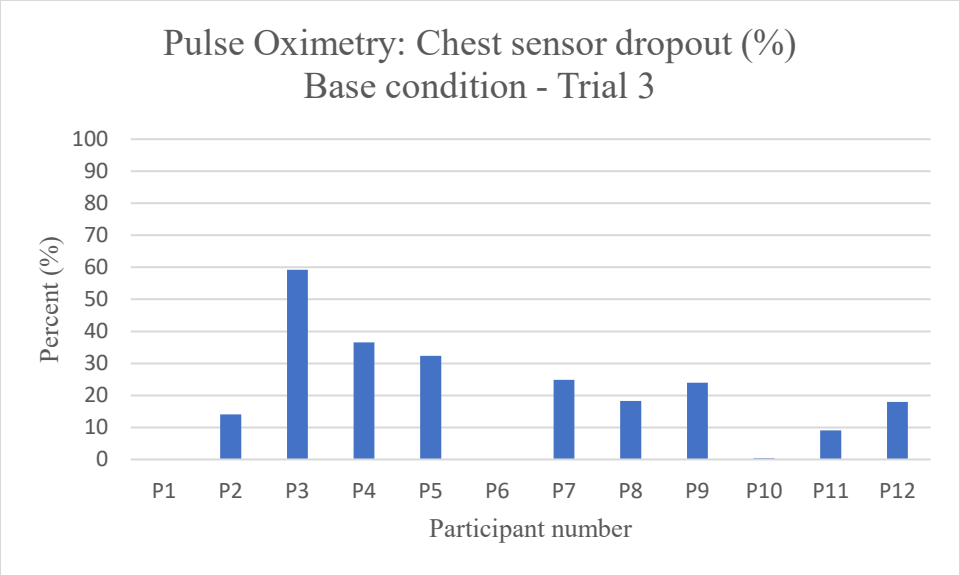


*Fig. B1-B3: Pulse oximetry dropout%, base condition, trials 1-3.*

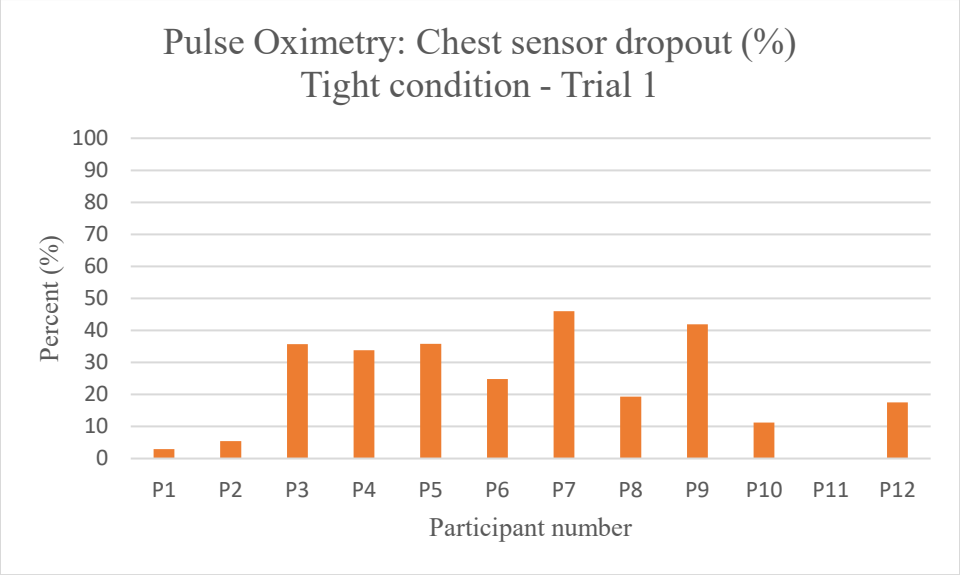

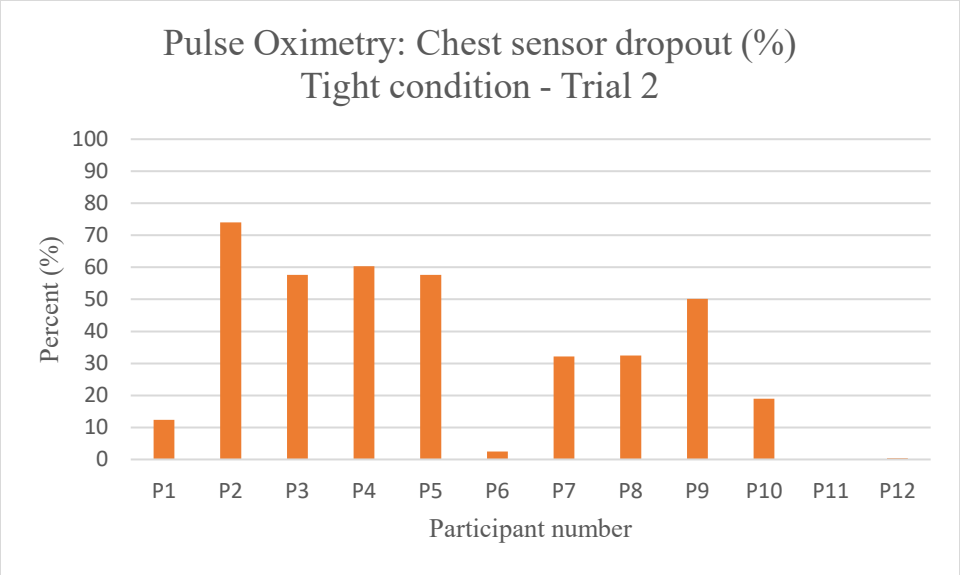


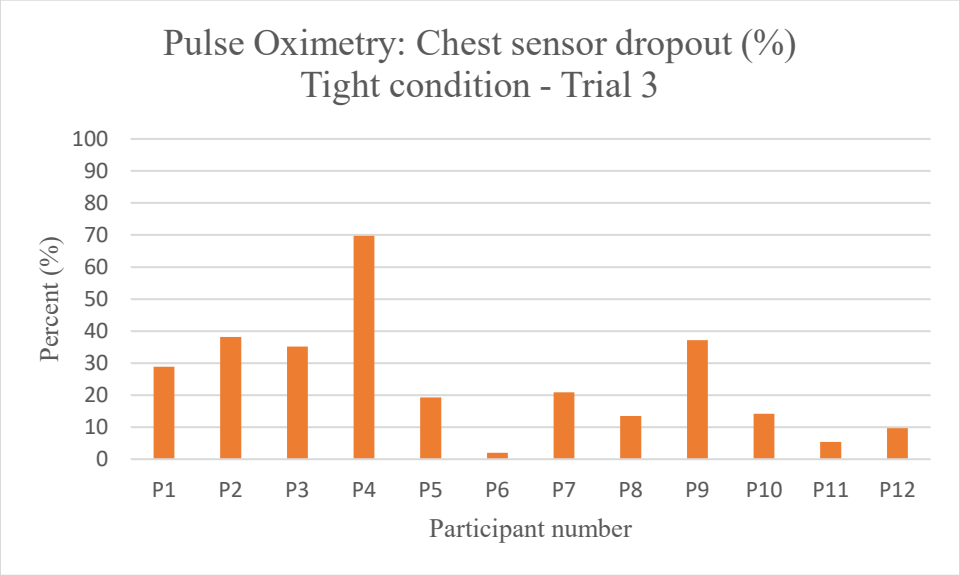


*Fig. B4-B6: Pulse oximetry dropout%, tight fit condition, trials 1-3*

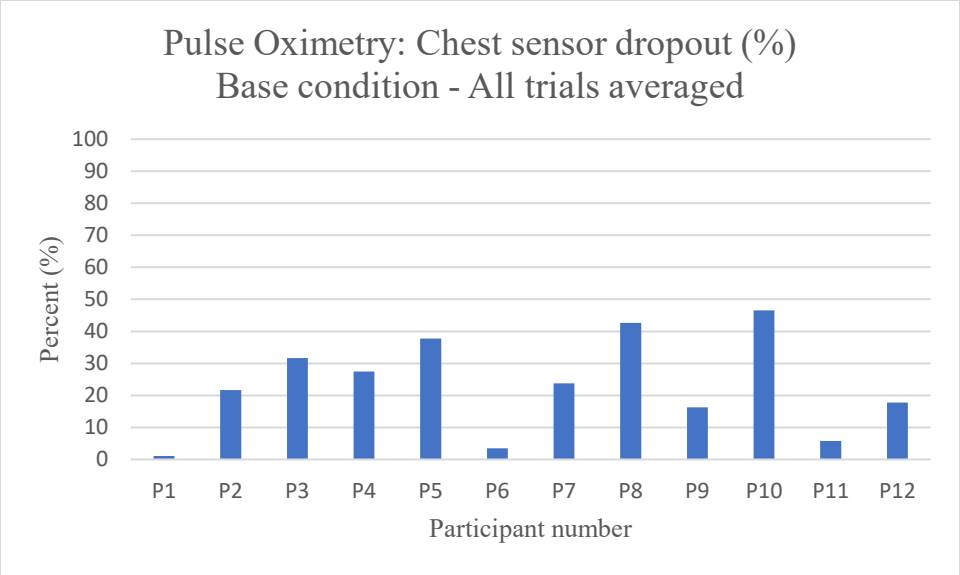


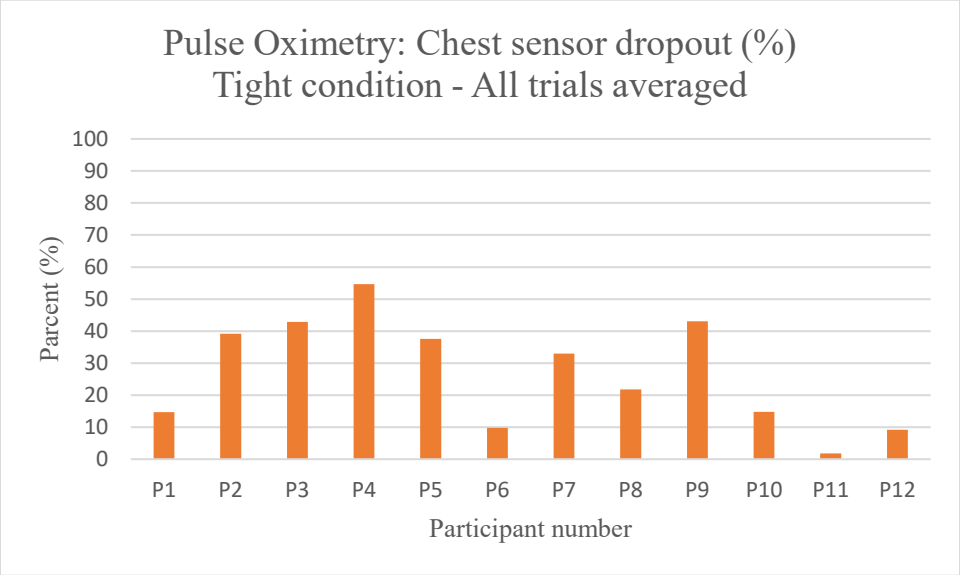


*Fig. B7-B8: Pulse oximetry dropout%, base fit condition all trials averaged, tight fit condition all trials averaged.*

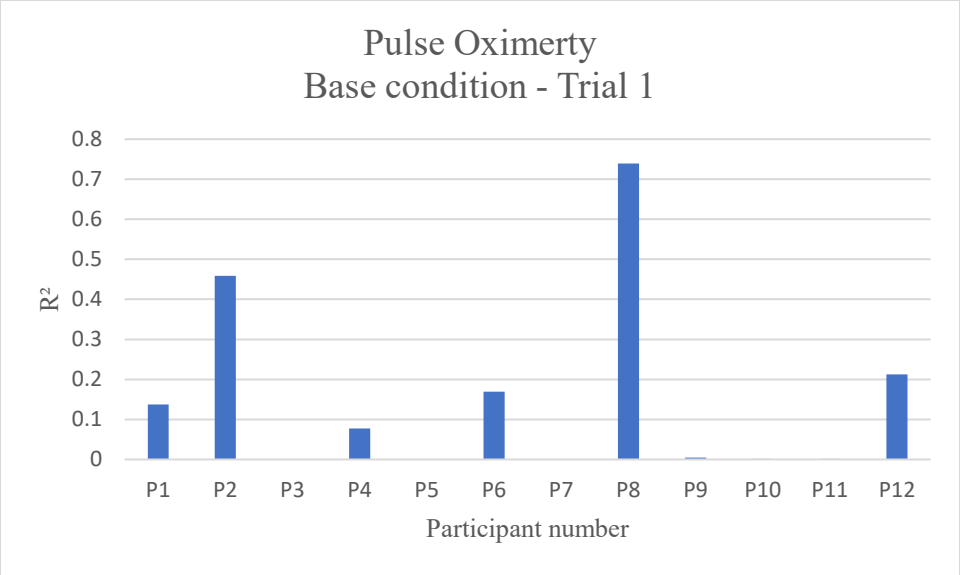
Pulse Oximerty
Base condition - Trial 1
0.8
0.7
0.6
0.5
0.4
0.3
0.2
0.1
0
R²
P1
P2
P3
P4
P5
P6
P7
P8
P9
P10
P11
P12
Participant number

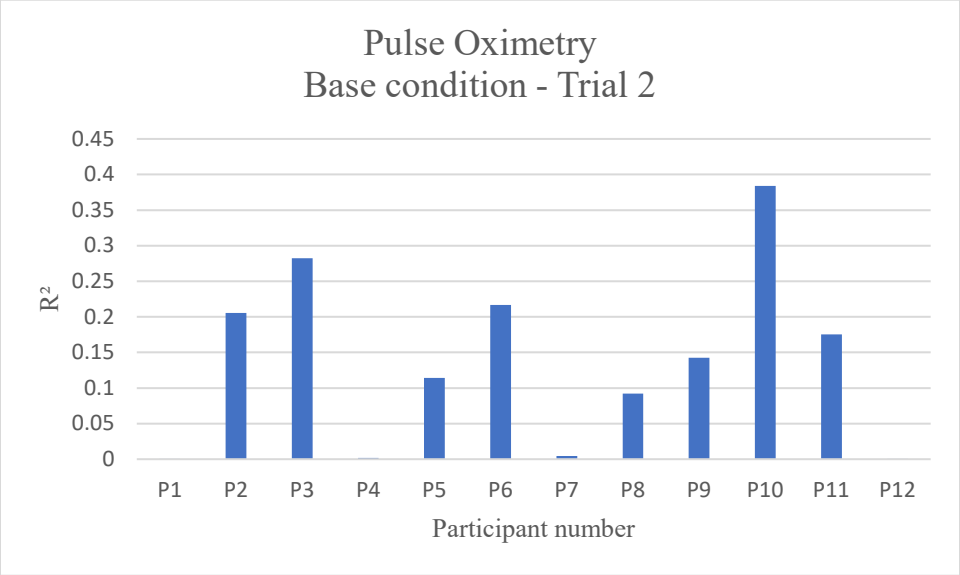
Pulse Oximetry
Base condition - Trial 2
0.45
0.4
0.35
0.3
0.25
0.2
0.15
0.1
0.05
0
R²
P1
P2
P3
P4
P5
P6
P7
P8
P9
P10
P11
P12
Participant number

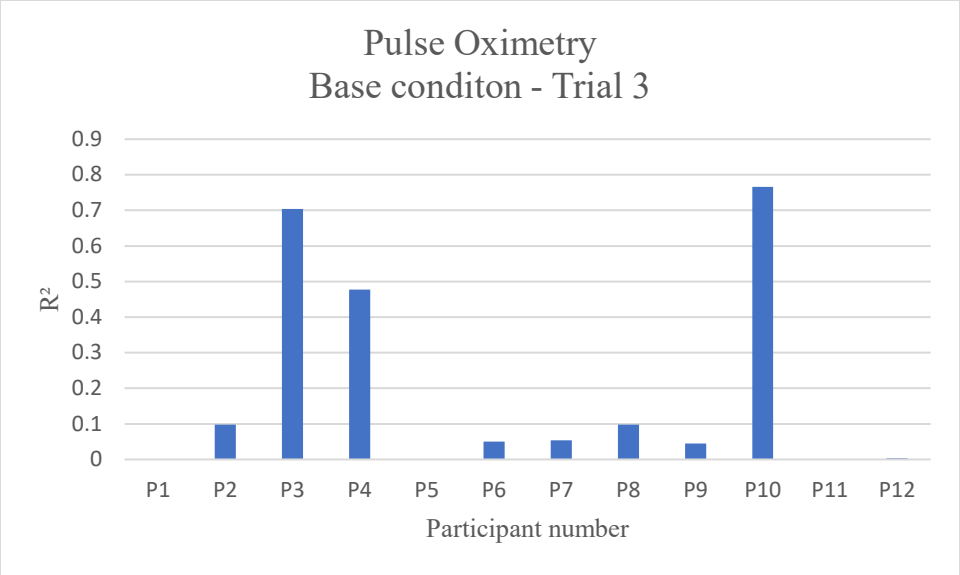


*Fig. B9-B11: Pulse oximetry $SpO_2$ coefficient of determination, base fit condition, trials 1-3*

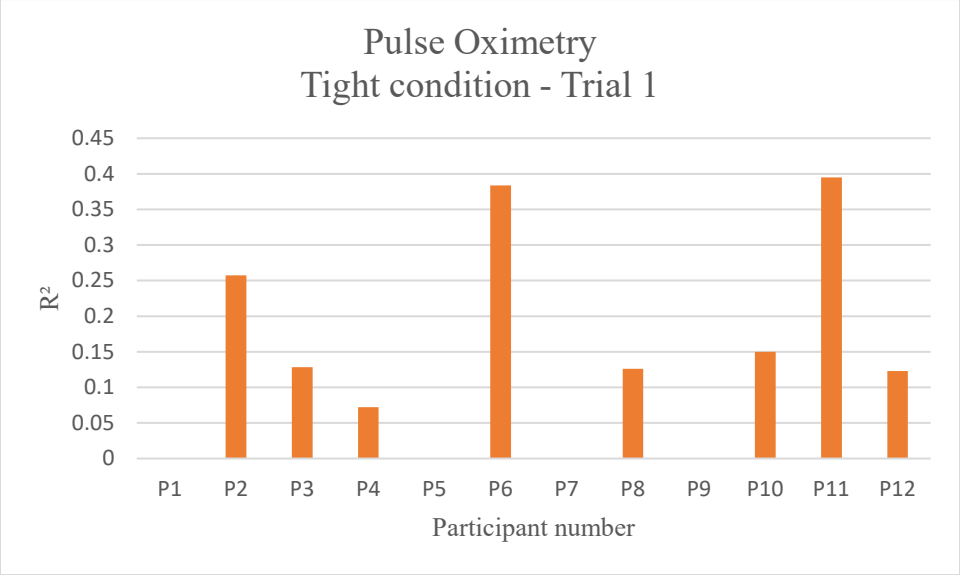

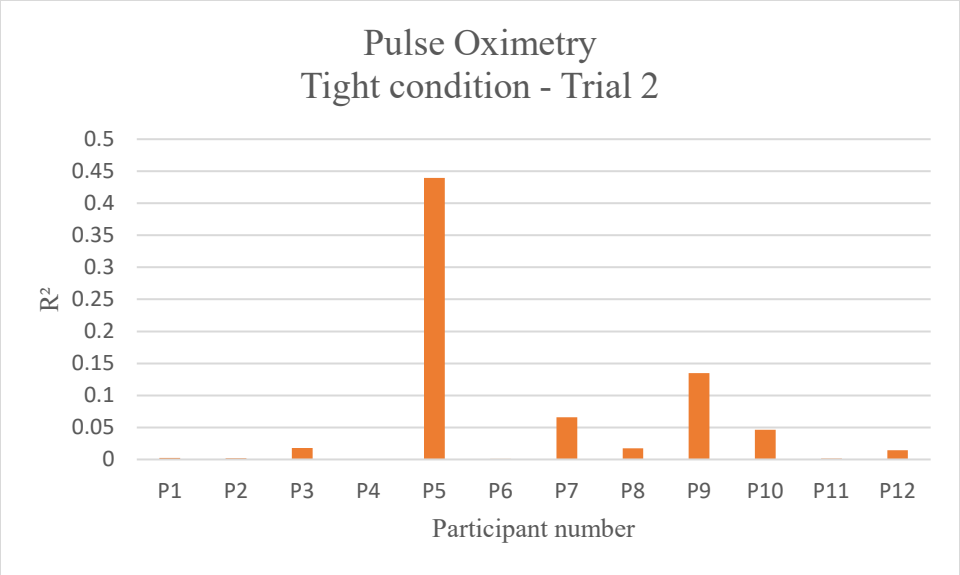


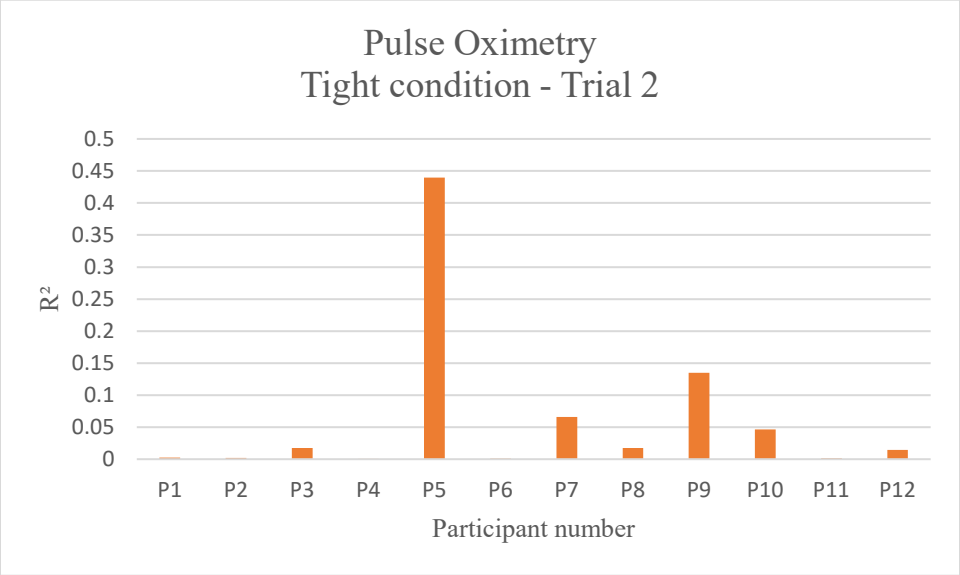


*Fig. B12-B14: Pulse oximetry $SpO_2$ coefficient of determination, tight fit condition, trials 1-3*

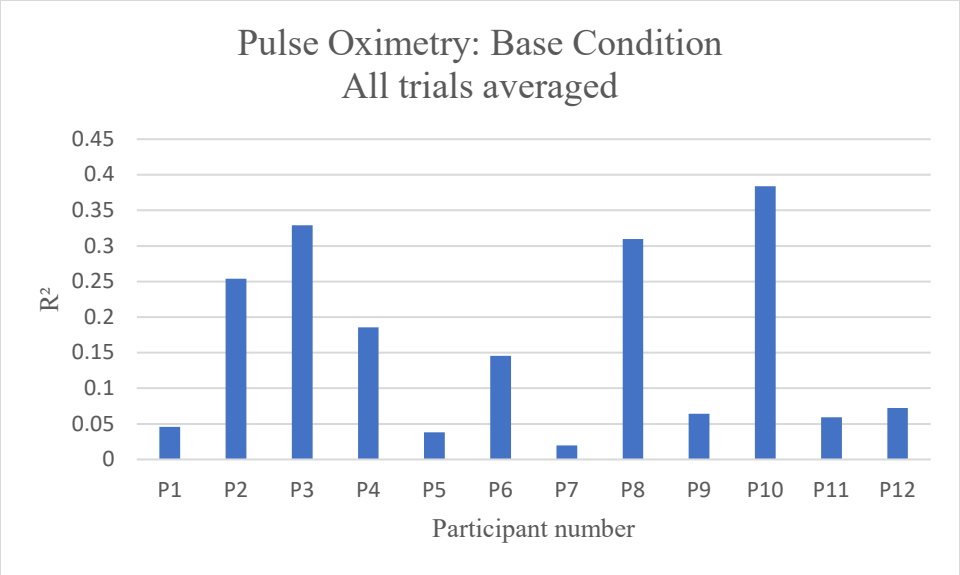


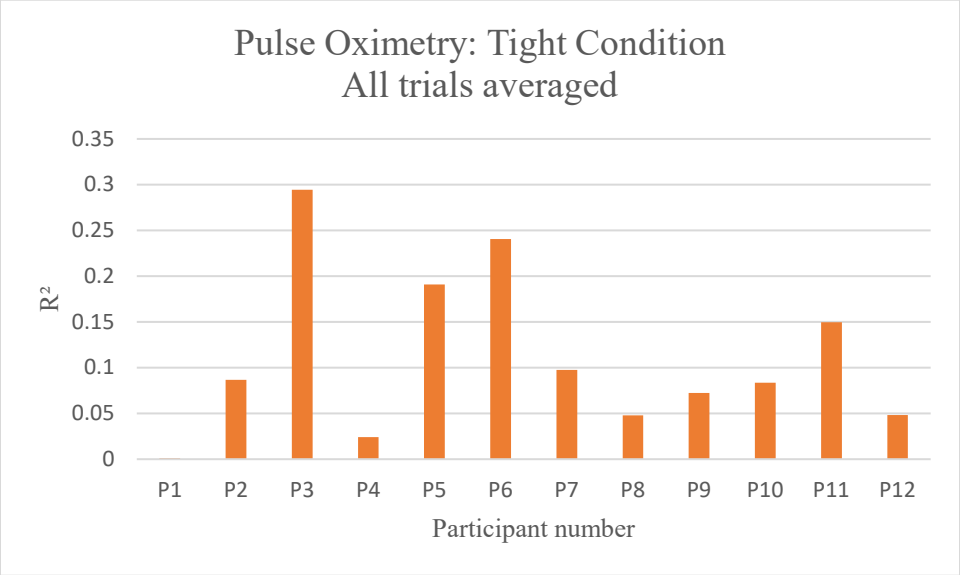


*Fig. B15-B16: Pulse oximetry $SpO_2$ coefficient of determination, base fit condition all trials averaged, tight fit condition all trials averaged.*

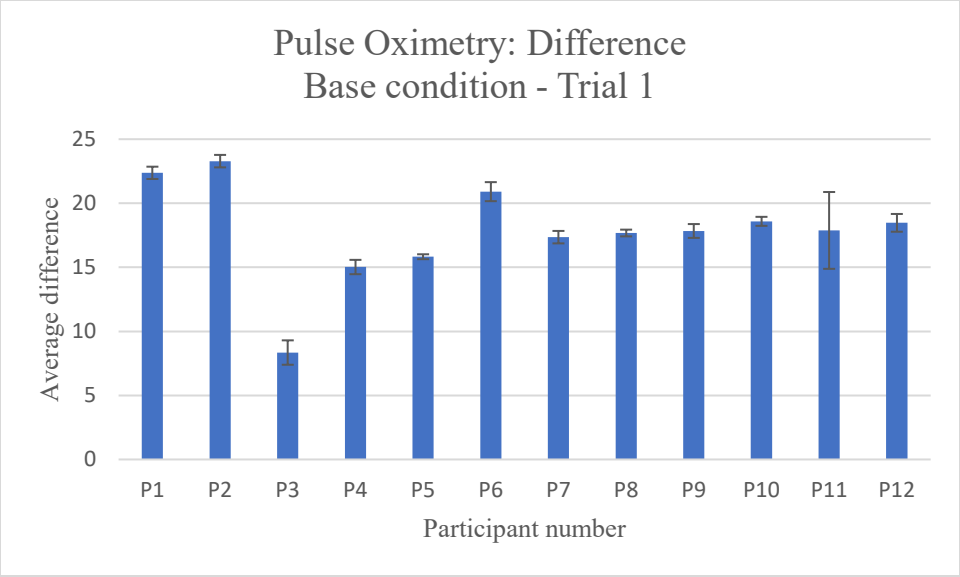
Pulse Oximetry: Difference
Base condition - Trial 1
Average difference
25
20
15
10
5
0
P1
P2
P3
P4
P5
P6
P7
P8
P9
P10
P11
P12
Participant number

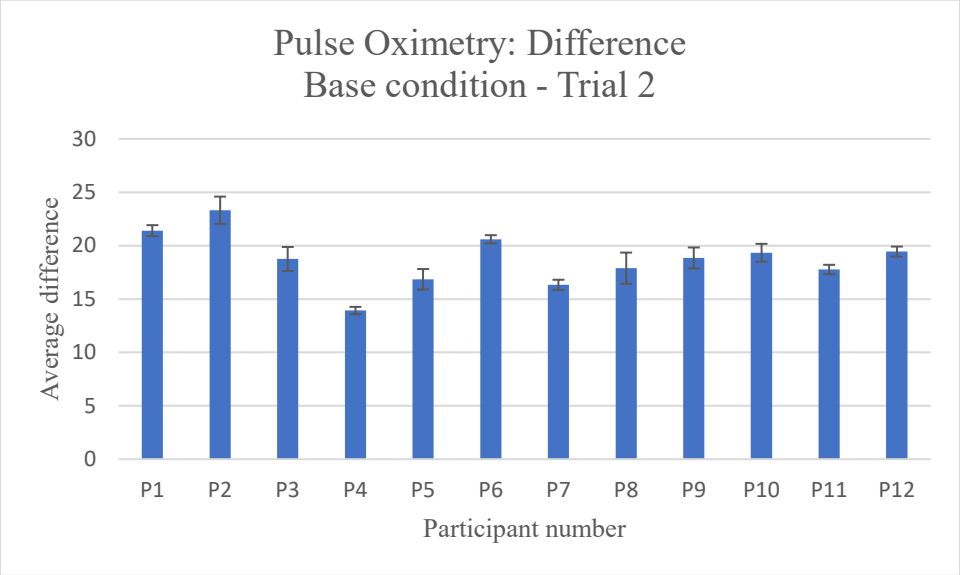
Pulse Oximetry: Difference
Base condition - Trial 2
Average difference
30
25
20
15
10
5
0
P1
P2
P3
P4
P5
P6
P7
P8
P9
P10
P11
P12
Participant number

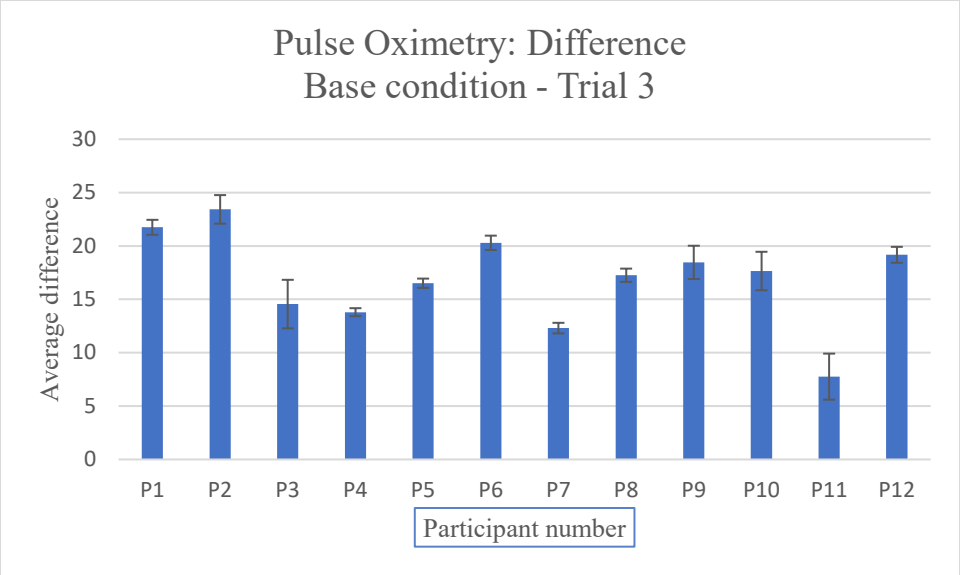


*Fig. B17-B19: Pulse oximetry $SpO_2$ average difference and standard deviation, base condition, trials 1-3.*

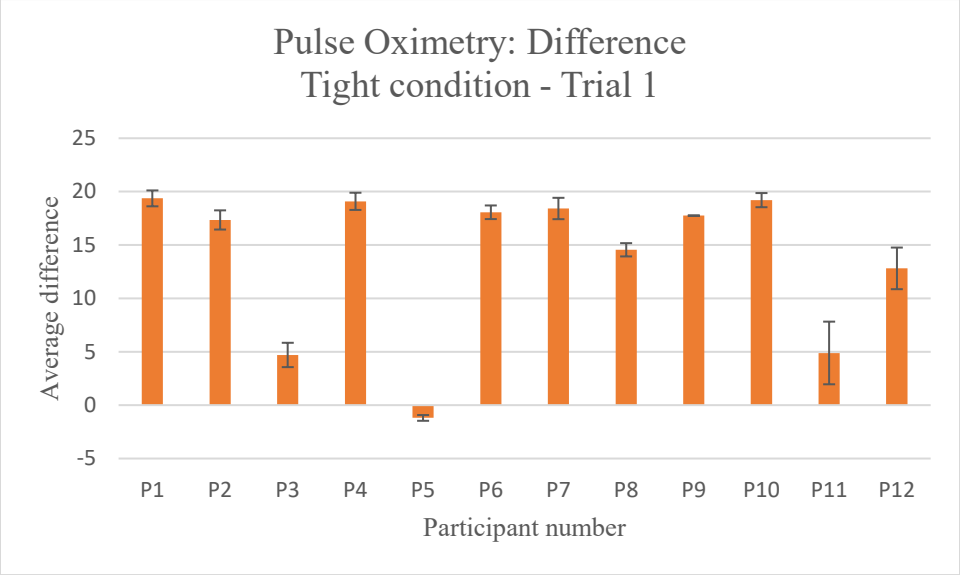

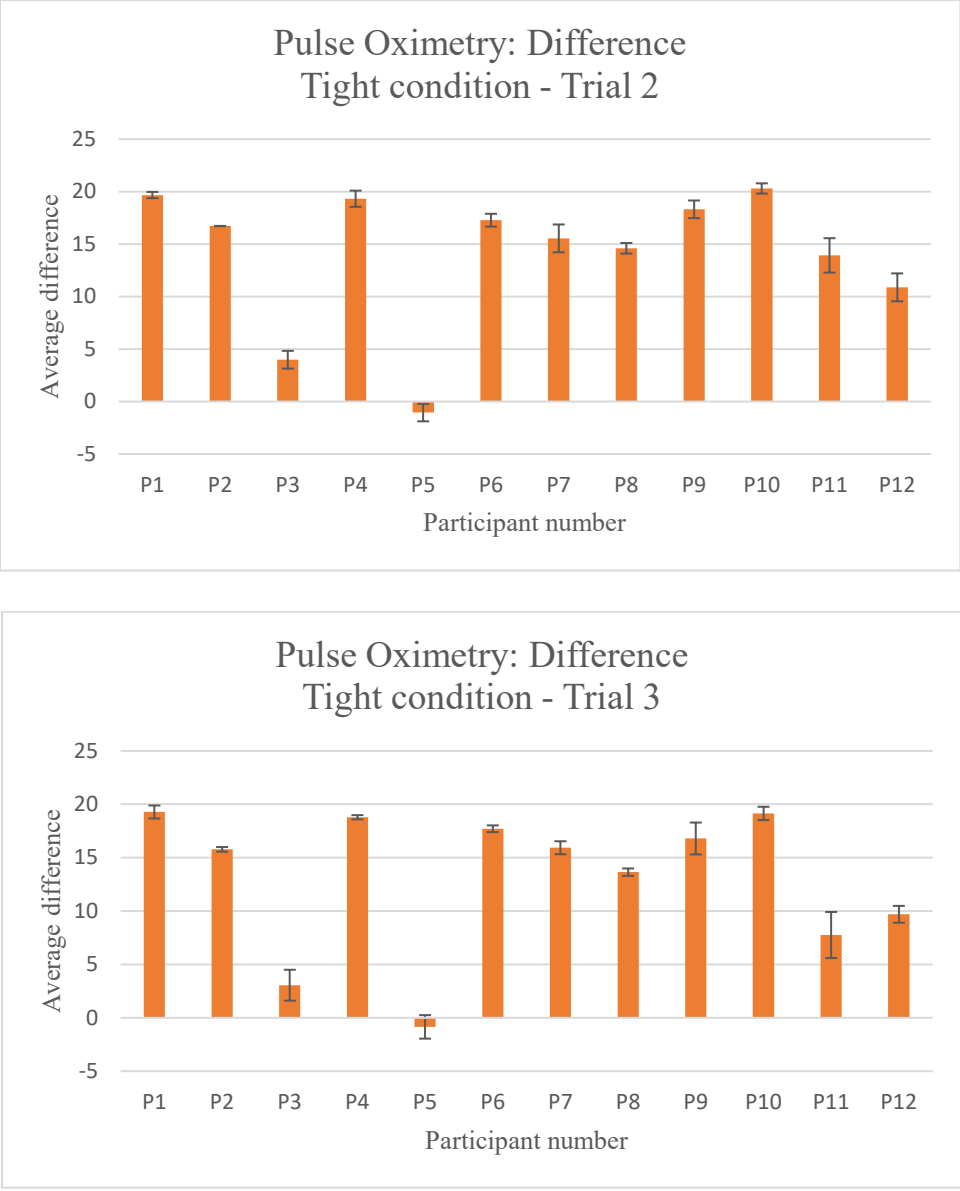


*Fig. B20-22: Pulse oximetry $SpO_2$ average difference and standard deviation, tight fit condition, trials 1-3*

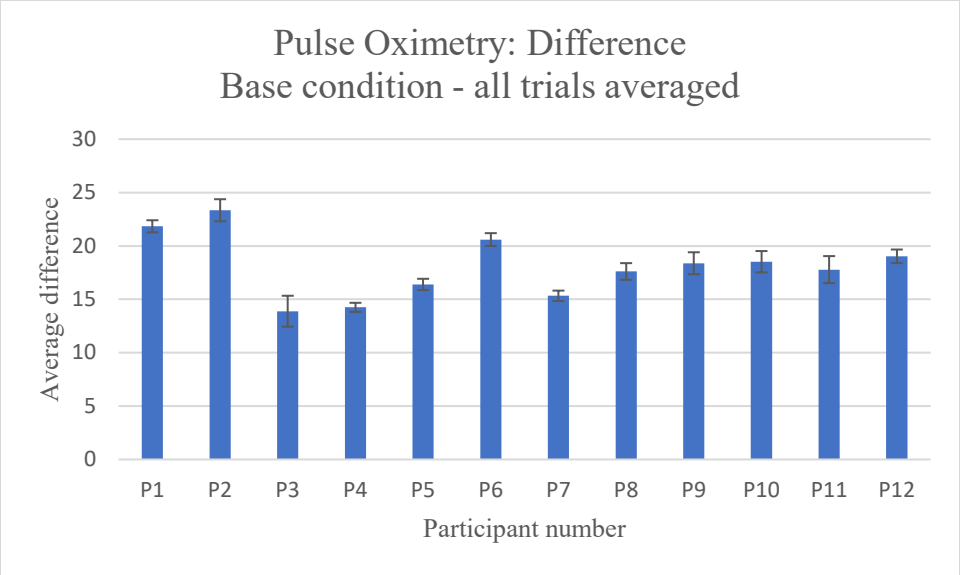


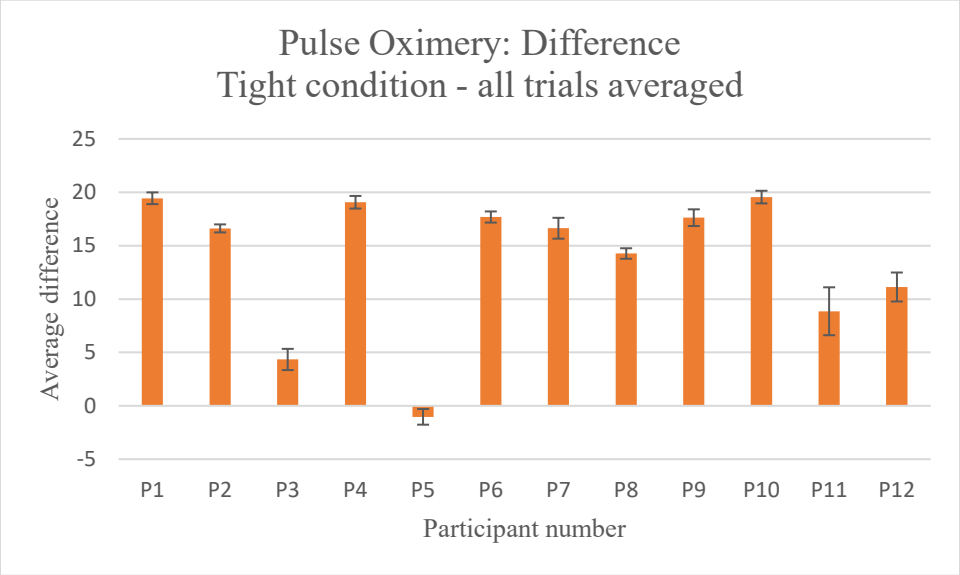


*Fig. B23-B24: Pulse oximetry $SpO_2$ average difference and standard deviation, base fit condition all trials averaged, tight fit condition all trials averaged.*

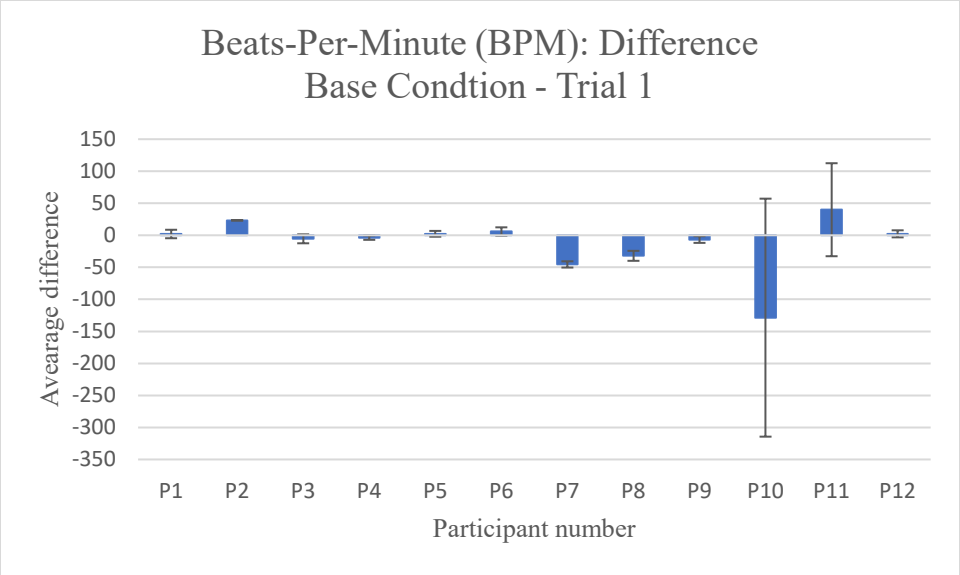
Beats-Per-Minute (BPM): Difference
Base Condtion - Trial 1
Avearage difference
150
100
50
0
-50
-100
-150
-200
-250
-300
-350
P1
P2
P3
P4
P5
P6
P7
P8
P9
P10
P11
P12
Participant number

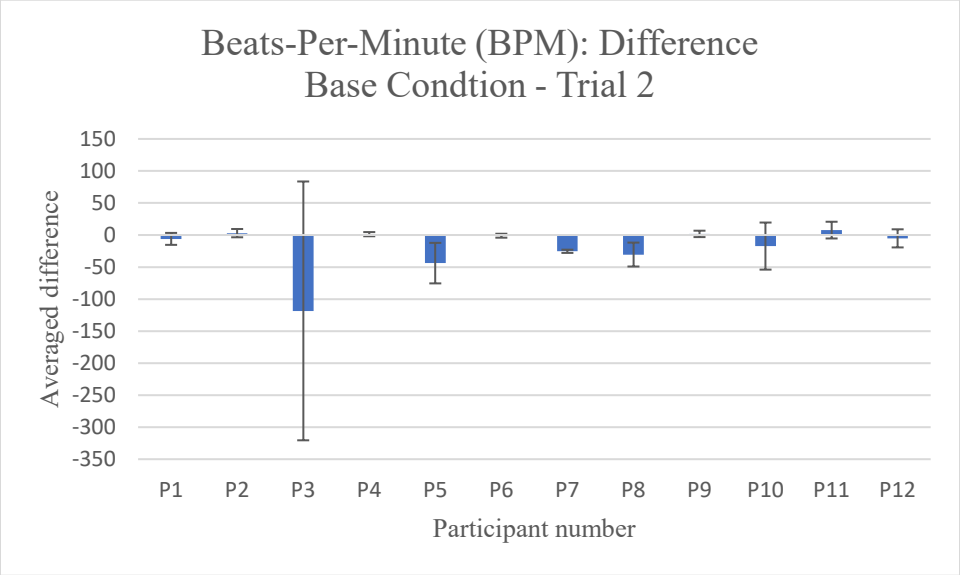
Beats-Per-Minute (BPM): Difference
Base Condtion - Trial 2
Averaged difference
150
100
50
0
-50
-100
-150
-200
-250
-300
-350
P1
P2
P3
P4
P5
P6
P7
P8
P9
P10
P11
P12
Participant number

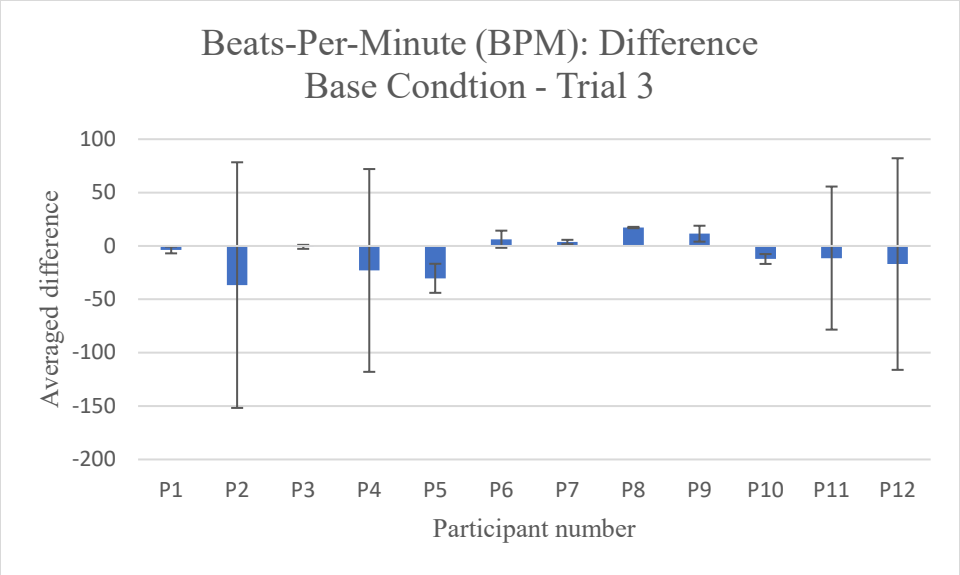


*Fig. B25-B27: Pulse oximetry BPM average difference and standard deviation, base fit condition, trials 1-3*

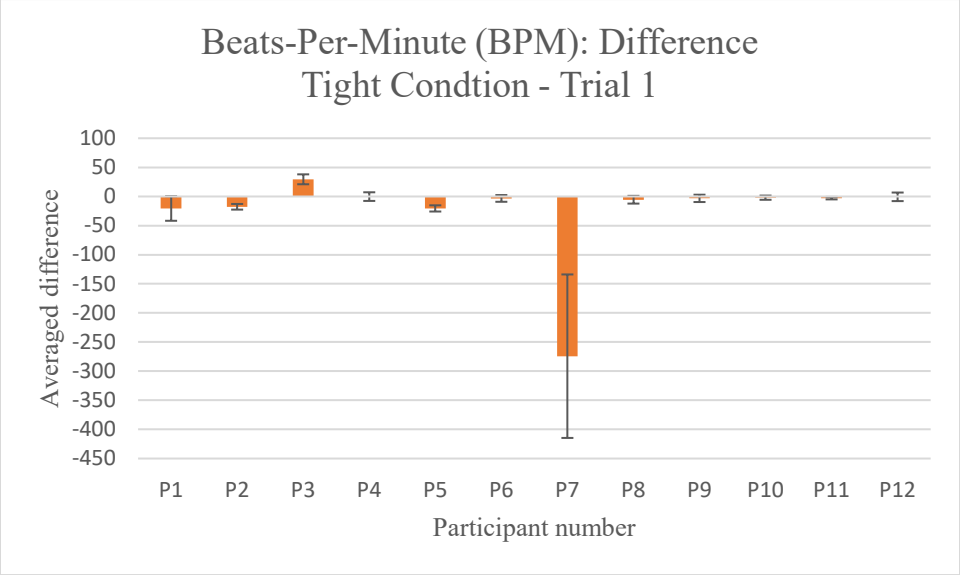

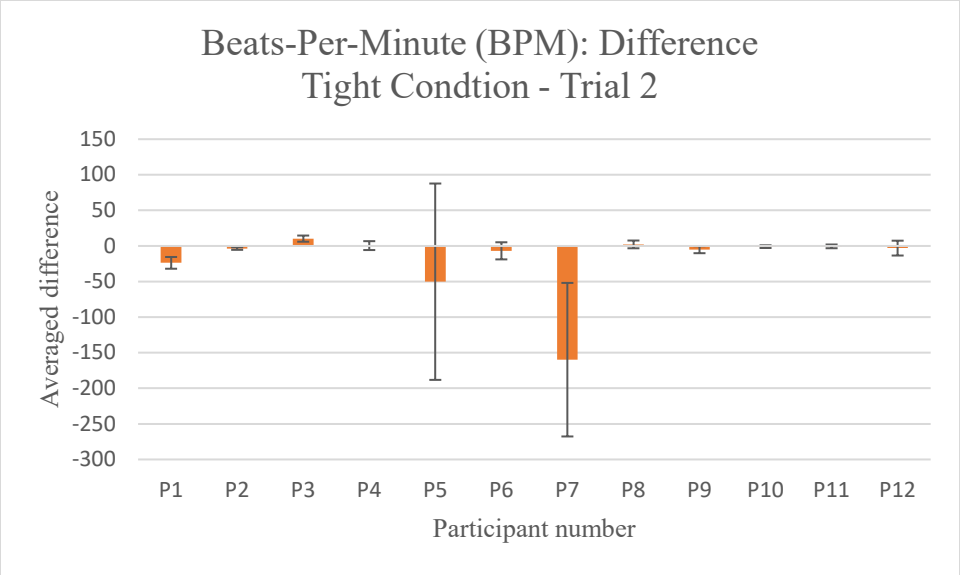


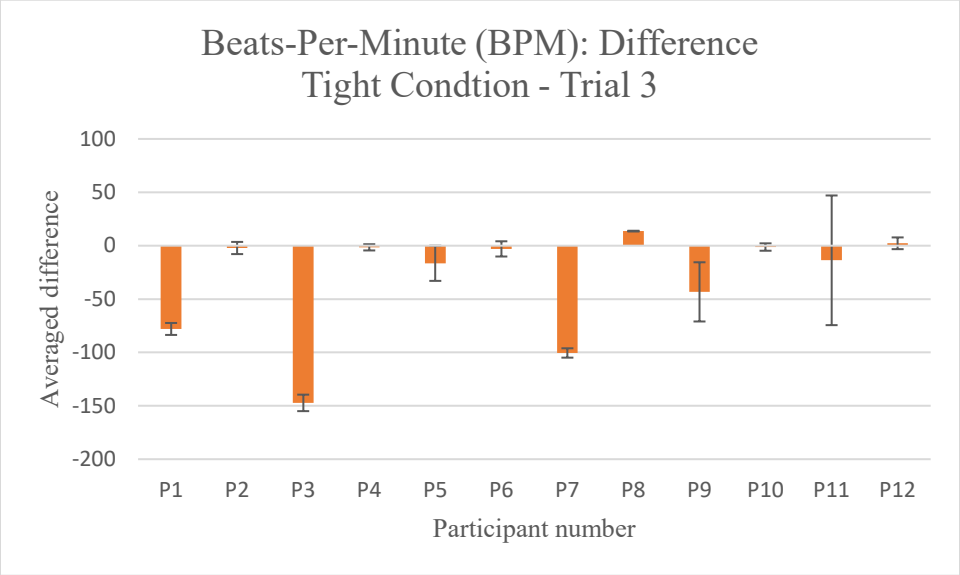


*Fig. B28-B30: Pulse oximetry BPM average difference and standard deviation, tight fit condition, trials 1-3*

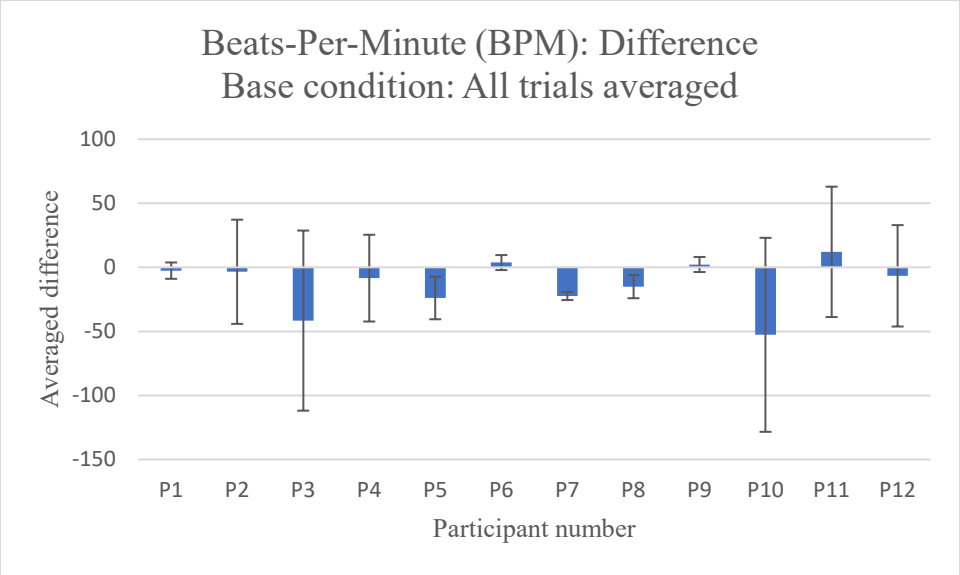


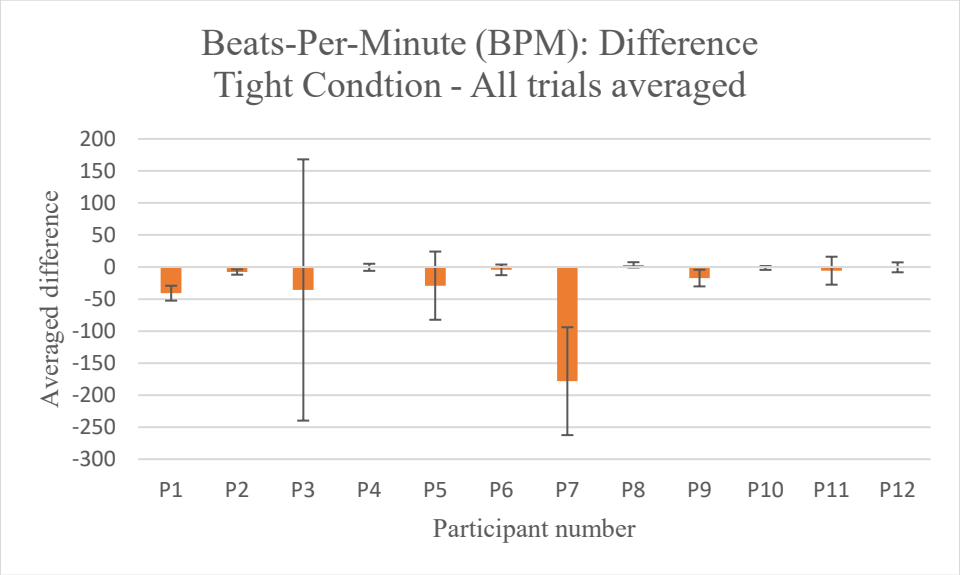


*Fig. B31-B32: Pulse oximetry BPM average difference and standard deviation, base fit condition all trials averaged, tight fit condition all trials averaged.*